TEMPORAL CHANGES IN THE SPATIAL PATTERNS OF WEAK LAYER SHEAR STRENGTH AND STABILITY ON UNIFORM SLOPES

by

Spencer Carl Logan

A thesis submitted in partial fulfillment
of the requirements for the degree

of

Master of Science

in

Earth Sciences

MONTANA STATE UNIVERSITY
Bozeman, Montana

May 2005

APPROVAL

of a thesis submitted by

Spencer Carl Logan

This thesis has been read by each member of the thesis committee and has been found to be satisfactory regarding content, English usage, format, citations, bibliographic style, and consistency, and is ready for submission to the College of Graduate Studies.

Katherine Hansen

Approved for the Department of Earth Sciences

David Lageson

Approved for the College of Graduate Studies

Bruce R. McLeod

STATEMENT OF PERMISSION TO USE

In presenting this thesis in partial fulfillment of the requirements for a master's degree at Montana State University, I agree that the Library shall make it available to borrowers under the rules of the Library.

If I have indicated my intentions to copyright this thesis by including a copyright notice page, copying is allowable only for scholarly purposes, consistent with "fair use" as prescribed in the U. S. Copyright Law. Requests for permission for extended quotation from or reproduction of this thesis in whole or in parts may be granted only the copyright holder.

Spencer Logan

May 2005

ACKNOWLEDGEMENTS

Many thanks to my committee, Katherine Hansen, Karl Birkeland, Richard Aspinall, and Kalle Kronholm, for their guidance and patience. Many people helped collect the data. Without them, this project would have been much smaller. Many thanks to Eric Lutz for all his help in the field in the summer and winter, for his assistance in organizing field days, and for his discussions on the ideas in this thesis. Kalle Kronholm, Karl Birkeland, Denny Capps, Jeff Deems, Ron Johnson, Katherine Hansen, Dave Lovejoy, Shannon Moore, and Simon Trautman also helped in the field and office. Linda Bishop and Grant Estey facilitated site access. I was partially supported by the Barry C. Bishop Scholarship for Mountain Research, the Department of Earth Sciences at Montana State University, and the National Science Foundation (Grant #BCS-0240310).

Most importantly, I received invaluable support and encouragement from my family and friends.

TABLE OF CONTENTS

TABLE OF CONTENTS - CONTINUED

LIST OF TABLES

LIST OF FIGURES

LIST OF FIGURES - CONTINUED

LIST OF FIGURES - CONTINUED

LIST OF FIGURES - CONTINUED

LIST OF FIGURES - CONTINUED

LIST OF FIGURES - CONTINUED

LIST OF FIGURES - CONTINUED

ABSTRACT

Avalanche forecasting involves the prediction of spatial and temporal variability of the stability of the snowpack. Greater spatial variability increases the uncertainty of forecasts and reduces the ability of a forecaster to extrapolate snowpack stability reliably. A greater understanding of the spatial patterns of stability, and how they change through time, could improve avalanche forecasting.

I examined temporal changes in shear strength and stability of three persistent weak layers at three different sites. Sites were located on uniform slopes to minimize factors that introduce variability or large-scale trends in the snowpack. At each site, shear strength and stability of the same persistent layer were measured in adjacent plots, sampled at intervals of one to eight days apart. Experimental variograms and pit-to-plot ratios provided measures of the spatial variability. Because adjacent plots began with similar conditions, differences between the plots were attributed to temporal change.

Shear strength of two buried surface hoar layers increased through time and became more variable. As the layers aged, the rate of strengthening decreased. Stability indices initially increased, then decreased as snowfall increased the slab stress. Changes in the spatial structure were most apparent when the layers were younger and gaining strength most rapidly. As the layers aged, the spatial measures provided less information.

Strength of depth hoar increased initially, then decreased as the depth hoar grew and bonds weakened. Spatial correlation increased over time between the first three plots. A strong wind event and warm weather led to considerable change to the snowpack between the third and fourth samples, complicating comparisons.

On these three weak layers, shear strength could be reliably extrapolated over a distance of at least 17 m on 86% of the days sampled, provided a sufficient number of tests were conducted to characterize the statistical distribution. The optimal spacing of tests changes as the autocorrelation length of shear strength changes. The number of tests required increases as the overall variability of shear strength increases. This suggests that test spacing is less important on older layers because the autocorrelation length is short, but more tests are required to characterize the slope statistically.

CHAPTER 1

INTRODUCTION

Forecasting snow avalanches is complicated by temporal changes in the spatial variability of the seasonal snowpack (McClung 2002a). In avalanche forecasting, information of limited spatial extent is extrapolated to areas of larger spatial extent. The amount of spatial variability within the snowpack affects the reliability of this extrapolation by introducing uncertainty (LaChapelle 1980; McClung 2002a). Assessing the variability within the data is an important, but often overlooked, aspect of avalanche forecasting.

Two snowpack properties of interest in avalanche forecasting are the shear strength of weak layers and the related snow stability (McClung and Schaerer 1993). Stability is the potential for snow to not avalanche relative to a given load (Greene et al. 2004), and is usually described as the ratio between strength of the weakest portion of the snowpack and stress of the snowpack above (Conway and Abrahamson 1984). The stability index is the ratio between the measured shear strength of the weakest layer and the calculated shear stress on that layer. Stability indices are calculated for individual stability tests. Stability tests may also measure relative stability, without calculating an index. Stability indices or relative stability are measurements of point stability. Avalanche forecasters extrapolate from point stability to estimate the overall slope stability. Spatial variability in the stability indices introduces uncertainty in the extrapolation to slope stability

Shear strength is a property of layers within the snowpack or of interfaces between layers, and is influenced by characteristics such the amount of bonding between snow grains. Fracturing of inter-granular bond leads to shear failure in a weak layer. If the fracture propagates a sufficient distance, an avalanche may result (Schweizer 1999). Locally weak areas are assumed to be susceptible to fracturing, while locally strong areas may prevent fracture propagation (Schweizer 1999). Identifying patterns of stronger or weaker areas is, therefore, important for avalanche forecasting.

There are several types of weak layers. Some, like subtle differences in new snow, may strengthen quickly. The most hazardous are persistent weak layers, like layers of depth hoar, buried surface hoar, or near surface facets, which may fracture and produce avalanches for weeks or months after forming (Birkeland 1998).

Forecasting for future avalanche hazard involves predicting the change within the snowpack, including how the spatial variability of strength and stability could change. Some of the temporal changes can be conceptualized as a curve tracking slope stability through time (Tremper 2001) (Figure 1). Birkeland and Landry (2002) related these trends to the spatial divergence and convergence of shear strength and point stability.

Weak layers often gain strength as they age (Jamieson and Schweizer 2000), increasing stability through time (Figure 1). As the slope stabilizes and adjusts to the load, small differences in the snowpack may be compounded. Based on soils research by Phillips (1999), Birkeland and Landry (2002) proposed that spatial variability might increase through time as the snowpack diverges, or becomes more dissimilar. Divergence increases uncertainty in forecasting because extrapolation of point stability becomes less reliable.

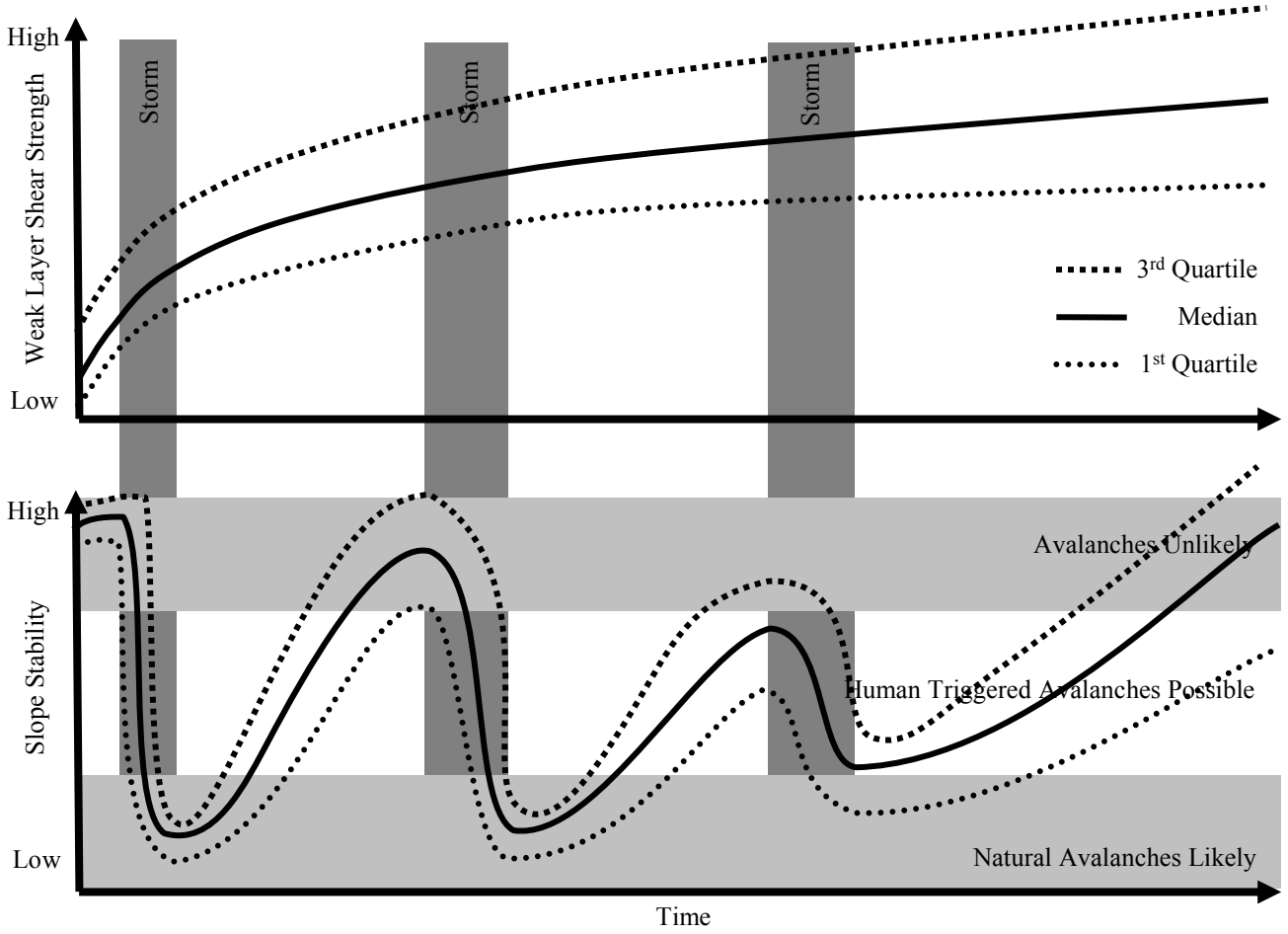

Figure 1. Conceptual diagram of changes in shear strength (top) and stability (bottom) of a persistent weak layer (adapted from Tremper 2001). Shear strength increases through time and becomes more variable. Stability changes as snowfall increases the load above the weak layer, then the weak layer gains strength and adjusts to the additional load.

A rapid change or perturbation to the snowpack, like substantial snowfall, can decrease slope stability and the stability indices (Figure 1), with the magnitude of the decrease related to the magnitude of the perturbation. If the perturbation is large enough, its influence could overwhelm previous differences in the snowpack and decrease the relative differences in shear strength. Such convergence, or decreasing spatial variability, would reduce the uncertainty in forecasting. There are indications that as slope stability decreases, point stability becomes increasingly spatially uniform (Kronholm and Schweizer 2003).

Better quantification of temporal trends in spatial variability of shear strength or point stability would improve avalanche forecasting. Knowing that the snowpack is diverging would allow an avalanche forecaster to seek data at a greater spatial density, or extrapolate over shorter distances and times. Conversely, if the snowpack is converging, reliable extrapolation should be possible over greater distances and for longer times.

I examined the temporal change in shear strength and stability indices of persistent weak layers over uniform slopes. I hypothesized that there are quantifiable temporal changes in the variability and spatial autocorrelation of shear strength and stability results, and focused on three primary questions:

1. What were the spatial structures of strength and stability indices on a single day?

2. How did the spatial structures of strength and stability indices change between days?

3. Were changes in spatial structures related to snowfall or other snowpack changes?

This research is the first to quantify temporal changes in spatial variability of shear strength and stability indices in a spatially explicit manner. I used linear trends and

variograms, spatially explicit by definition, and additional, non-spatial methods to analyze the spatial structure of strength and stability. The spatial structure would then indicate how spatially variable the shear strength and stability were on a given day.

To assess changes in the spatial structure, I compared the spatial structure of adjacent plots sampled on different days. Based on previous research (Birkeland and Landry 2002), I anticipated that changes in the spatial structure could be related to observed changes in the snowpack, such as metamorphism or increases in slab thickness. Small or gradual changes would lead to increasing spatial variability, while large or rapid changes to the snowpack would decrease spatial variability. The intention was to improve the understanding of spatial and temporal variability of the snowpack, in order to improve avalanche forecasting.

CHAPTER 2

LITERATURE REVIEW

Avalanche Processes

Avalanches are falling masses of snow that may contain ice, rocks, or soil (McClung and Schaerer 1993). Two types of avalanches are commonly differentiated: loose snow avalanches involving mostly surface snow, and slab avalanches. In a slab avalanche, a fracture occurs within a weak snowpack layer, and then propagates outwards. The propagating fracture isolates a block of snow that then moves down-slope (McClung and Schaerer 1993). Slab avalanches are more dangerous to people, and therefore most research concentrates on them. My research concentrated on two commonly measured properties of the snowpack that influence the potential for a slab avalanche to initiate, the weak layer shear strength and the stability index.

Imagine a wooden block sitting on a tilted shelf. The vertical force of gravity acting on the block can be resolved into two components, one perpendicular and one parallel to the slope (Easterbrook 1993). The two force components, the slope angle, the physical properties of the block, and properties of the shelf determine how steep the shelf can tilt before the block slides. Failure (sliding down the shelf) results if the slope parallel force exceeds the friction caused by the slope perpendicular force. If friction is stronger, the block stays in place.

Slope perpendicular and slope parallel components of force also act on snowpacks, but the snowpack can respond by deforming. McClung and Schaerer (1993)

define three types of deformation within the snowpack: compression, tension, and shear (Figure 2). Compression is deformation perpendicular to the snow surface; it increases density and tends to promotes strengthening (Tremper 2001). Tensile deformation results from creep, a down-slope movement of snow layers or the entire snowpack. Shear deformation is induced as snow grains move past each other, generally parallel to the slope. Shear stress is caused by the combination of all three types of deformation, and is not uniform throughout the snowpack (McClung and Schaerer 1993).

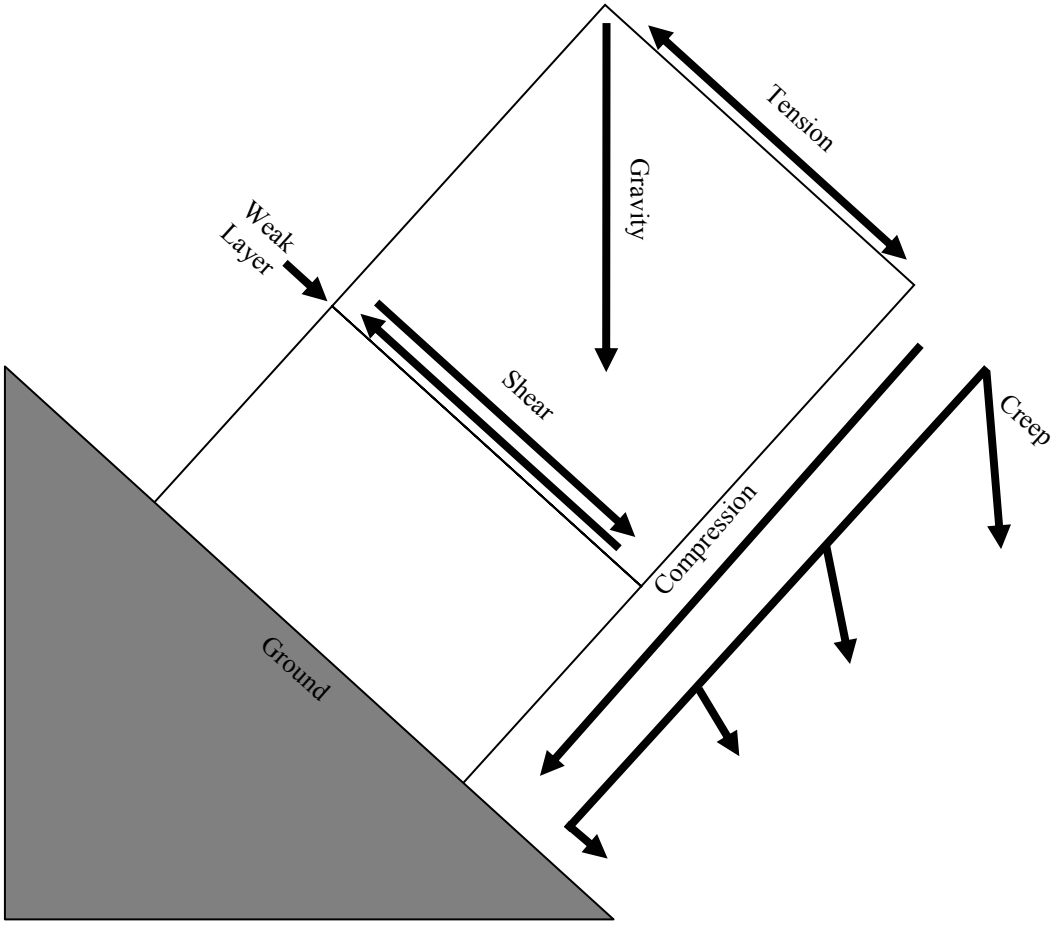

Figure 2. Diagram of the forces on the snowpack. Shear deformation promotes failure, and is indicated here along the weak layer parallel to the slope. Compression, tension, and gravitational deformation contribute to creep.

Each layer may deform at a rate different from others, causing stress concentrations within layers or at layer interfaces (Jamieson 1999a).

A snowpack layer or interface can become a failure plane if the shear stress exerted by the layers above —termed the slab—exceed the shear strength of the layer—termed the weak layer (McClung and Schaerer 1993). Slab avalanches initiate through the fracturing of bonds between snow grains within the weak layers (McClung and Schaerer 1993). This may lead to a fracture that propagates outwards along the interface or layer. To avalanche, the fracture must propagate fast enough to fracture the weak layer in shear over a sufficiently large area, and then fracture the overlying slab in tension (McClung and Schaerer 1993; Louchet 2000). Slowly propagating fractures or fractures that do not extend over a sufficient area could allow the snow grains to sinter and re-form bonds, effectively closing the fracture and preventing it from reaching a critical size (Schweizer 1999).

Stability is the potential for snow to not avalanche relative to a given load (Greene et al. 2004). If stability is good, avalanches are unlikely or require large triggering forces. If stability is poor, natural avalanches are likely in certain types of terrain, and the force required to trigger an avalanche is small (Greene et al. 2004). Assessing the stability of the snowpack and projecting changes in stability into the future are the primary goals of avalanche forecasting (McClung 2002a). Forecasters usually extrapolate from stability tests, essentially point measurements, to the overall slope stability. Spatial variability in the measurements of stability introduces uncertainty in the extrapolation.

A stability index, the ratio between the shear strength of the weak layer and the shear stress exerted by the slab, can be calculated for stability tests (Conway and Abrahamson 1984). Stability tests measure snowpack stability by applying a load to the snowpack until the weak layer fractures. Different types of stability tests load the snowpack in different manners, and have different resolutions and scales of results. As an example, a rutschblock test tests a 3 m^2 area of snow and the stability result can be one of seven categories (Föhn 1987a). Quantified loaded column tests (Landry et al. 2001) isolate a 0.09 m^2 column, and record the force at which the weak layer fractures with a force gage. Shear strength of the weak layer can be calculated using the quantified loaded columns (Landry et al. 2001). Shear frame tests, used in this project, measure the force at shear fracture of weak layers (Jamieson and Johnston 2001). The stress on the weak layer is calculated from measurements of slab thickness, density, and slope angle. A stability index is then the ratio of the shear strength at failure and the calculated slab stress (Jamieson and Johnston 2001).

The Seasonal Snowpack

The old adage says, “Every snowflake is unique”. Myers (1997) cited snow as the ultimate example of heterogeneity, because variability exists at the fundamental level of the unique snowflakes. However, all snowflakes share a common crystalline structure. Snowflakes formed under similar conditions have similar forms because factors like temperature, super-saturation of the air, and storm characteristics exert strong influences on the shape of the snowflake (McClung and Schaerer 1993).

Falling to the ground, these similar snowflakes form layers within the snowpack. Layers are aggregates of individual snow grains that are somewhat homogenous and

exhibit similar characteristics (Colbeck et al. 1990). Processes operating on the snowpack can form other layers on or within the snowpack. Although composed of relatively homogeneous grains, layer properties may vary from location to location, making them spatially heterogeneous (Colbeck 1991).

Snow grains metamorphose under the influence of various factors (McClung and Schaerer 1993). Some factors, such as terrain and substrate, are temporally static through the winter, but can differ with location and greatly influence the metamorphism of nearby snow (Birkeland et al. 1995; Arons et al. 1998). Other metamorphic factors such as weather and diurnal fluctuations of temperature and solar radiation change through time. This leads to the potential for layer properties to vary spatially, and for the spatial variations to change through time.

Types of Weak Layers

Some instabilities form as new snow falls and the snowpack adjusts to the load (McClung and Schaerer 1993). These are usually along interfaces between the old snow surface and the new snow, or interfaces between layers produced within a storm. Such instabilities are usually transient, and after a few days, no longer produce avalanches (McClung and Schaerer 1993).

Other types of weak layers are persistent, and may remain as a weak layer in the snowpack for weeks or months (Jamieson 1999b; McClung and Schaerer 1993; Tremper 2001). The persistent weak layers are the most hazardous layers, and account for the majority of weak layers in fatal avalanches (Jamieson and Schweizer 2000). Of the persistent weak layers, buried surface hoar comprises the weak layer more than any other

grain type in intermountain climates (Jamieson and Schweizer 2000), and depth hoar is of great concern in continental climates (Tremper 2001).

Avalanche Forecasting

Avalanche forecasting involves an estimate of both current and future snow stability (LaChapelle 1980), and attempts to minimize uncertainty about temporal and spatial variability of stability (McClung 2002a). McClung (2002a) emphasized instability over stability because information about instability has the lowest uncertainty.

Avalanche forecasting is a process that combines information at various scales and inductively integrates them to make a prediction (LaChapelle 1980). Avalanches occur at scales different from the scales at which many measurements are made. Fracturing occurs on scales of the grain and layer (10^{-4} to 10^{-1} m) and avalanches occur at the slope scale (5×10^{1} to 10^{2} m; Kronholm 2004). When compared to avalanches, stability tests are essentially point measurements, with individual test sizes ranging from 0.025 m^2 (shear frames) to 3 m^2 (rutschblocks). There is potential that the measurement scale is unable to represent properly the scale of the avalanche process.

How does a forecaster take the point measures of stability and scale the results to the slope? The information used is not limited to just stability tests. Forecasts are based on a combination of meteorology, snow physics, and empirical evidence (LaChapelle 1980). Information is grouped into three classes based on the amount of uncertainty within the data (Birkeland 1997; McClung and Schaerer 1993). Data with less uncertainty is representative at shorter spatial scales (Hageli and McClung 1999), because it is specific information about a specific location. As the scale at which information is

representative increases, the uncertainty about specific locations must increase to account for greater potential variations.

Data Classes

Class I data have the least uncertainty of the data classes. Class I data are direct measures of stability, either by testing the snowpack to failure or observing failure that has already occurred. Class I data include stability tests, at scales from 0.025 m^2 to 3 m^2, and the observation of and deliberate triggering of avalanches (or lack of them) at the slope scale. Class I data are often collected in a manner that does not allow for the estimation of variability within the results. Only one or two adjacent stability tests or a single rutschblock are common. Avalanche observations are only a presence/absence measurement, because there is no way to judge how close a slope was to avalanching. Deliberate triggering can sometime be done in a progressive manner, allowing an estimate of the force required to trigger an avalanche, but repeatable measures require many similar slopes.

Class II data are primarily data about snowpack stratigraphy, and include information about the presence, strength, and loading of weak layers. Stratigraphy influences stability, but stability cannot be directly measured from Class II data. Class I and II data are collected through targeted sampling (McClung 2002b). The measurement location is judged to be representative of the area of interest, or to represent the weakest conditions of the area of interest.

Meteorological factors comprise Class III data. Changes in weather can have a large impact on the snowpack, but the effects on stability may not be direct, multivariate, or less than certain. Meteorological factors are extrapolated from a few measurement

locations, and may have considerable error at the local scale. The local error, combined with the less than direct effects on stability, leads to large amounts of uncertainty in the influence of meteorological factors on stability.

Forecasting Stability

The prediction of current instability at particular locations is the most common type of avalanche forecasting, conducted by recreational backcountry travelers to the authors of public avalanche bulletins. The forecast relies upon extrapolation of data to the area of interest. Uncertainty within the extrapolations must be minimized, because greater uncertainty leads to greater forecasting errors.

The primary way of minimizing uncertainty in the extrapolation of stability is to collect Class I data as close to the area of interest as possible. Stability test locations are selected to maximize safety and "representativeness" of the results, so are located on the slope of interest (least uncertainty), or on slopes of similar steepness, aspect, and elevation (greater uncertainty). Targeted sampling (McClung 2002b), where tests are located in areas where weak snowpacks and poor stability are expected, is also used to reduce the uncertainty about the most unstable snowpack structures.

Quantifying the variability of the results is a critical and often overlooked component of avalanche assessment. More variability within the results increases the uncertainty and decreases the reliability of the extrapolation.

Because the snowpack is spatially variable, extrapolating stability test results always introduces uncertainty. Research into the spatial variability of stability (Jamieson 1995; Kronholm and Schweizer 2003; Landry 2002), and therefore the ability to extrapolate stability results, has come to different conclusions about the amount and

importance of the variability. Greater understanding of the spatial structure of shear strength and stability would improve the reliability of stability test extrapolation.

Forecasting for future instability requires anticipating factors that will change instability over time. The estimates must include the appropriate amount of uncertainty. Weather forecasts are one of the primary factors used, and the avalanche forecaster has to scale synoptic weather forecasts to the area of interest.

Another factor is how the spatial variability of instability might change in the future. Will the variability of instability increase? If so, by how much and how will the ability to extrapolate spatially be reduced? If the spatial variability of instability decreases, does that make spatial extrapolation easier and more certain? Examining the changes in the spatial structure of shear strength and stability through time would help to answer questions such as these.

This study focuses on the spatial variability of Class I and II data at the scale of a small slope. What kind of statistical extrapolation is possible over relatively short distances? Class III data are incorporated into the analysis of any potential site-wide spatial trends and in the analysis of temporal changes.

Earth Surface Systems

In *Earth Surface Systems*, Phillips (1999) applied concepts from chaos theory, complex systems, and non-linear dynamics to understanding natural systems. Phillips made the case that the approach was applicable to most natural systems. Birkeland and Landry (2002) applied ideas from *Earth Surface Systems* (Phillips 1999) to the snowpack to help explain spatial patterns of stability and temporal changes in the patterns.

One of the central threads of *Earth Surface Systems* (Phillips 1999) is that both order and disorder are possible within a system, especially if observed at different scales. Physical rules control the development of systems. At any one location, slight, local variations in those physical rules control the development of the system's local characteristics. In the case of avalanches, initiation requires a slope steeper than 25° covered with snow, but different storms can deposit snow across the slope in different manners. Regional avalanche forecasts are possible because of patterns in stability that exist over an entire mountain range, but interpreting spatial patterns at scales such as individual slopes can be quite hard (Birkeland and Landry 2002).

Phillips (1999) suggested that spatial variations develop through time. From an initially similar state, small local variations create differences in the system. As time continues, small differences are amplified and spatial variation increases. The increase in spatial variability occurs because of slight variations in the dynamics of the system, and does not require external input. Large perturbations—external forcing—can overwhelm the system and force it to converge to a uniform state (Birkeland and Landry 2002). External forcings are rare in the systems that Phillips (1999) describes, but are common to the snowpack, where large storms can occur and may dramatically change the snowpack stability (Tremper 2001).

Coastal soils in North Carolina provided an example of increasing spatial variability through time (Phillips 1993). Two soils were located on adjacent, old marine terraces, the older dating from the middle Pleistocene, and the younger soil dating from the late Pleistocene. Climate, biota, and parent material were similar. Only one soil

family was mapped on the younger terrace, with little variation. Seven soil families were mapped on the older terrace, with considerable differentiation between the families.

Phillips (1993) interpreted the findings as evidence of deterministic spatial chaos, where spatial variability tends to increase through time. Spatial differentiation would occur even under nearly uniform environmental factors, and the spatial variability of soil structure would not necessarily exhibit small-scale, systematic patterns. If pedogenesis was not chaotic, soils would tend to converge towards a spatially uniform climax soil type. Convergence would dampen variations through time, where chaotic evolution would tend to amplify small variations.

Similarly, if spatial variability exists in the snowpack, and increases through time, the snowpack system should be deterministically chaotic. Divergence should be the tendency. In the absence of major perturbations, the snowpack properties should become more variable. Small perturbations or slight differences in initial conditions at two locations could lead to increasingly different characteristics through time. The result is variation that falls within finite limits (Phillips 2000) and may follow patterns or exhibit spatial correlation. A major perturbation—in the snowpack, most likely significant snowfall—could force the snowpack towards a uniform state, something rarely observed in soils (Birkeland and Landry 2002).

Spatial Variability of the Seasonal Snowpack

Considerable attention has been paid to spatial variations of snowpack stratigraphy, strength, and stability at many scales, from mountain ranges (Birkeland 2001) to individual slopes (Harper and Bradford 2003; Kronholm 2004; Landry 2002). Studies conducted by different researchers, in different avalanche climates, using

different types of tests, reach different conclusions about the significance of the variability of stability present within the snowpack. The use of different tests, sampling arrays, and differences of weak layers complicates comparisons of the various studies.

Spatial Variability of Snowpack Stratigraphy

Several studies have examined microstructural variations in the snowpack (Harper and Bradford 2003; Kronholm 2004; Kronholm et al. 2004). While Harper and Bradford (2003) found considerable structural variations on short scales—the order of 10^{-4} to 10^{-1} m—general structural characteristics were continuous throughout the snowpack over slope scales. They attributed much of the structural variability reported in other studies to effects of variations in local conditions, or to problems associated with point measurements of continuous processes.

Birkeland et al. (1995) measured the average penetration resistance of the entire snowpack in a more wind-drifted area than Harper and Bradford (2003) or Kronholm et al. (2003). Birkeland et al. (1995) found that variations in average penetration resistance were related to snow depth, influenced by wind deposition and scour, and variations in the substrate.

Kronholm et al. (2004) reported the penetration resistance and spatial variability of seven layers over a small slope, including a layer of buried surface hoar. Geostatistical analysis was used to quantity the spatial variability of each layer. The surface hoar layer had the least variability of penetration resistance, but had little spatial autocorrelation. Penetration resistance in the other layers had considerably more spatial variability, and the authors attributed the variations primarily to wind and topography.

Spatial Variability of Stability

Kronholm (2004) combined stability and structural measurements to examine the spatial variability of both using geostatistics. He sampled wind-effected, high alpine slopes using an array of 24 ramrutsch stability tests, and 119 structural profiles from the SnowMicroPen. He found results from adjacent tests tended to be correlated, unlike Landry (2002).

Kronholm (2004) had too few stability tests fracturing on the same weak layer to perform much geostatistical analysis on the stability results. In the stability results he was able to analyze, the slope scale trend accounted for most of the spatial structure, and the residuals offered no additional spatial structure. This was attributed to either insufficient resolution of the stability test used (ramrutsch), or lack of spatial structure in addition to the slope-scale trends.

Conway and Abrahamson (1984) conducted one of the earliest studies of the spatial variability of snowpack stability. Using a modified shear frame test, they measured shear strength and stability just above crown lines of recent avalanches and on cross-slope transects on slopes that had not failed. They later reanalyzed the data as a stationary random process, and looked for spatial autocorrelation (Conway and Abrahamson 1988). They found a smaller coefficient of variation and much higher mean stability on slopes that had not failed. They reported correlation lengths for shear strength between 0.2 and 1.3 m. To estimate the variance in stability across a slope adequately, Conway and Abrahamson (1988) suggested tests spaces 0.5 m apart and spanning 3 m.

Using the rutschblock, Jamieson and Johnston (1993) and later Jamieson (1995) measured stability variations across relatively uniform potential avalanche slopes. They found that any one rutschblock score was within ± 1 score of the slope mean 97% of the time. This was taken to mean that a single rutschblock could represent the overall slope stability. However, rutschblocks are scored on a scale from 0-7, so a range of three scores represents 37% of the potential range of scores. One slope had a large range of scores, from one to five with a median of three. There were weaker areas associated with a layer of buried surface hoar. In spite of low rutschblock scores, the slope did not avalanche while being sampled.

Working on more variable slopes, Campbell and Jamieson (2004) found clusters of weaker and stronger rutschblock scores. These were related to variations in terrain, observable differences in the weak layers, or changes in slab properties. Large variations in adjacent scores were not uncommon. Sampling the same slope, with similar snowpack conditions, in two different years, they found similar, terrain-controlled patterns of rutschblock scores.

Stewart and Jamieson (2002) used a modified compression test spaced closely across potential starting zones. Clusters of related scores were found, but no correlation length was reported (Kronholm 2004).

Landry (2002) and Landry et al. (2004) studied spatial variability over relatively uniform slopes. He used the quantified loaded column test (QLCT) (Landry et al. 2001), and grouped 50 tests into five pits, equally spaced across a 30 m by 30 m plot. Large variations in test results occurred on some slopes, while the coefficient of variation on other slopes was as low as 6%. Landry (2002) did not analyze his results in a spatially

explicit manner, instead using the semi-spatial pit-to-plot ratios (see page 37 for a full discussion of the ratio and the semi-spatial nature). Of the 54 pits examined, 33 (61%) pits represented the plot-wide results (Landry et al. 2004). Several times, the weakest and strongest test results were within 0.5 m of each other (Landry 2002). No relationships between non-representative pits and topography, substrate, or observed stratigraphic differences were found (Landry 2002; Landry et al. 2004).

Temporal Variability of Stability

As part of Landry's (2002) study, he collected data from three plots on the same slope, measuring the same buried surface hoar layer over three weeks. In addition, 80-100 SnowMicroPen profiles were collected in two of the plots (Birkeland et al. 2004). Because the plots were spread across the slope, differences between the plots could not be attributed to time alone.

Birkeland and Landry (2002) were the first to address temporal change in the spatial variability of slope-scale stability. They used the coefficient of variation of each pit and pit-to-plot ratios as indicators of variability. They proposed that a weak layer starting from a relatively uniform condition would gain strength, accompanied by an increase in spatial variability of stability tests. An event of large enough magnitude would cause convergence and a decrease in the spatial variability. The authors explained the divergent and convergent behavior, identifying a forcing event between the second and third day of sampling.

Birkeland et al. (2004) compared the SnowMicroPen signals for the surface hoar layer on the first two days. No spatial structure was found within the signals for either plot. Significant change occurred in signal variance and maximum penetration

resistance. The authors found no significant difference in layer thickness between the two days. This was contrary to the results expected from the model of surface hoar strengthening (Jamieson and Schweizer 2000). The authors attributed the lack of thinning to the low-density slab and lack of force on the layer. The increase in maximum resistance was an indication of increasing bonding of the surface hoar grains to the adjacent layers.

Using a different method of layer delineation with the same data, Lutz et al. (2004) found significant thinning of the weak layer, and strengthening of the interface between the weak layer and underlying layer. These changes correlated with the increase in shear strength measured using the QLCT. Additional analysis of several layers within the slab is ongoing (Birkeland et al. 2004).

Jamieson and Johnston (1999) tracked multiple surface hoar layers through time, and recorded more than 300 temporal comparisons. Their work had no spatial component, and they assumed the study sites to be spatially uniform. The factors most significant to temporal strengthening of buried surface hoar layers were slab thickness, total snowpack thickness, and surface hoar grain size (Jamieson and Johnston 1999). Thickness and depth were related to the load above the surface hoar layer, with increased load increasing the rate of strengthening. Layers composed of larger surface hoar grains increased in shear strength at a slower rate than did layers of smaller grains. Age of the surface hoar layer was a statistically significant variable. Implications of layer age were not discussed by the authors, nor were changes in strengthening rates compared to the age of the layer.

Spatial and Temporal Variability and Avalanche Forecasting

The amount of variability in shear strength and stability results influences the reliability of extrapolation and predictions made using the data. Because avalanche forecasting is spatial in nature (extrapolating information from the point of observation to the area of interest) the spatial structure of the variability is of interest. If the stability data are autocorrelated, samples placed within the correlation distance under-represent the potential variability of slope stability. Quantifying typical correlation lengths of stability results could improve prediction at distances less than the correlation length, and help space stability tests to represent better the variability of point stability.

All studies of spatial variability of stability have examined the variability within the results, but have drawn different conclusions. Some studies have found that only a few test results can represent the overall slope stability (Jamieson 1995; Jamieson and Johnston 1993) and that there were regions of weaker or stronger snow associated with terrain features (Campbell 2004). Other studies have shown that the stability test used had considerable variation across the study sites, and results were not always representative (Landry 2002; Landry et al. 2004). Only two studies have quantified the spatial structure of the results, one using trend surfaces (Kronholm 2004), and the other autocorrelation along transects (Conway and Abrahamson 1988). My first research question focused on describing the spatial structures of strength and stability indices on a single day. This included looking for areas that were weaker or stronger, quantifying any slope-scale trends across the site, and determining autocorrelation within the test results.

Studies have suggested that spatial variability changes through time, and suggested some potential mechanisms driving the change (Birkeland and Landry 2002).

This was the focus of my second and third research questions: does spatial variability change through time, and can the changes be related to other changes in the snowpack? In exploring the spatial structure of stability, I planned to collect data in a manner that would allow me to examine the changes through time.

CHAPTER 3

METHODOLOGY

Field Methods

Site Selection

This study used three field sites in the mountains of south central Montana (Figure 3). The study sites fall within the intermountain avalanche climate zone (Mock and Birkeland, 2000). Intermountain avalanche climates exhibit characteristics between the moderate temperatures, dense snowfall and deep snowpacks of maritime climates and the low temperatures, and shallower, low-density snowpacks of continental climates (Mock and Birkeland, 2000). Intermountain climates exhibit a variety of avalanche and snowpack conditions, including persistent weak layers (Tremper, 2001).

Two of the sites had been used in previous research (Birkeland and Landry 2002; Birkeland et al. 2004; Landry et al. 2004). Several other sites were prepared, but the snowpack never developed persistent weak layers in the winters I conducted fieldwork.

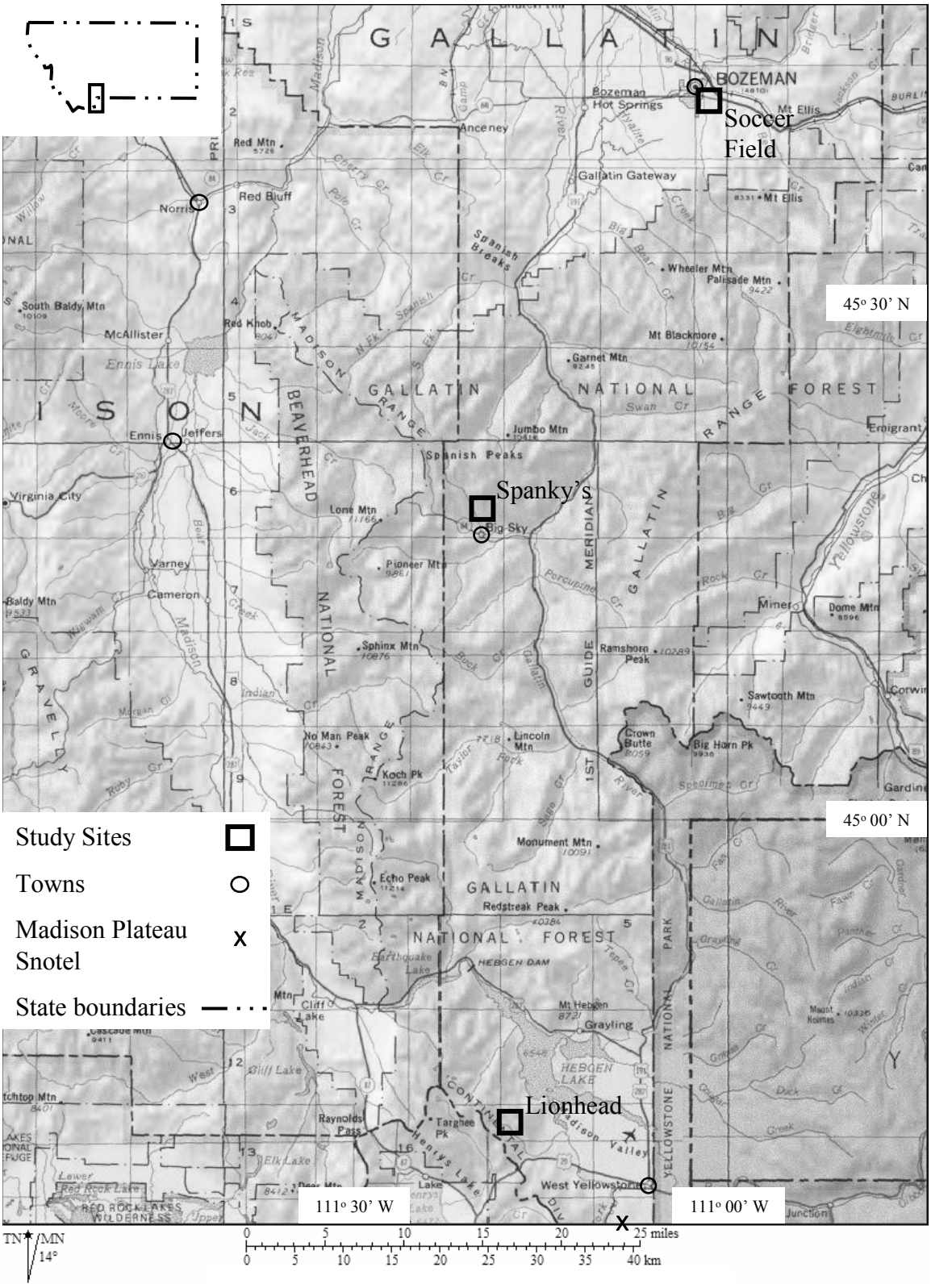

Figure 3. Map of the study site region (base map from National Geographic TOPO!).

Site selection considered uniformity of slope, slope angle, substrate, potential wind exposure, and avalanche safety. The slopes needed to be planar, with as little difference in slope angle and aspect as possible. Slight variations were unavoidable because the slopes were natural, but change was less than 5^{o} in angle or aspect. The sites were selected to minimize differences in vegetation or substrate. The sites were placed in mid-slope forest clearings to minimize wind redistribution of the snow.

The sites had slope angles between 25° and 30°, so creep was similar to an avalanche starting-zone but the slope would be unlikely to avalanche. The sites could not be too hazardous, because I hoped to sample when the snowpack stability was low. The Lionhead site proved to be well sited when avalanche debris ran within 2 m of the site.

Field Site Descriptions

Among the goals of the 2003-2004 field season was the sampling of a flat, uniform site. Heavy snowfall at the end of December 2003 provided a field site in Bozeman, MT. At the end of 2003, we fenced off a portion of the soccer fields at Montana State University and established a site within walking distance of the field crew's homes.

The Soccer Field (Figure 4) site was located on the Montana State University campus on a level, grass playing field at an elevation of 1480 m (45° 39.8' N 111° 02.8' W, Figure 5). No obstructions or large objects were within 20 m of the site (Figure 4). A weather station was located within 100 m of the site (Figure 5), and that weather data incorporated in the analysis (Western Regional Climate Center 2004).

Figure 4. Photo mosaic of the Soccer Field, taken during the sampling of Plot 3.

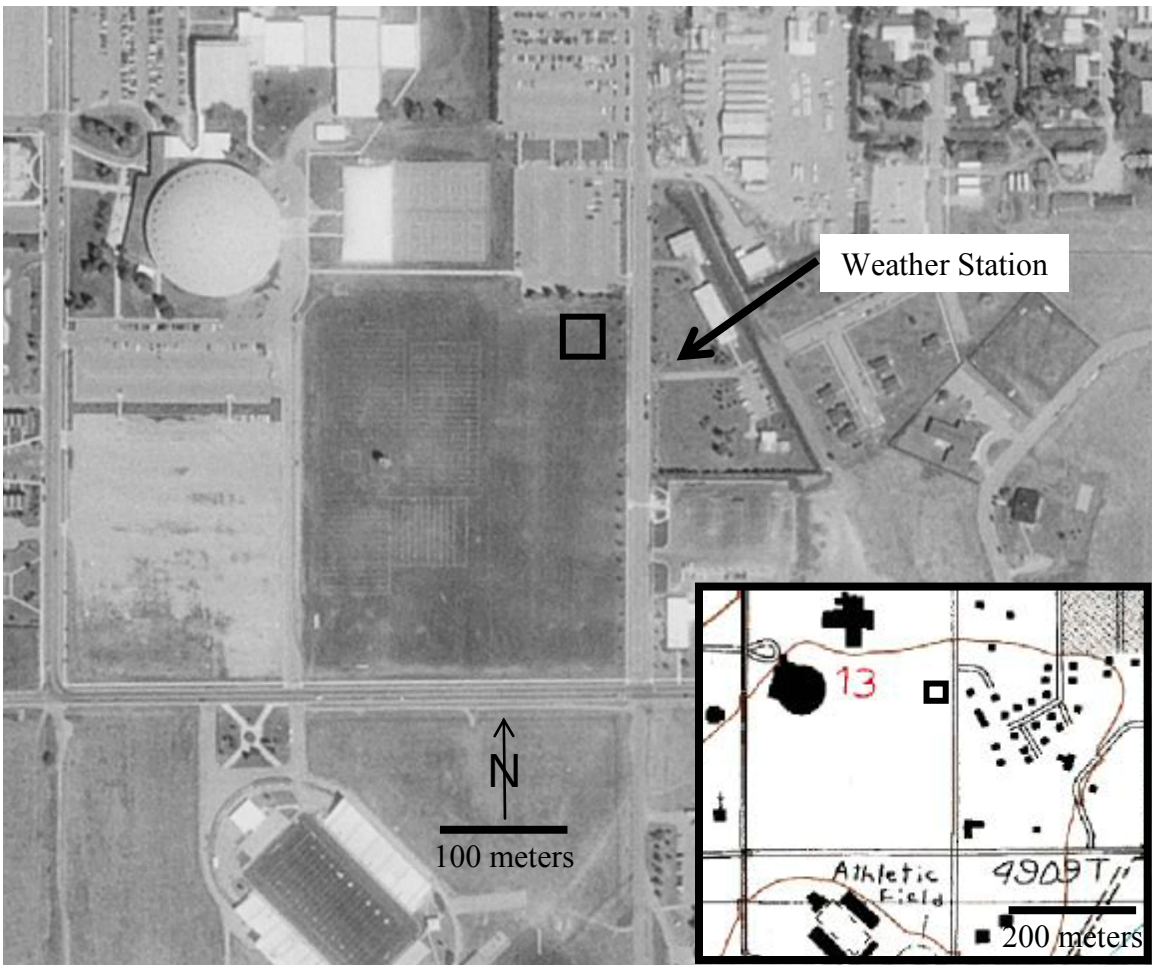

Figure 5. Air photo and topographic map of the Soccer Field Site. The site location is indicated by the square. Contour interval is 6.5 m.

The Spanky's site is 3.5 km north of Big Sky, Montana (45° 19.3' N 111° 22.7' W, Figure 6). The site is in a wind-sheltered, grassy opening in the forest with an east-northeast aspect at an elevation of 2640 m. The average slope angle is 27° and varies less than 5°. Vegetation ranges from grasses and forbs to shrubs 0.4 m high. When sampled, the weak layer was more than 1 m above the ground, so vegetation and substrate were unlikely to have influenced the weak layer. There were several 20 m tall trees approximately 20 m upslope from the site, and the southern edge of the clearing was approximately 20 m south of the site (Figure 7). Weather data used in the analysis was obtained from The Yellowstone Club (Leonard 2004), 5 km south of the field site.

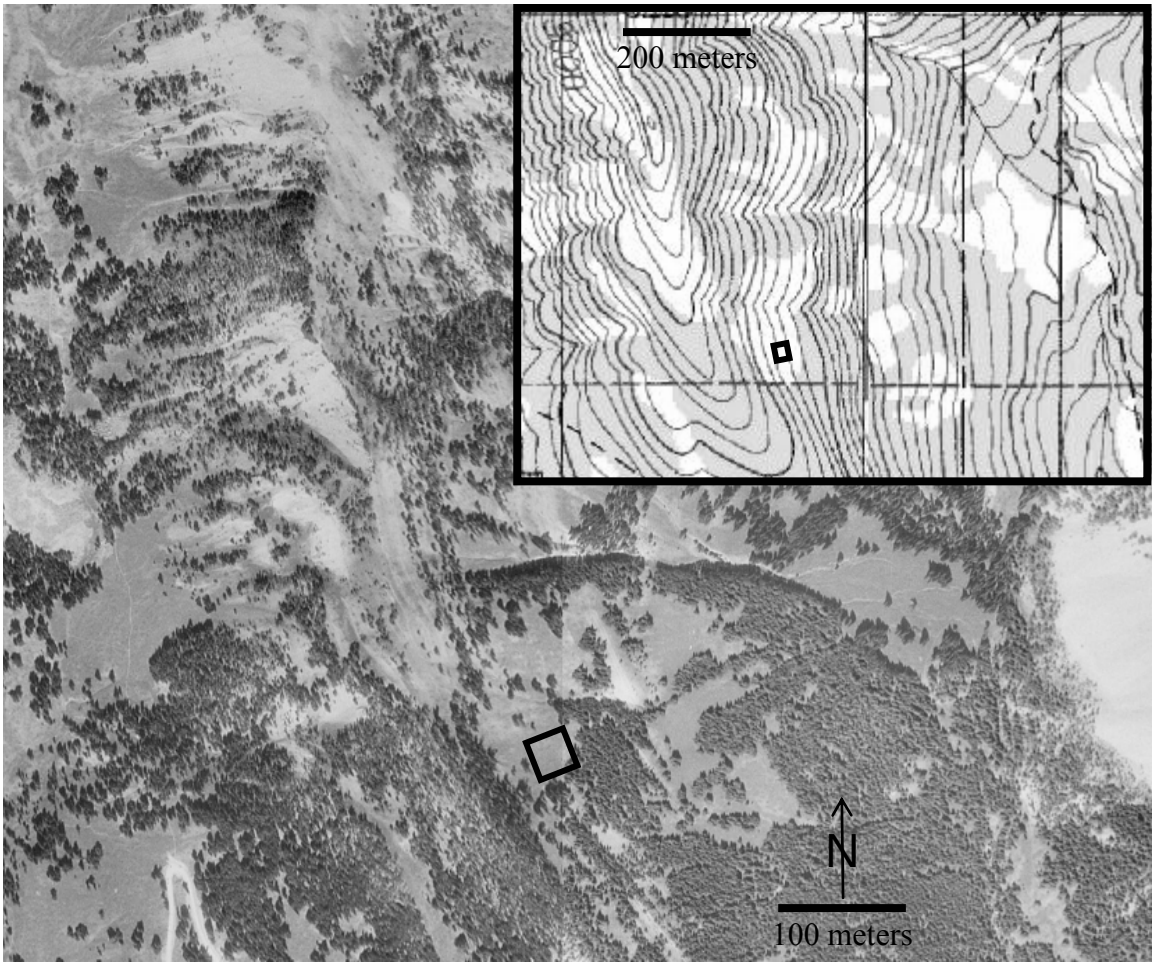

Figure 6. Air photo and topographic map of the Spanky's Site. The site location is indicated by the square. Contour interval is 13 m.

Figure 7. Photo of the Spanky's site, taken during sampling of Plot 3.

The Lionhead site is located 17 km west of West Yellowstone, Montana, on the Idaho-Montana border (44° 42.2' N 111° 17.6' W, Figure 8). The site is in a clearing at the base of a glade, at an elevation of 2340 m with a northeast aspect. The average slope angle is 27° with 6° of variation across the site. The Lionhead site had more shrubs than the Spanky's site, but the shrubs were no taller. Again, the weak layer was more than 1 m above the ground when sampled and should have been uninfluenced by the shrubs. The closest tree was 15 m tall, and located 2 m below the lower left corner of the site (Figure 9). Trees on the slopes 30 m above the site provided some shelter from potential avalanches on steeper slopes above. Weather data used in the analysis came from the Madison Plateau Snotel site (Natural Resources Conservation Service 2004), 25 km east of the Lionhead site.

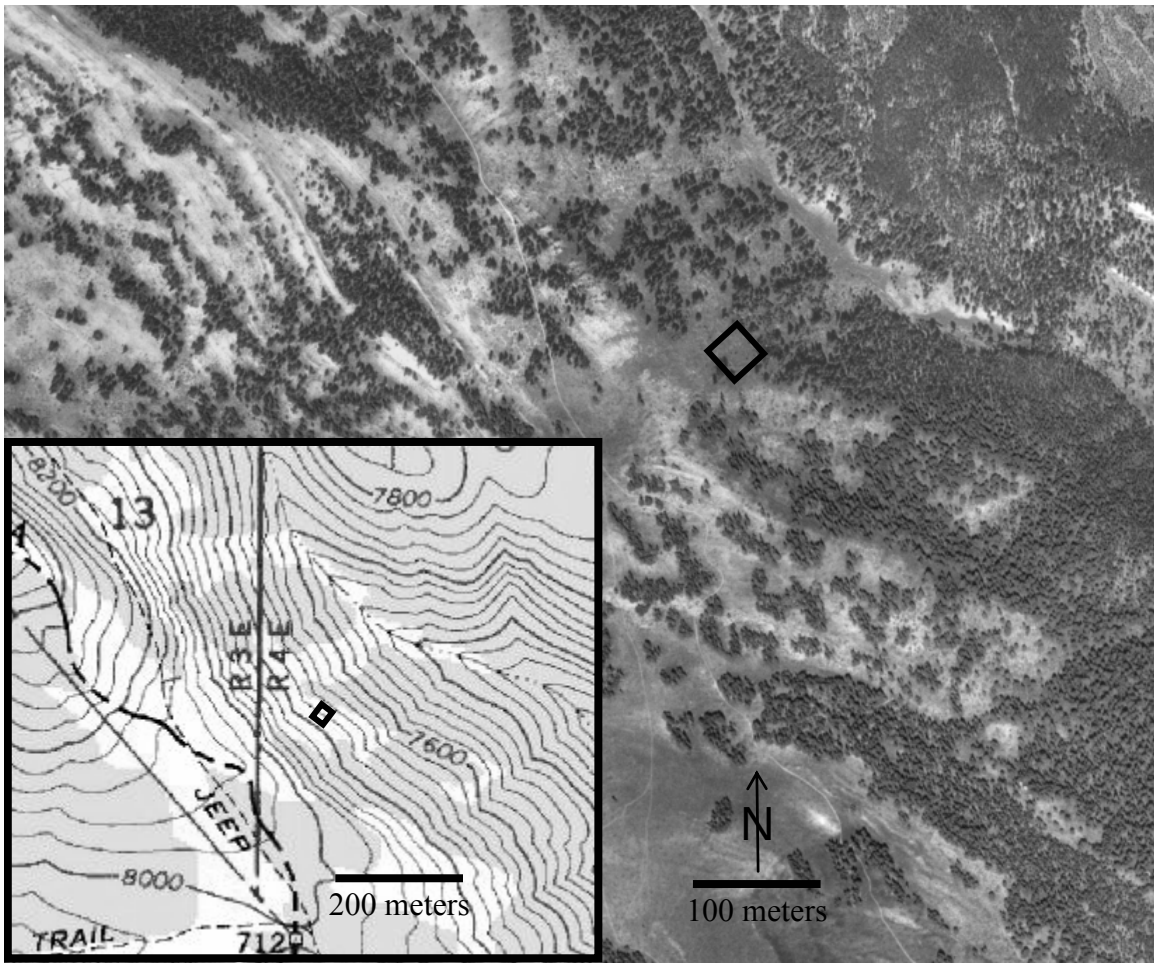

Figure 8. Air photo and topographic map of the Lionhead site. The site location is indicated by the square. Contour interval is 13 m.

Figure 9. Photo mosaic of the Lionhead site, taken during the sampling of Plot 4.

Site Layout

Each site consisted of four 14 m x 14 m plots in two rows, separated by 3 m wide 'alleys,' for a total of 961 m^2 (Figure 10). Layout of the sites in the summer of 2003 allowed for sites to be located minimizing across-plot differences in substrate, vegetation, or angle. Plot corners were marked by rebar, with 2 x 4 x 100 cm wooden slats wired on as markers. This facilitated accurately locating the plots in winter.

Site layout began by establishing the top site boundary using a measuring tape stretched horizontally across the slope, and rebar placed to mark the top four plot corners. Layout proceeded down-slope, using right triangles to insure square plots. Where variations in slope shape (slight concavities or convexities) distorted the plots, the distortion within plots was minimized by adjusting the width of the alleys.

Sampling Array

The alleys, sampled first, provided a measure of the sites' "initial conditions," and tested whether or not the plots began with generally similar characteristics. Any site-wide trends could be identified from the samples. The alley samples consisted of 48 shear frame tests in 12 pits of four tests, with test centers 50 cm apart (Figure 10).

Sampling the first plot occurred within a few days of the alley sample. Five main pits and four smaller pits grouped the shear frame tests. The five main pits allowed for pit-to-pit and pit-to-plot comparisons (Birkeland and Landry 2002). The smaller pits were included to improve variogram calculations. Test centers were located 0.5 m apart.

A full manual study profile (Greene et al. 2004) was conducted for each plot adjacent to Pit 1. In addition to the stability tests, profiles were collected with the SnowMicroPen (SMP), a high-resolution penetrometer. Interpretation of the SMP signal

provides detailed stratigraphic information (Johnson and Schneebeli 1999; Schneebeli et al. 1999; Pielmeier and Schneebeli 2003; Kronholm 2004; Birkeland et al. 2004).

Optimization of the sampling array became an involved process. Sampling of a plot had to be completed within one day to minimize temporal change, which placed a constraint on the number of shear frame tests that could be conducted. Preliminary studies conducted in the winter of 2000-2001 by Landry (2002), Birkeland and Landry (2002), the winter of 2001-2002 by myself, and Kronholm (2004) in Switzerland, indicated that five or six pits of 10-12 tests for a total of 60 tests per plot seemed a

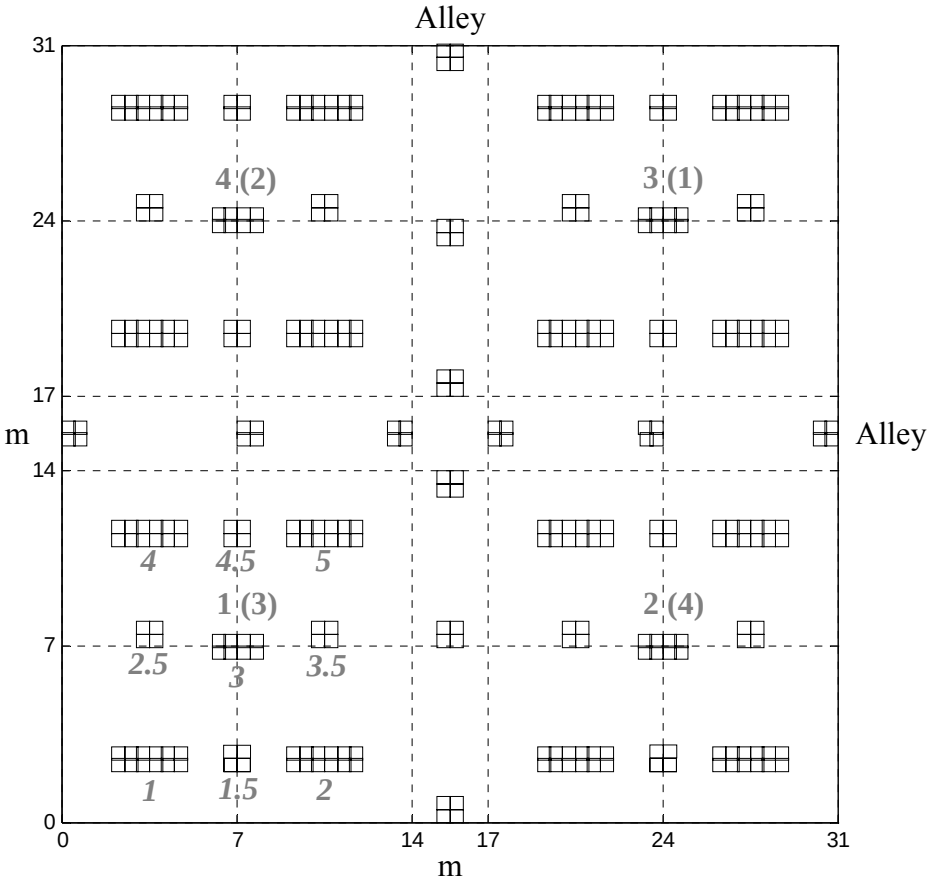

Figure 10. Location of stability tests for the alley and all four plots. Plot numbers for the Soccer Field and Spanky's are indicated in gray and in parentheses for Lionhead. The five main and four smaller pits are numbered in italics for Plot 1

realistic undertaking. After sampling the Soccer Field, I found that more tests were possible to complete and would improve the calculation of the variograms. Four smaller pits were added, bringing the total number of shear frame tests to 72.

To compare and refine the sampling array, I wrote several MATLAB programs. Given a set of coordinates to sample from, the program would sample a pre-defined matrix, and then calculate variograms from the sampled values. Variograms from different coordinate sets could be compared by sampling the same pre-defined matrix. The performance of a coordinate set could be assessed using several pre-defined matrices, which could be varied by changing the range of values, the amount of random noise, or the autocorrelation between values.

Shear Frame Test

The shear frame test measures the shear strength of specific weak layers or interfaces within the snowpack (Greene et al. 2004). Shear frames allow specific layers to be measured, where most other stability tests can test only the weakest layer in the snowpack. A thin metal frame of known area is placed into the layer just above the layer of interest, then a force gage attached. A rapid pull on the gage produces brittle fracturing in the weak layer. The stability index is calculated by dividing the maximum force recorded by the gage by the area of the frame.

When performed by skilled operators using similar methods, there is little inter-operator difference (Jamieson and Johnston 2001). Jamieson and Johnston (2001) report mean coefficients of variation of 18% for shear frames on sloping sites. To maximize my ability to compare results among plots, the same operator conducted all the shear frame tests at a site.

The tests began with the excavation of a vertical wall at the down-slope side of the pit. After identifying the target weak layer, the slab was carefully removed to leave about 20 cm of snow above the weak layer. Test centers were located at 50 cm intervals using holes from the previously measured SMP profiles. The operator prepared the final bench by carefully removing all but 5-10 cm of the slab.

There are two common sizes for shear frames, 0.01 m^2 and 0.025 m^2 (Greene et al. 2004). The smaller frames are used to test the strength of relatively strong weak layers. In my study, the weak layer was not strong enough to require the use of the small frame, so the 0.025 m^2 frame was used for all the sampling days.

The frame was inserted carefully until the bottom edge of the frame was 2-5 mm above and parallel to the weak layer (Jamieson and Johnston 2001). The weak layer tracked at the Lionhead site was quite fragile, so the frame could not be placed as closely as recommended, and was inserted 5-10 mm above the weak layer. Any slab projecting above the frame was removed, and then the frame isolated by carefully cutting around it with a thin putty knife. The recording force gage was attached to chains at the front of the isolated frame (Figure 11). The operator applied force parallel to the layer, and loaded the frame to test failure within one second. The rapid loading produced brittle fracturing within the weak layer.

If the operator felt that test was faulty, most often because of improper preparation, he placed a second test as closely as possible to the first, and recorded that value. A test result was not discarded because the result seemed too strong or weak.

Figure 11. Kalle Kronholm conducting a shear frame test. The frame has just failed, and the force at failure is being read.

Two force gages were used, one calibrated in 0.05 kg increments from 0.2 to 5 kg of force, the other calibrated in 0.2 kg increments from 2 to 20 kg of force. The test precision decreased with the use of the 2 to 20 kg gage.

Shear strength (Pa) for each test (T_{250}) was calculated by dividing the force in kilograms recorded at failure (F_{fail}) by the frame area (T_{frame}), in square meters, so that,

$$T_{250} = \frac{F_{fail} g}{A_{frame}}$$

where g is the acceleration due to gravity. Multiplying T_{250} by 0.65 provided a value of shear strength independent of the frame area, T_{∞} (Föhn 1987b). To calculate the stability index (S), T_{∞} was divided by the shear stress of the slab,

$$S = \frac{T_{\infty}}{\rho g h \sin(\alpha)}$$

where ρ was slab density (kg m^{-3}), h slab thickness measured slope normal (m), and α the slope angle (Landry et al. 2001).

Data Analysis

Analysis of results from each plot proceeded in a similar fashion. Initially, I recorded results in notebooks. Halfway through the field season, I began using personal digital assistants (PDAs) for data recording. The PDAs ran spreadsheet software, allowing me to assess data quality in the field and reduce the time required for data entry and pre-processing.

Statistical Measures of the Plots

Two statistical descriptors described the plot-wide characteristics: the median and quartile coefficient of variation (QCV). The QCV is a robust measure of the relative spread of the data, and is defined as:

$$QCV = \frac{(Q3 - Q1)}{(Q3 + Q1)}$$

where *Q1* and *Q3* are the first and third quartiles, respectively. The QCV is similar to, but not equivalent to, a parametric coefficient of variation (Spiegel and Stephens 1999). The median and the QCV quantify the central tendency and relative spread of the plots. Non-parametric statistics were used because the distributions of shear strength were not normal for Spanky's Plots 2, 3, and 4, and Lionhead Plot 3. The data were not transformed because no single, simple transformation could be used across all the data sets, and the use of a robust variogram reduced the need for normally distributed results.

Pit-to-Plot Analysis

A semi-spatial method to analyze the spatial variability of a plot was the pit-to-plot ratio (Birkeland and Landry 2002; Landry 2002; Landry et al. 2004). Pit-to-plot ratios characterized the ability of a single pit to represent the results of the entire plot, and therefore indicated whether a pit could be reliably extrapolated across a plot. A pit was "representative" of the plot if there was no statistically significant difference ($p > 0.05$) between the results in a pit and the results of all the tests for a plot.

The nonparametric Wilcoxon Test, identical to the Mann-Whitney test, was used to compare the individual pits to the pooled results (Neter et al. 1996). The Wilcoxon Test assumes only that the two data distributions are identical, but not necessarily normal. At each of the sites, the distribution of test results of at least one plot was not normal. The Wilcoxon test is less powerful than a standard t-test if the distribution of results is normal, so pits showing some evidence of being non-representative ($0.05 < p < 0.1$) were noted. To increase the conservativeness of the test, results from all the main pits were pooled, and individual pits compared to the pooled result (Landry 2002; Landry et al. 2004).

If more pits were statistically representative of the plot, the pit-to-plot ratio was high and the plot was less spatially variable. Lower pit-to-plot ratios indicated fewer representative pits and greater spatial variability. A pit was representative of the plot if there was no statistically significant difference between the results in a pit and the results of all the tests for a plot. Boxplots were used to facilitate analysis, with whiskers extending to the 0.05 and 0.95 quantiles, the box indicating the 0.25 and 0.75 quantiles,

and the median indicated by a dotted line. Individual values smaller than 0.05 quantile or larger than 0.95 quantile were indicated by circles (for example, Figure 21, p. 54).

Pit-to-plot ratios are not spatial measures, because the locations of the tests are not explicitly considered in the analysis. The location of the pits within the plot, or the location of the test within the pit, does not matter. Pit-to-plot ratios do provide a measure of how representative of the overall results a group of measures is, and whether the results from one pit could be reliably extrapolated across the distances of a plot.

Geostatistical Analysis

Spatial correlation within the data was broken into two components, so that the value at a location **s** was the sum of a large scale trend *t(s)* and randomly varying residuals *ε(s)*,

$$Z(\mathbf{s}) = t(s) + \varepsilon(s)$$

Trend surface analysis was used to analyze the large-scale linear trend, t(s), and variograms were used to analyze the correlation within the residuals, ε(s).

Linear trend surfaces described any plot-wide trends, and variograms measured spatial autocorrelation among the tests (Cressie 1993). Trend surfaces used regression on the measurement locations as predictor variables. The large-scale linear trend, *t(s)*, was composed of slope in the X and Y directions, $a_2(x)$ and $a_3(y)$ respectively, and the intercept, a_1, such that

$$t(s) = a_1 + a_2(x) + a_3(y).$$

The trend was removed if it was significant ($p < 0.05$) and explained more than 10% of the variability in the data ($R^2 > 0.10$). The residuals, *ε(s)*, were used in the subsequent variogram analysis. If the trend explained less than 10% of the variability, it

had no discernable effect on the subsequent variogram analysis. The trend was not removed and the variogram analysis used the raw data

Using linear trends does not imply that trends present in the snowpack were actually linear. The physical process could be far more complicated. Trend surfaces can represent any longer-range trends within the data, and can be used to filter the trend before analysis by other methods (Webster and Oliver 2001). Linear trends were relatively easy to interpret and adequately described plot-wide trends present in the data. I did fit higher order trends to several of the data sets, but the explanatory power and fit of the higher order surfaces never justified their use.

Variograms quantify the spatial autocorrelation within a data set by calculating the average variance between data points over distance (Webster and Oliver 2001). The location and result of each measurement was explicitly included in the analysis. Only recently have variograms been applied to shear strength and stability data (e. g. Kronholm 2004), although variograms have been applied to other snowpack properties such as depth or snow water equivalent (Blöschl 1999).

Experimental variograms, calculated from measured data, are an accepted way to analyze continuous data measured at scattered locations (Blöschl 1999; Deutsch and Journel 1998; Myers 1997; O'Sullivan and Unwin 2003; Webster and Oliver 1990; Webster and Oliver 2001). I did not fit any model variograms to the strength or stability data in this study, because model variograms offered poor fits to the data.

Like most statistical methods, variogram analysis makes assumptions about the data and the underlying process. One of the first assumptions is that that the process of interest is spatially continuous across the data set. A layer within the snowpack is

continuous at the scales of this study, so the assumption is valid (Colbeck 1991; Kronholm 2004).

The data are also assumed to come from a stationary random process. Stationarity means that the mean must be the same across the plot, or that no site-wide trends influence the results. Fitting trend surfaces to the data and using the residual is the accepted method for assuring that this assumption is not violated.

Many processes interacting in complex and non-linear manners influence the characteristics of a physical process, such as shear strength of a weak layer. Although the processes are highly deterministic, they cannot yet be fully quantified. The resulting characteristics can be treated as statistically random (Phillips 1999; Webster and Oliver 2001), the second half of the assumption of a stationary random process. The assumption does not imply that the process or results are random, only that the statistical model is valid (Webster 2000). The classic example is that of rolling dice (Webster and Oliver 2001). Conceptually, the position of the die could be measured, the forces acting on the die quantified, and the outcome calculated. Practically, die rolls are treated as a random process, with the result drawn with equal probability from the set [1, 2, 3, 4, 5, 6].

Likewise, the result of a shear frame test could be drawn from a set of values with a probability distribution. Each test could have a different set and probability distribution. Tests closer together probably have a more similar set and distribution than do tests located farther apart. We can observe spatial autocorrelation in many processes, so we assume that the result of the processes are similarly autocorrelated. The assumed correlation leads to the assumption that the difference between data points depends only

on the distance between them, and not the absolute position. Non-spatial statistics assume that the difference between data points is not related to distance.

The classic experimental variogram, *γ(h)*, was estimated from the data by

$$\gamma(h) = \frac{1}{2N(h)} \sum_{N(h)} \left(Z(s_i) - Z(s_j)\right)^2$$

where $Z(s_i)$ and $Z(s_j)$ are the values at locations separated by h, and $N(h)$ is the number of point-pairs separated at that distance (Cressie 1993). The classic variogram was sensitive to outliers and non-normal distributions, leading to high semivariance and little indication of spatial correlation.

For this project, the Cressie and Hawkins (Cressie 1993) robust variogram provided better results because outliers are weighted less weight (see p. 45), and the results were less influenced by non-normal distributions of shear strength. The semivariance, *γ(h)*, was defined as

$$\bar{\gamma}(h) = \frac{\left(\frac{1}{|N(h)|} \sum_{N(h)} |Z(s_i) - Z(s_j)|^{1/2} \right)^4}{2\left(0.457 + \frac{0.494}{|N(h)|}\right)}$$

where the terms are the same as described previously (Cressie 1993). The robust variogram scales the point-pair differences to resemble a Gaussian distribution, then re-scales the semivariance to the original values. The Cressie and Hawkins robust variogram was selected after comparing the classical and several robust variogram results from several of the plots (Lark 2000).

Several components are important for interpreting the variogram (Figure 12). The sill occurs where the semivariance "levels off." The leveling typically corresponds to the

overall variance. The range is the distance that the variogram reaches the sill, and is indicative of the spatial scale of the process (Blöschl 1999). At distances larger than the range, there is no longer correlation.

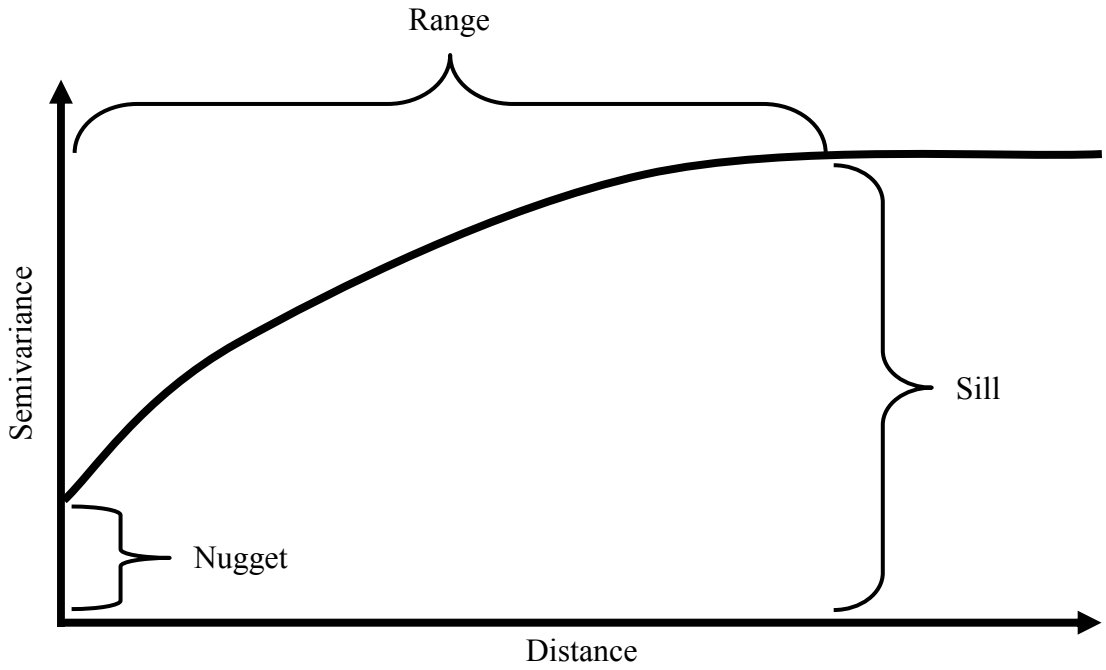

Figure 12. Variogram example, with important elements labeled.

The nugget is the difference between zero and the semivariance at the shortest lag, where the variogram intersects the y-axis. The nugget is variance that cannot be resolved by the measured data (Myers 1997). Nuggets may have several causes, ranging from lack of data at shorter distances, to inherent variability at scales shorter than the measurements (Burrough 1983). The nugget ratio is the nugget compared to overall variance; higher nugget ratios are indicative of greater fundamental error in the measurements, or variability that the measurements cannot resolve (Blöschl 1999; Myers 1997).

Variogram models did no fit the experimental data well. Because of this I estimated the nugget by fitting a line through the semivariance of the two smallest bins

(Figure 13). The ratio between the extrapolated nugget and the overall variance was used as an estimate of the nugget ratio. I used the term "nugget ratio estimate" to differentiate it from a true nugget ratio. The range was estimated from the distance to the largest peak in semivariance, or the distance at which the experimental variograms "leveled off."

In this project, the variograms were plotted as circles of varying gray tones, keyed to the number of point-pairs within that bin (Figure 13). In the analysis, this allowed less weight to be given to bins with many or few point-pairs if they seemed anomalous. Light gray (20%) circles indicate bins with less than 50 point-pairs, darker gray (40%) bins with 51-100 point-pairs, darker gray (60%) bins with 101-150 point-pairs, and darkest gray (80%) bins with more than 151 point-pairs. The gray divisions correspond, roughly, to the distribution of point-pairs per bin using a lag distance of 0.6 m (median 83, interquartile range of 55 to 130 point-pairs). Differences in tone are easily identified and differentiated (Tufte 1983). To aid in interpretation, a light line connects the circles, but does not indicate any fitted model. A dashed horizontal line indicates the plot-wide variance.

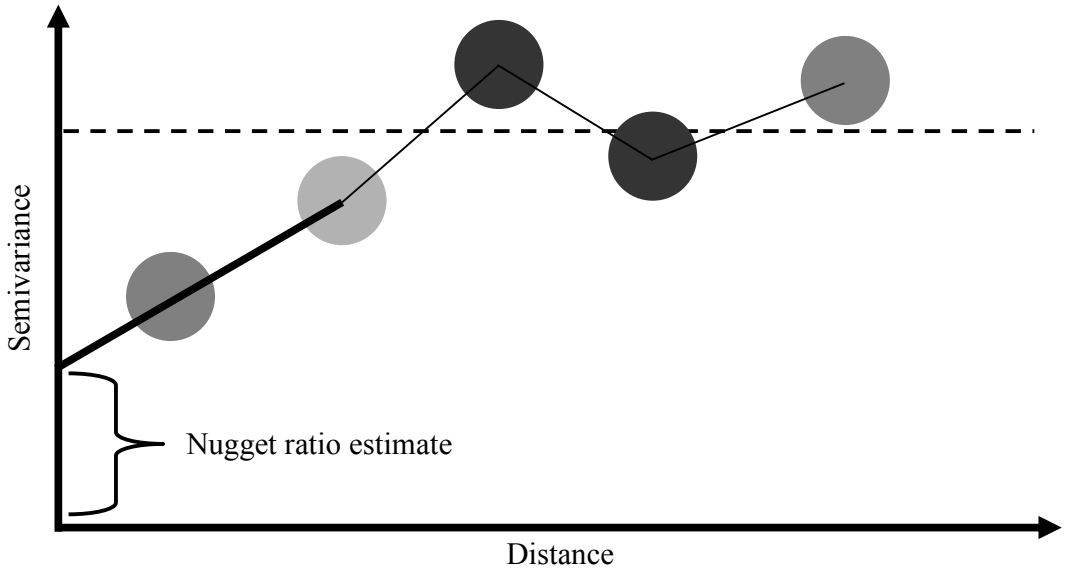

Figure 13. An example variogram, plotted as for this project. Light gray (20%) circles indicate bins with less than 50 point-pairs, darker gray (40%) bins with 51-100 point-pairs, dark gray (60%) bins with 101-150 point- pairs, and darkest gray (80%) bins with more than 151 point-pairs. To estimate the nugget ratio, a line was fit through the two smallest bins (heavy black), and compared to the overall variance (dashed line).

Temporal change in shear strength was assessed by comparing variograms of a plot with those of the previously sampled plot. Comparing variograms required the assumption that the individual plots began from similar initial conditions. Sampling the alleys provided indications of the initial conditions within the plots. With such an assumption, differences in variograms could be attributed to temporal change rather than spatial differences.

Assessing Divergence and Convergence

The temporal trends were measured by the differences between measures of a plot and the one sampled prior. Increasing spatial variability between plots was a sign of divergence (Phillips 1999). Indicators of divergence would be decreases in the range of the variograms, increases in the nugget ratio estimate, decreases in the pit-to-plot ratios (few representative pits), and increases in the QCV. Increasing ranges, pit-to-plot ratios, and decreasing QCV would indicate convergence and increasing spatial uniformity. An increase in the range was used as an indication of increasing spatial autocorrelation. An increase in the pit-to-plot ratios indicated more pits representative of the second plot, and therefore increasing spatial uniformity. A decrease in the QCV, while not a spatial measure, indicated a decrease in the relative range of shear strength values measured.

I explored and ultimately rejected other methods for assessing spatial variability and temporal trends. Most methods were not applicable to this study because they relied upon measuring or estimating temporal change at fixed locations. One method was to

randomly pick a series of point pairs and measure the difference between them through time (Phillips 1995). An increase in the mean difference between the points indicated divergence while a decrease in mean difference indicated convergence. Because stability tests are destructive, different plots had to be used, and prevented the application of the technique. Space-time geostatistics also relied upon measurements at the same location or general vicinity.

Phillips (2000) used changes in stratigraphic soil columns to estimate changes in Kolmogorov entropy, which were then related to temporal trends. This method seemed promising, because detailed snow profiles are commonly collected and the estimation of Kolmogorov entropy was easily calculated. The method measured convergence or divergence in the slope normal direction, and a single profile provided no spatial information. I had hoped to extend the entropy estimates to SMP profiles, but the entropy estimates will not be practical until layer delineation can be done rapidly.

Examples of Variogram Analysis

A simulated data set (Figure 14) showed an obvious trend of decreasing values from the upper left to the lower right. One hundred twenty one regularly spaced measurements were taken from this data, at the locations indicated in white. There was a significant linear trend ($p < 0.001$) in the sampled data that overwhelmed any indications of correlation at longer distances (Figure 15). With the trend removed, the variogram had a range of 15 units, and suggested that another, more closely spaced sample would indicate greater correlation (Figure 15).

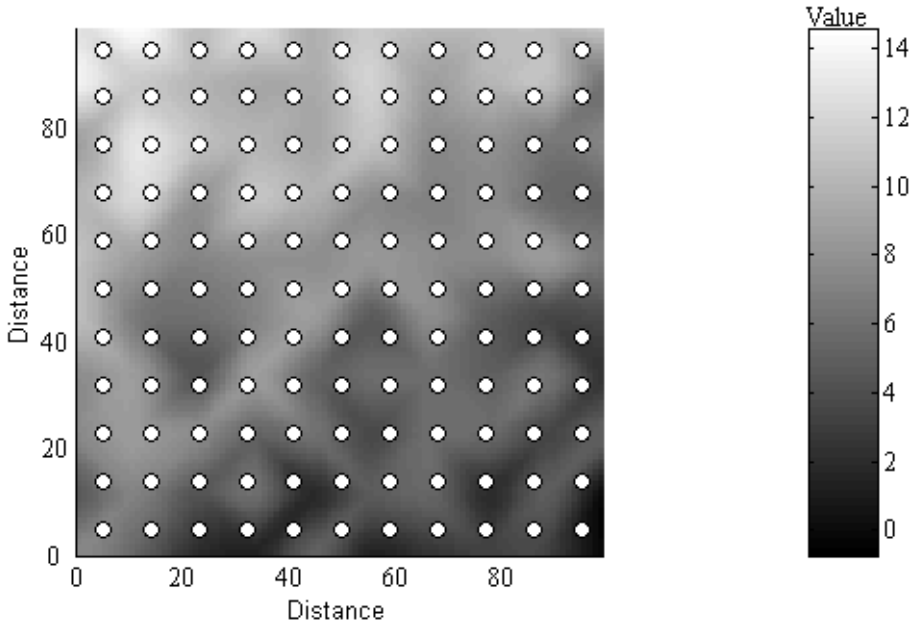

Figure 14. An example data set, with a trend from lower right to upper left. White circles indicate the regularly spaced sample locations.

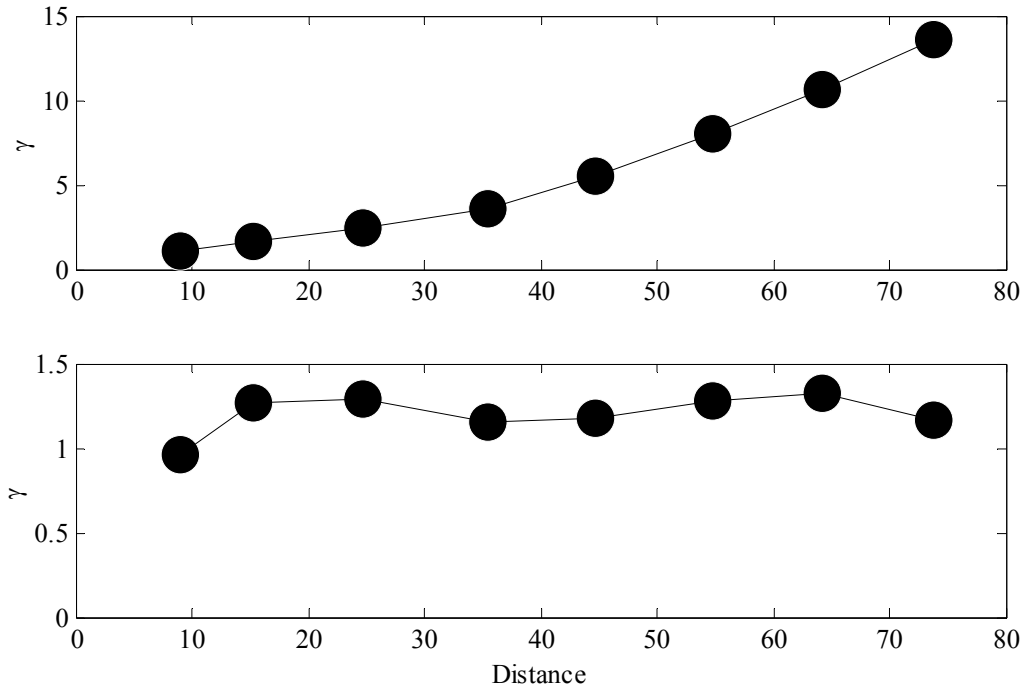

Figure 15. Variograms of the sampled data values including the linear trend (top), and after the linear trend was removed (bottom).

The influence of removing extreme values from the data set is evident using the Spanky's Plot 2 data (Figure 16). Six test results, the 3 strongest and the three weakest, were removed from the data set. The number of point pairs was reduced by 25%, or almost 500 point pairs. The semivariance decreased markedly, but the pattern of the variogram remained similar. In this study, no outliers were removed because the interpretation of the variograms was not changed or "improved" by removing only a few outliers. Justifying the removal of data points was complicated by the sample method (only valid results were recorded) and the small sample size.

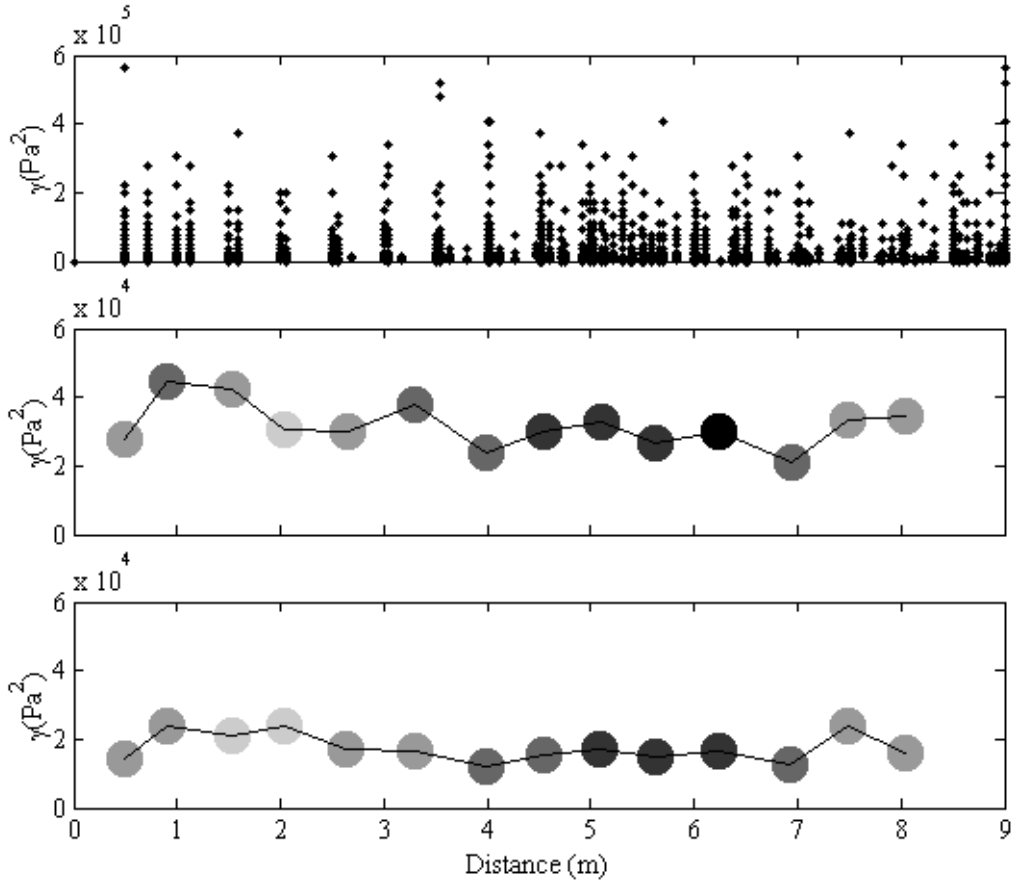

Figure 16. An example of the effect of outliers on the variograms. On top is the variogram cloud. In the middle is a variogram with all point-pairs included (2557 point-pairs), and on the bottom is a variogram with the three highest and lowest values removed (2081 point-pairs). Gray circles indicate the number of point pairs within bins: 20% gray less than 50 point-pairs, 40% gray 51-100 point-pairs, 60% gray 101-150 point- pairs, and 80% gray more than 151 point-pairs.

To demonstrate the effect of different lag distances, Spanky's Plot 1 data were plotted with four different lag distances (Figure 17). The overall variance was reached at 5 m. The two spikes, at 0.6 and 4.1 m, were reduced by using larger lag distances, but at the expense of increasing the nugget ratio. Larger bin widths included more point-pairs.

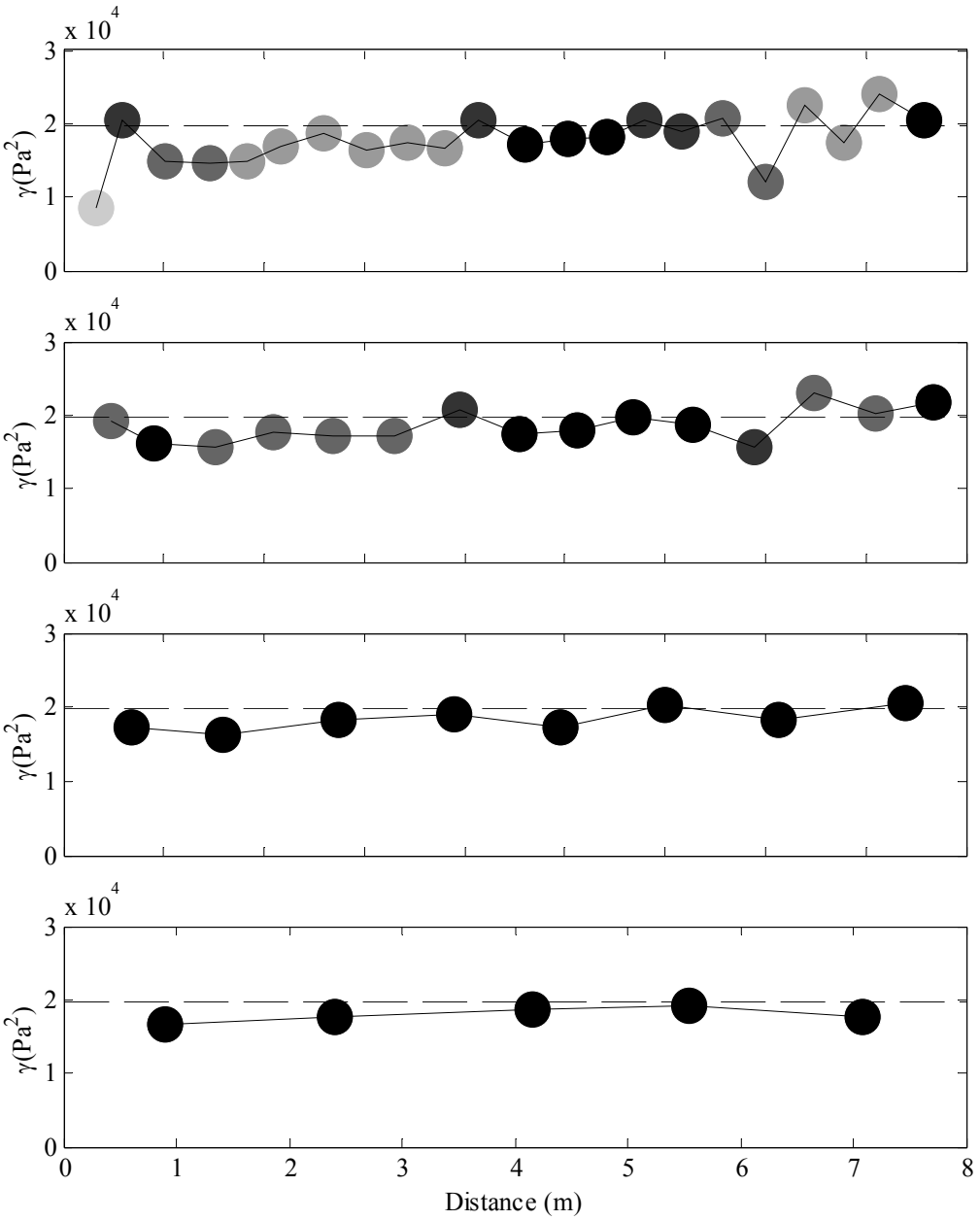

Figure 17. Variograms of Spanky's Plot 1 shear strength, indicating effects of differing bin widths. Bin widths, from top to bottom, are 0.4 m, 0.6 m, 1.1 m, and 1.6 m. Gray circles indicate the number of point-pairs within bins: 20% gray less than 50 point-pairs, 40% gray 51-100 point-pairs, 60% gray 101-150 point-pairs, and 80% gray more than 151 point-pairs.

CHAPTER 4

RESULTS

Soccer Field

Conditions prior to sampling

The Soccer Field snowpack began with small storms in early December 2003 (Figure 18). Several centimeters of snow fell December 4, but melted under warm temperatures December 6 and 7. The remnant snow probably formed the basal ice layers observed in subsequent sampling. Additional snowfall December 8-11 and 14 brought the recorded snow depth to 8 cm. This was followed by a snow-free period of 10 days during which faceted and depth hoar grains developed in the thin snowpack. Snowfall December 25-30, with 20 cm recorded on the 26, buried the faceted layer (Figure 19).

The site was laid out and alleys sampled December 31, 2003, six days after the faceted snow was first buried. At that time, the field crew had not considered conducting stability tests on the flat site. After experimenting with the shear frames, I found that I could get consistent shear frame results on the faceted layer. Sampling of the alleys had progressed too far to conduct the appropriate tests in them, but we were able to use shear frames on all the plots.

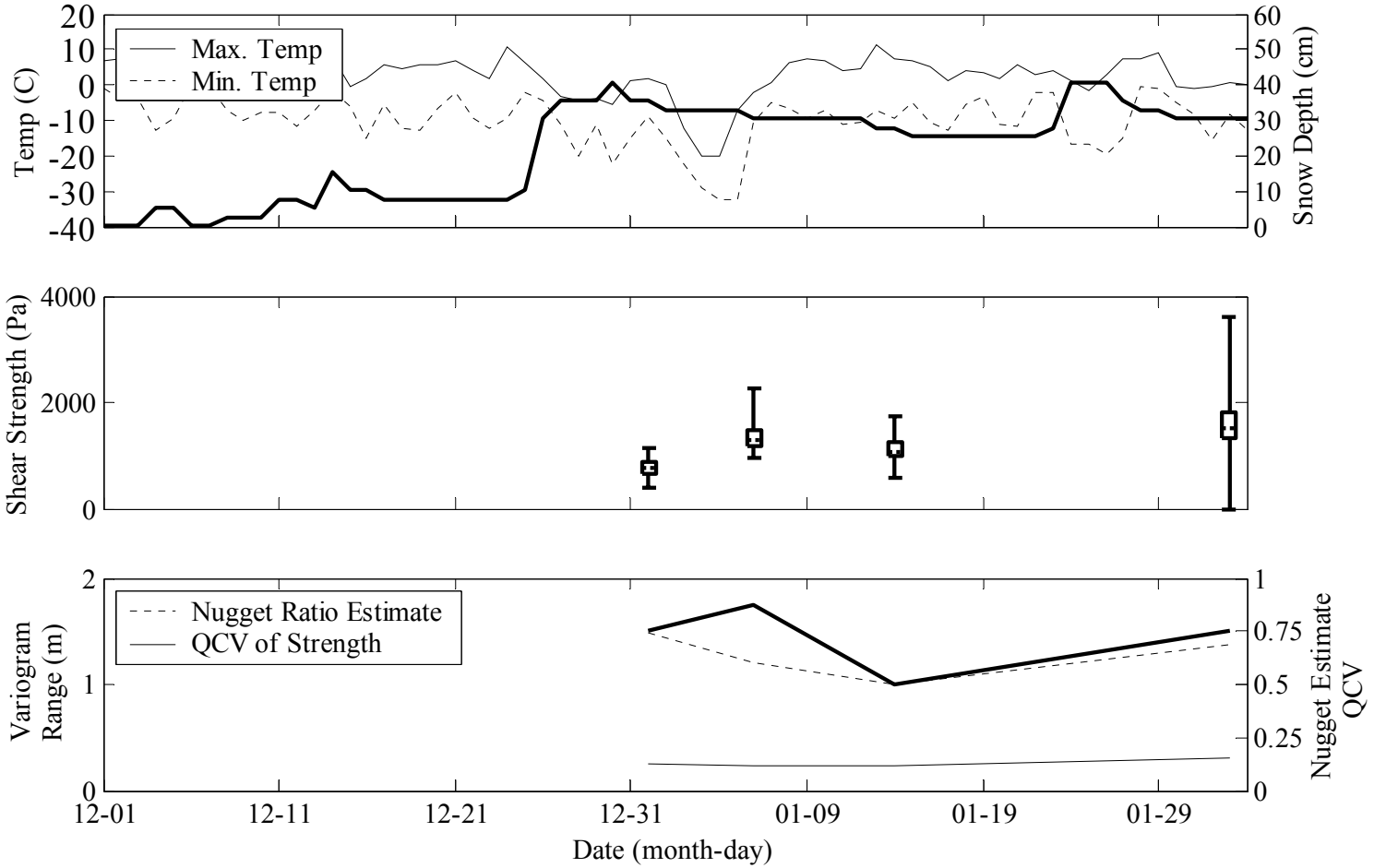

Figure 18. Weather data (top), box plot of shear strength (middle; dotted lines indicate medians, boxes the interquartile range, whiskers extend to 0.05 and 0.95 quantiles), and summaries of the statistical and spatial characteristics (bottom) of the Soccer

Three factors differentiated the Soccer Field from the other two sites. One, stability could not be calculated because there was no gravitational or slope angle component. Second, the Soccer Field was used to refine the sampling strategy. Only the five main pits were sampled: additional pits were not added until analysis of Soccer Field data indicated additional tests were necessary and feasible.

The third factor involved the shear frame test itself. Unlike the buried surface hoar sampled at the other sites, shear frames were not ideal for the facets and depth-hoar interface at the Soccer Field. Inserting the base of the frame an equal distance above the interface could be quite challenging, especially as the slab aged, faceted, and became weaker. Fractures on the depth hoar were often ragged and poor quality (Johnson and Birkeland 2002).

Plot 1

Sampling of Plot 1 occurred on the first day of the New Year, January, 1 2004. Median shear strength was 748 Pa, with a QCV of 0.128 (Table 1; Table 2). Most failures were poor quality (Q3) and quite rough. The shear frames failed near the top of the depth hoar layer (Figure 19).

There was some evidence of a linear trend in the data ($p = 0.06$; Table 3). The variogram (Figure 20) had a nugget ratio estimate of 0.75, almost pure nugget. As indicated by the range, all the variability within the data occurred at distances within the pits, so none of the pit-to-plot ratios were significant (Figure 21).

Table 1. Characteristics of the slab and weak layer for each of the plots at the Soccer Field site. Insufficient slab measurements were made in Plot 1 to calculate QCVs.

	Alley	Plot 1	Plot 2	Plot 3	Plot 4
Median slab thickness (cm)	---	27	24.2	22.8	22
QCV of slab thickness	---	---	0.344	0.349	0.354
Median slab density ($kg\ m^{-3}$)	---	200	181	210	248
QCV of slab density	---	---	0.361	0.340	0.337
Median shear strength (Pa)	---	784	1294	1068	917
QCV of shear strength	---	0.128	0.118	0.115	0.150
Median stability index	---	---	---	---	---
QCV of stability index	---	---	---	---	---

Table 2. Rates of change of slab and plot characteristics between Soccer Field plots.

	Alley and Plot 1	Plots 1 and 2	Plots 2 and 3	Plots 3 and 4
Number of days between:	1	6	9	18
Change in Median Slab Thickness ($cm\ d^{-1}$)	---	-0.5	-0.2	0
Change in Median Slab Density ($kg\ m^{-3}\ d^{-1}$)	---	-3	3	2
Change in Median Shear Strength ($Pa\ d^{-1}$)	---	85	-25	-8
Change in Median Stability (d^{-1})	---	---	---	---
Significance, change in Strength	---	< 0.001	< 0.001	< 0.001
Significance, change in Stability	---	---	---	---

Location Soccer Field, Plot 1
Date 20040101
Time 1030
Observer SL
Aspect 0
Inclination 0

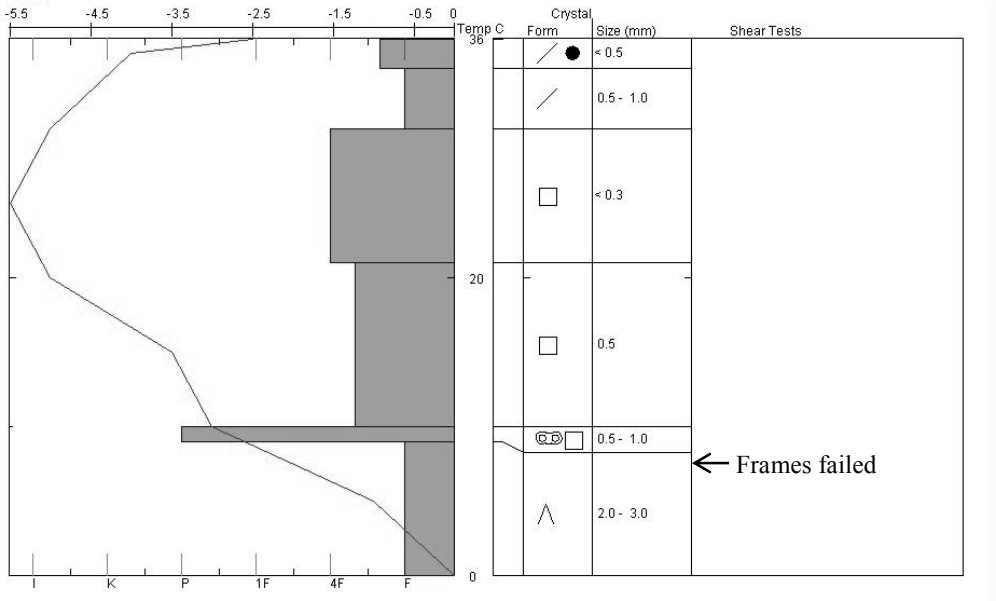

Figure 19. Manual Profile for Soccer Field Plot 1

Table 3. Significance, correlation, and coefficients of linear trends of Soccer Field shear strength.

	p value	R^2	a_1	a_2	a_3
Plot 1	0.060	0.105	0.8033	0.0056	-0.0118
Plot 2	0.328	0.041	1.2110	0.0139	0.0071
Plot 3	0.190	0.061	1.2359	-0.0135	-0.004
Plot 4	0.307	0.044	1.8901	-0.0132	-0.0277

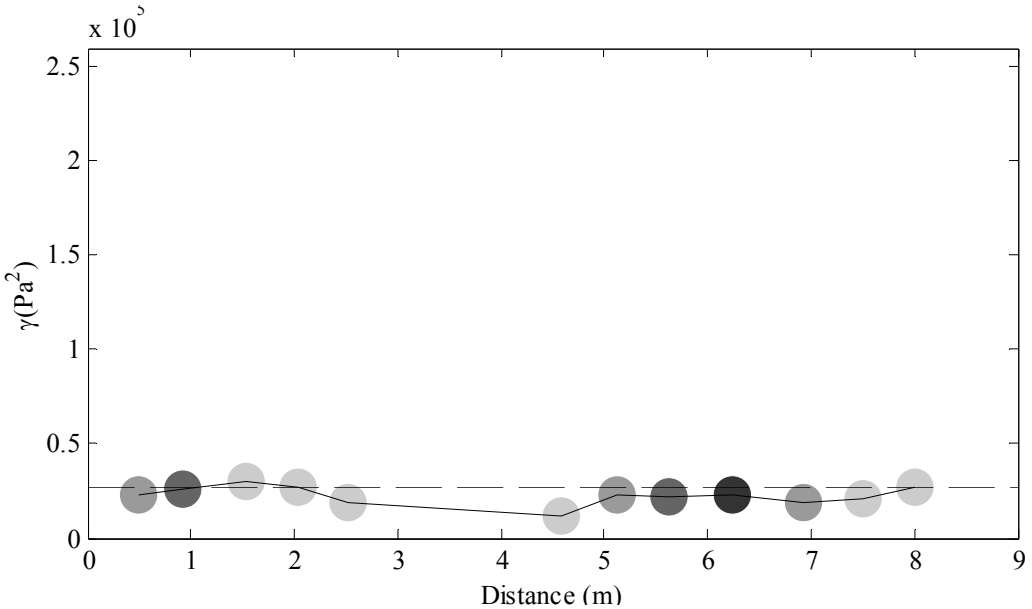

Figure 20. Variogram of Soccer Field Plot 1. Gray circles indicate the number of point-pairs within bins: 20% gray less than 50 point-pairs, 40% gray 51-100 point-pairs, 60% gray 101-150 point-pairs, and 80% gray more than 151 point-pairs.

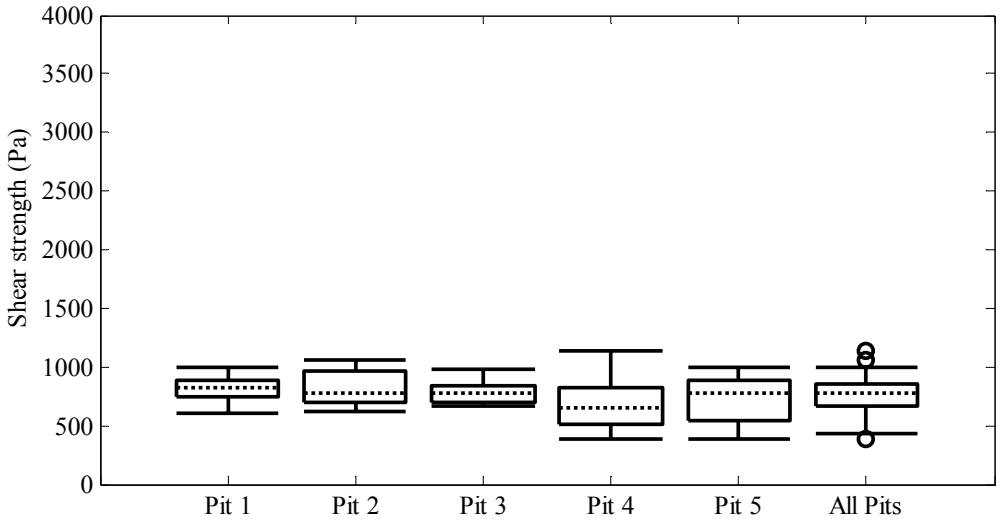

Figure 21. Box plots for pit-to-plot comparisons of shear strength for Soccer Field Plot 1. All pits were representative of the plot. Dotted lines indicate medians, boxes the interquartile range, whiskers extend to 0.05 and 0.95 quantiles, and circles indicate outliers.

Plot 2

We sampled the second plot January 7, 2004 at the end of a very cold 6 day period (Figure 18). Maximum temperatures on January 4 and 5 were -20° C. Temperatures began warming on January 6, and the weather station recorded a decrease of 3 cm in snow depth on the 6th. Median shear strength increased when compared to Plot 1 (Table 2). The shear quality was much more variable than Plot 1, ranging from smooth planar (Q2) to roughly planar (Q3; Figure 22).

There was no evidence of a linear trend in the shear strength data (Table 3). The variogram (Figure 23) had a nugget ratio estimate of 0.6 and a range of 1.75 m. The range indicated that autocorrelation occurred at the intra-pit distances. All pits were representative of the plots (Figure 24).

Location	Soccer Field, Plot 2
Date	20040107
Time	1030
Observer	SL
Aspect	0
Inclination	0

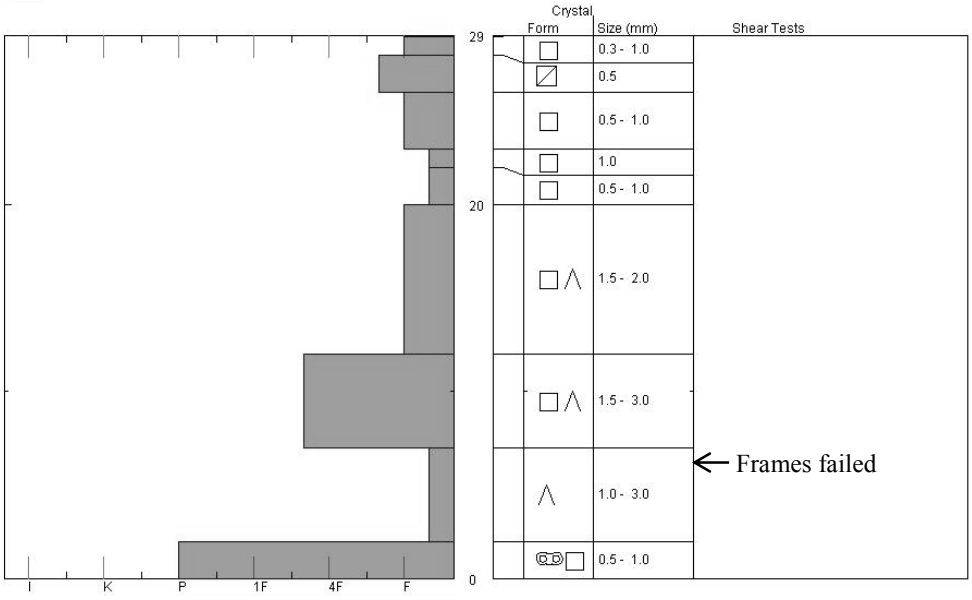

Figure 22. Manual profile for Soccer Field Plot 2

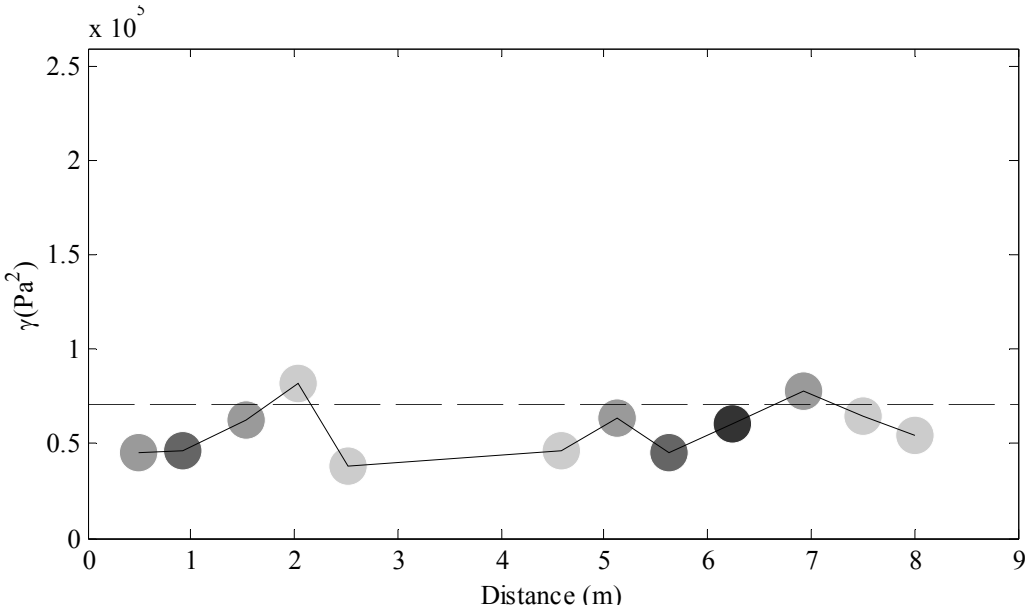

Figure 23. Variogram of the Soccer Field Plot 2, plotted with a lag distance of 0.6 m. Gray circles indicate the number of point-pairs within bins: 20% gray less than 50 point-pairs, 40% gray 51-100 point-pairs, 60% gray 101-150 point-pairs, and 80% gray more than 151 point-pairs

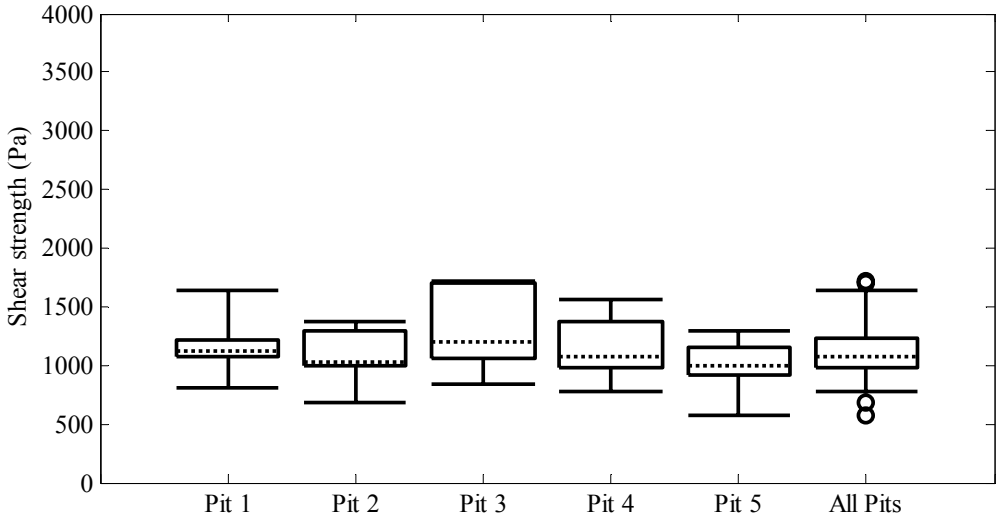

Figure 24. Box plots for pit-to-plot comparisons of shear strength for Soccer Field Plot 2. All pits were representative of the plot. Dotted lines indicate medians, boxes the interquartile range, whiskers extend to 0.05 and 0.95 quantiles, and circles indicate outliers.

Plot 3

Plot 3 was sampled January 15, 2004. Temperatures in the week between Plot 2 and 3 samples were relatively warm, with mean maximum temperature of 7° C (Figure 18). The snowpack continued to consolidate, as seen in the thinning and increase in slab density (Table 1). Median shear strength decreased from that of Plot 2, but variability remained quite similar (Table 2). Shear frame failures were more planar (Q1) than those in Plot 2, possibly the result of a greater difference in hardness between the slab (4F to P) and depth hoar (Figure 25).

Location	Soccer Field, Plot 3
Date	20040114
Time	0900
Observer	KB
Aspect	0
Inclination	0

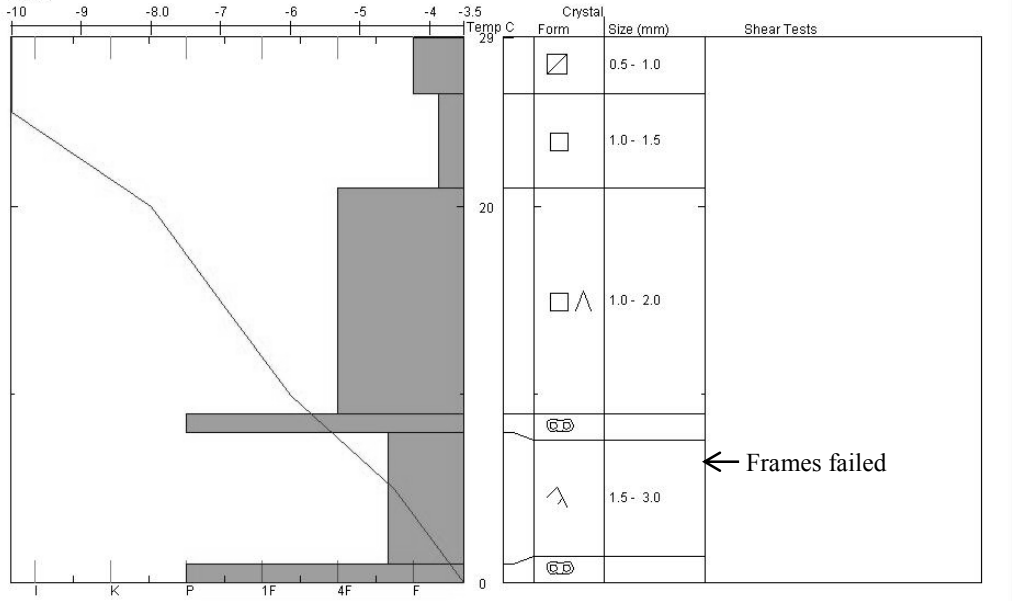

Figure 25. Manual profile for Soccer Field Plot 3

There was no evidence of a linear trend in the shear strength data (Table 3). The nugget ratio estimate was 0.5. The peak semivariance within the pit occurred at 1 m. The semivariance within pits was less than the semivariance between pits (Figure 26).

The Plot 3 variogram was the first to suggest that there was greater autocorrelation within pits than between pits. Although all pits were representative of plot shear strength (Figure 27), Pit 5 was the least representative pit of the plots sampled so far.

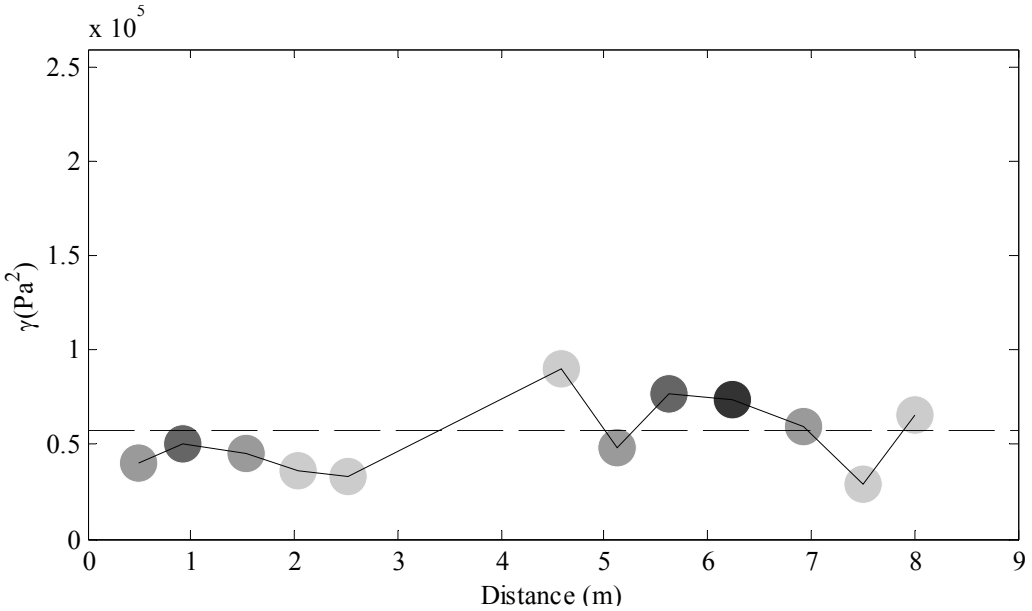

Figure 26. Variogram of Soccer Field Plot 3, plotted with a lag distance of 0.6 m. Gray circles indicate the number of point-pairs within bins: 20% gray less than 50 point-pairs, 40% gray 51-100 point-pairs, 60% gray 101-150 point-pairs, and 80% gray more than 151 point-pairs.

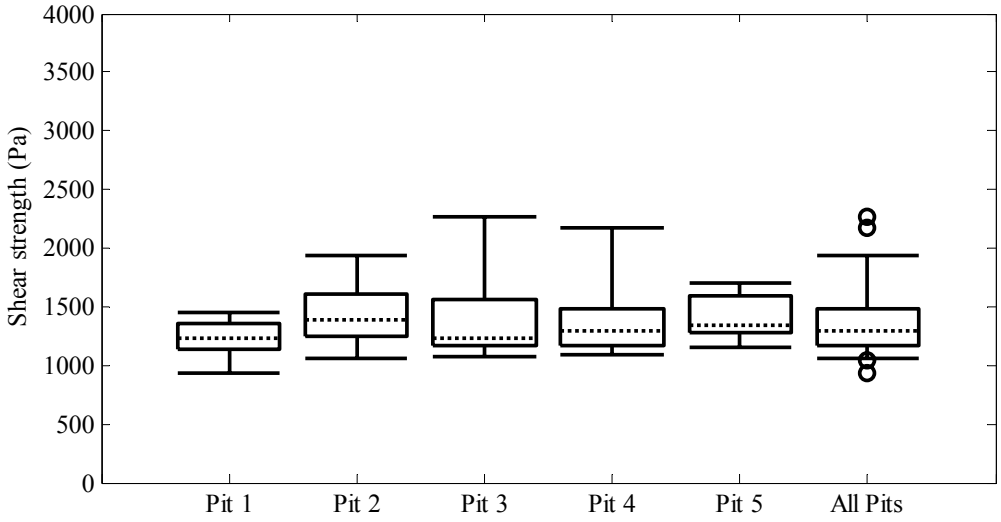

Figure 27. Box plots for pit-to-plot comparisons of shear strength for Soccer Field Plot 4. All pits were representative of the plot. Dotted lines indicate medians, boxes the interquartile range, whiskers extend to 0.05 and 0.95 quantiles, and circles indicate outliers.

Plot 4

Plot 4 was sampled February 3, 2004. Temperatures had remained steady for eight days after Plot 3 was sampled, with mean maximum temperatures of 6° C (Figure 18). Snowfall occurred January 23-26, with a storm total of 18 cm. Strong winds followed the storm, scouring the snow surface. The snowpack depth measured at Plot 4 was slightly thinner than Plot 3 (Table 1), indicative of wind scouring, while the snow depth recorded at the wind-sheltered weather station increased 3 cm (Figure 18). No manual profile was available.

Shear frame failure occurred at two distinct depths. There was a highly variable ice lens near the top of the depth hoar layer. Tests would fail just above the lens where it was present, and they were consistently stronger than tests failing in the depth hoar ($p < 0.001$). The ice lenses did not seem to represent tracks of pedestrians or other disturbances of the depth hoar layer. The lens may have formed as water infiltrated into the snowpack, then froze.

There was no evidence of a linear trend in the shear strength data (Table 3). Both failures were included in the variogram analysis because there were not sufficient results from either to calculate a variogram from just one of the failures. Including both failures greatly increased the variance. The nugget ratio estimate was 0.69, and the variogram indicated no autocorrelation of shear strength (Figure 28). As in Plot 3, semivariance was greater between pits than within pits, but the differences between pits were not statistically significant (Figure 29). All pits were representative of the plot.

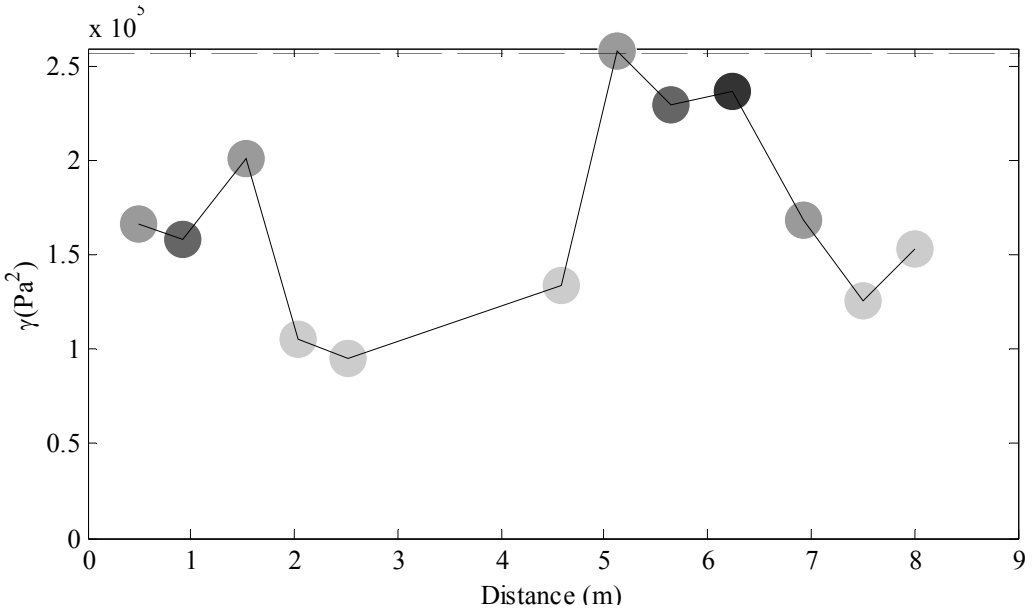

Figure 28. Variogram of Soccer Field Plot 4, plotted at lag distance of 0.6 m. Gray circles indicate the number of point-pairs within bins: 20% gray less than 50 point-pairs, 40% gray 51-100 point-pairs, 60% gray 101-150 point-pairs, and 80% gray more than 151 point-pairs

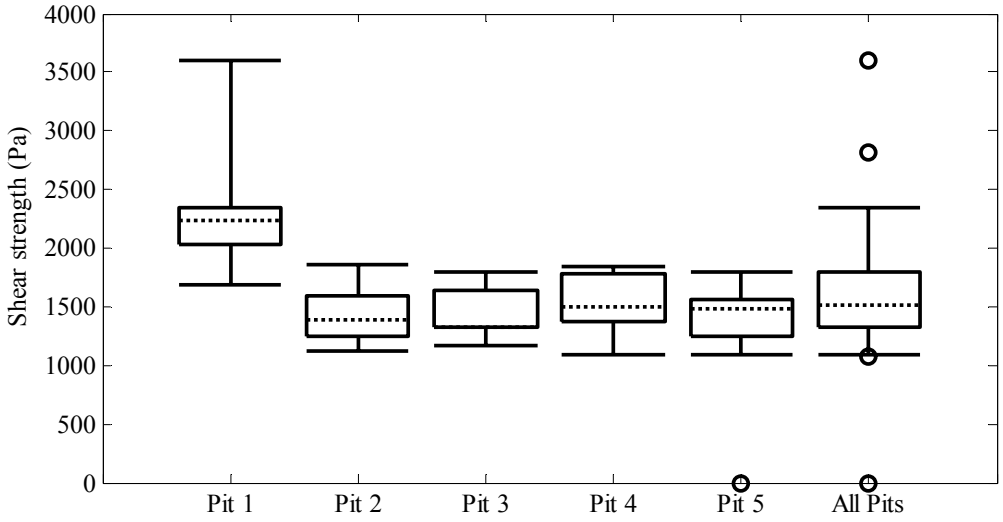

Figure 29. Box plots for pit-to-plot comparisons of shear strength for Soccer Field Plot 4. All pits were representative of the plot, though Pit 1 is quite skewed by several strong measurements. Dotted lines indicate medians, boxes the interquartile range, whiskers extend to 0.05 and 0.95 quantiles, and circles indicate outliers.

Pit-to-Plot Ratios of the Soccer Field

All pits were representative of their respective plots. This was expected. A level site was desirable as a test site because it should have a uniform snowpack. A uniform snowpack should be similar at all locations, with the lack of site-scale trends increasing the likelihood that all pits would be representative of the plots. None of the plots had significant linear trends (Table 3), and all pits did represent the respective plots.

Moreover, if all the variance occurred within a pit, as the variograms for Plot 1 and 2 indicated, any pit should be capable of characterizing the plot. Plots 3 and 4, where the semivariance within a pit was less than variance between pits would be more likely to exhibit inter-pit differences. Pits in Plot 4 may have been representative because failures on the ice lens occurred in all pits, increasing the intra-pit variance.

Temporal change

The change in shear strength between Plots 1 and 2 was significant (Table 2; Figure 18). The relative spread of the results decreased slightly, even though results from Plot 2 were skewed by the two strong test results (Table 1). Shear quality of the fractures became more planar between the two days.

Shear strength decreased significantly (Table 2) between Plots 2 and 3. Relative spread changed little, although the distribution of Plot 3 was more symmetrical than Plot 2 (Figure 18).

Variograms were hard to interpret. Subtle changes between the three variograms indicated convergence (Figure 18). The nugget ratio estimates decreased and the ranges increased, indicating increasing spatial autocorrelation through time. However, the nugget ratio estimates remained large, so the changes in range should be interpreted

cautiously. The QCV decreased between Pits 1 and 2, and did not change between Pits 2 and 3 (Table 2), supporting convergence. The pit-to-plot ratios did not change and provided indication of temporal trends.

Considerable change occurred in the snowpack over the two weeks between the sampling of Plots 3 and 4. The presence of the intermittent ice lens complicated comparisons between Plot 4 and Plot 3. The increase in strength from Plot 3 to Plot 4 (considering only failures in the depth hoar) was significant ($p < 0.001$; Table 2). The nugget ratio estimate and the QCV of shear strength both increased. The divergence indicated would be consistent with the presence of the ice lens and resulting spatial variability.

Spanky's Site

Conditions prior to sampling

A layer of near-surface facets topped with surface hoar developed during a high-pressure weather pattern prior to January 22, 2004. As early as January 10 an observer reported "nice surface hoar on top" of the snowpack (Chabot 2004). Snowfall began on January 23, with 25 cm of snowfall reported by the Gallatin National Forest Avalanche Center (2004) on January 24 (Figure 30).

We sampled the alleys on January 26, 2004 and Plot 1 three days later. Sampling of the remaining plots occurred at near weekly intervals, with Plot 2 sampled on February 5, Plot 3 a week later on February 12, and Plot 4 sampled on February 20. Slab and weak layer properties were characterized for the five sample days (Table 4; Table 5).

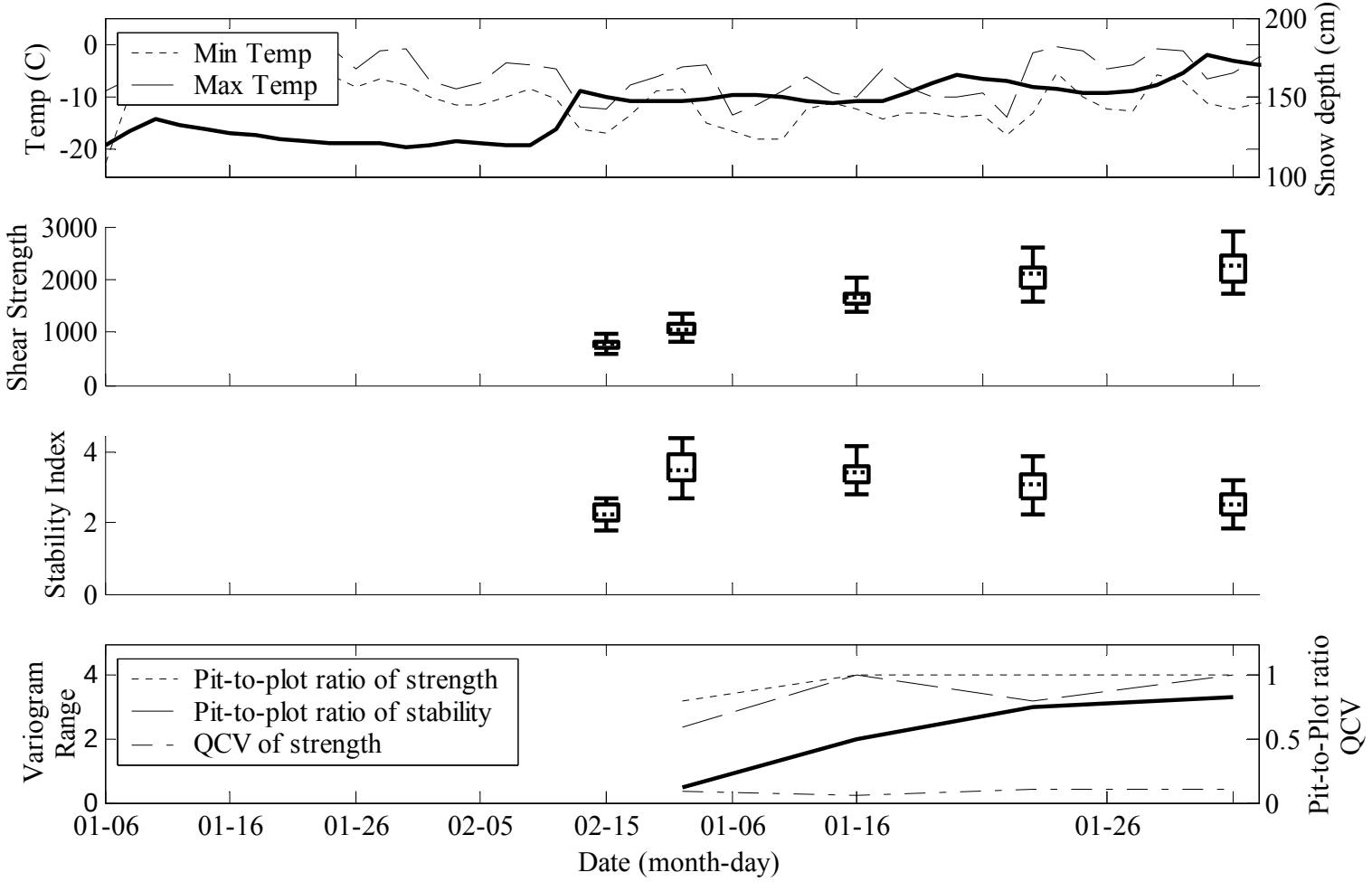

Figure 30. Weather data (top), box plots of shear strength and stability ratios (middle; dotted lines indicate medians, boxes the interquartile range, whiskers extend to 0.05 and 0.95 quantiles), and summaries of the statistical and spatial characteristics (bottom) of the Spanky's site. The weather data was collected from The Yellowstone Club, Montana, 5 km south of the site.

Table 4. Characteristics of the slab and weak layer for each plot at the Spanky's site.

	Alley	Plot 1	Plot 2	Plot 3	Plot 4
Median Thickness (cm)	45	34	47	66	72
QCV of Thickness	0.018	0.002	0.011	0.023	0.014
Median Density (kg m^{-3})	98	129	157	148	183
QCV of Density	0.041	0.034	0.015	0.024	0.011
Median Shear Strength (Pa)	764	1049	1648	2118	2256
QCV of Strength	0.091	0.093	0.060	0.096	0.107
Median Stability Index	2.3	3.5	3.4	3.1	2.5
QCV of Stability Index	0.092	0.099	0.067	0.108	0.111

Table 5. Rates of change of slab and plot characteristics between Spanky's plots.

	Alley and Plot 1	Plots 1 and 2	Plots 2 and 3	Plots 3 and 4
Number of days between:	3	7	7	8
Change in Median Slab Thickness (cm d^{-1})	-4	2	3	1
Change in Median Slab Density (kg m^{-3} d^{-1})	10.3	4	-1.3	4.4
Change in Median Shear Strength (Pa d^{-1})	95	86	67	17
Change in Median Stability (d^{-1})	0.40	-0.01	-0.04	-0.08
Significance, change in Strength	< 0.001	< 0.001	< 0.001	< 0.001
Significance, change in Stability	< 0.001	0.211	< 0.001	< 0.001

The Alleys

Snowfall prior to sampling added 25 cm to the slab above the weak layer (Figure 30). A 1 cm thick layer of small facets overlaid the surface hoar layer, and small facets were observed between the surface hoar grains (Figure 31). The remainder of the slab

consisted of broken and fragmented precipitation particles. A high avalanche hazard existed due to the rapid loading of a weak snow layer (Gallatin National Forest Avalanche Center 2004).

I found no significant linear trend in the shear strength or stability indices of the Alley sample (Table 6), so no site-wide trends were present. I therefore assumed the four plots were relatively similar at this point in time.

Location Spanky's Alley
Date 20040126
Time 1140
Observer SL
Aspect 80
Inclination 28

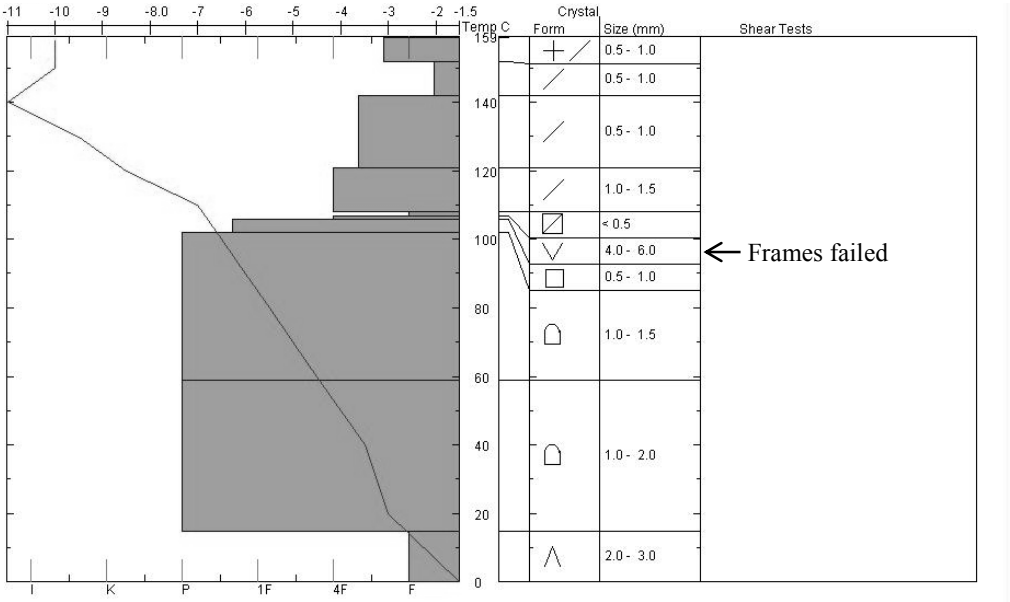

Figure 31. Manual profile for Spanky's Alley

Table 6. Significance, correlation, and coefficients of the linear trends in shear strength and stability indices at the Spanky's site. Trends that were significant and explained more than 10% of the variability are indicated in bold.

		p-value	R2	a1	a2	a3
Alley	Shear Strength	0.335	0.047	732.2569	3.0899	-1.4311
	Stability Index	0.293	0.053	2.3023	0.0064	-0.0072
Plot 1	Shear Strength	0.293	0.053	1127	-7.4	-3.4
	Stability Index	0.335	0.047	3.889	-0.0367	-0.0128
Plot 2	Shear Strength	0.192	0.037	1799.9	-5.8	-0.9
	Stability Index	0.738	0.009	3.3626	0.0062	-0.0084
Plot 3	Shear Strength	0.240	0.009	2402.4	0.300	-15.2
	Stability Index	**0.004**	**0.149**	4.2653	-0.0038	-0.0469
Plot 4	Shear Strength	0.216	0.216	2712.3	-6.6	-17.4
	Stability Index	**0.023**	**0.104**	3.2659	0.004	-0.0325

Plot 1

Warm temperatures rapidly settled and consolidated the slab in the three days between the Alley and Plot 1 samples (Figure 30; Table 5). The surface hoar layer remained an avalanche hazard and a few avalanches were released in steeper, wind-loaded terrain in the nearby Big Sky Mountain Resort. At the study site it appeared that as the slab settled, the layer of facets above the surface hoar layer interpenetrated the surface hoar grains (Figure 32). Two compression tests failed moderately (CT 17 Q2) on the surface hoar layer (Figure 32).

Location	Spanky's Plot 1
Date	20040129
Time	1130
Observer	SL
Aspect	80
Inclination	26

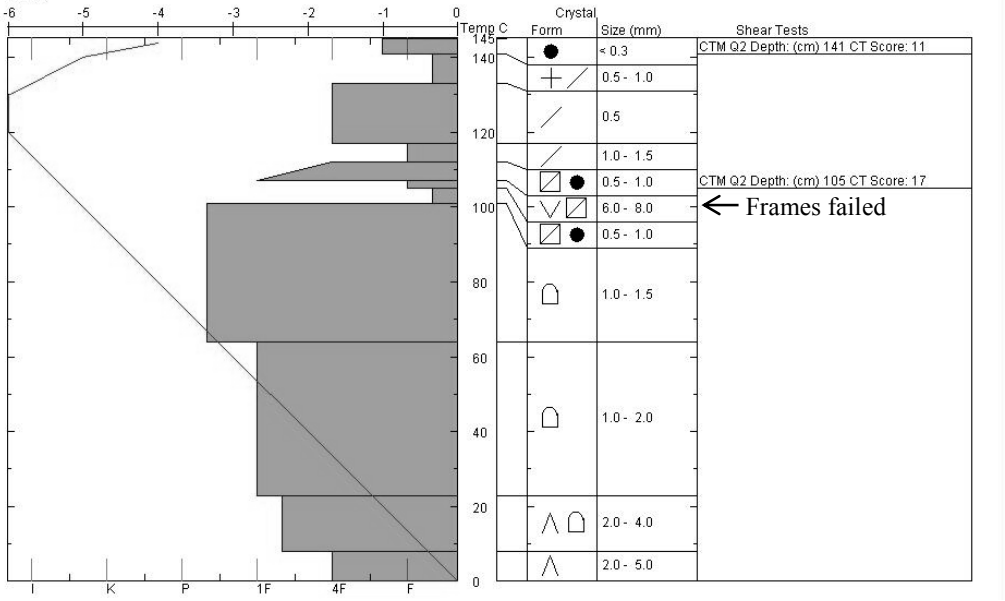

Figure 32. Manual profile for Spanky's Plot 1

We conducted a total of 90 shear frame tests in Plot 1, fitting additional shear frame tests between Pits 1 and 2 (Figure 33). The relatively thin slab made for easy digging and test preparation, and several hours of daylight remained after the 72 initial tests were finished. The field crew decided that additional tests could be inserted easily between the pits with spacing tighter than the 0.5 m intervals already used, and an additional 18 tests were done. The additional tests provided short pair distances and shorter minimum distances between tests than the other plots sampled.

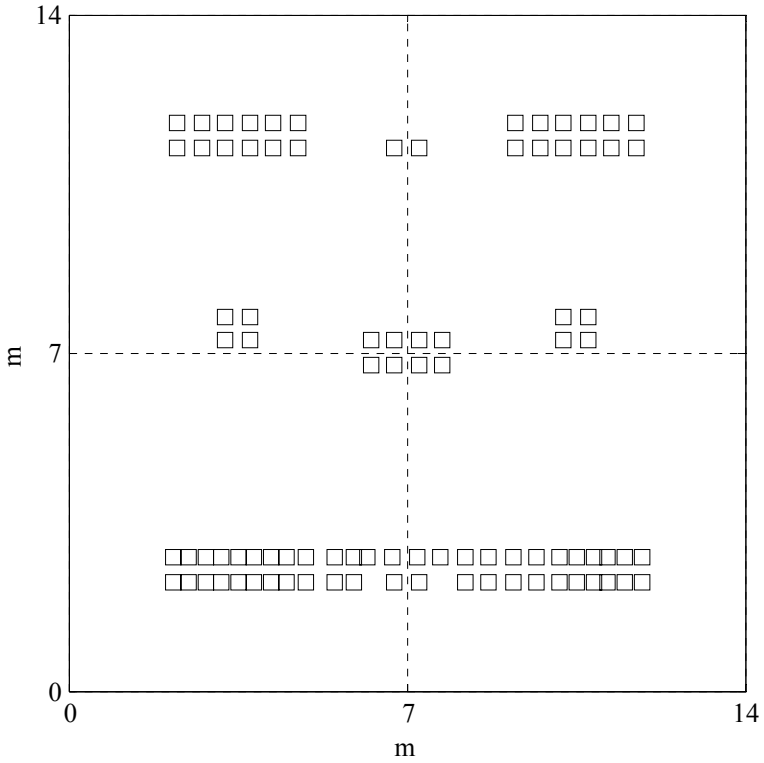

Figure 33. Layout of sampling array used for shear frames in Spanky's Plot 1.

Both the median shear strength and the median stability indices increased compared to the alley sample (Table 5). No evidence of linear trends existed in either the strength or stability indices (Table 6). The shear frame test with the lowest shear strength was within 0.5 m of one of the tests with the highest shear strength. Landry (2002) noted such close proximity of very high and very low results.

The robust variogram indicated spatial correlation at short distances with a range of 0.5 m and a nugget ratio estimate of 0 (or 0.25 if calculated from the 1st and 3rd lag distance; Figure 34, Figure 17). The point pairs in the 0 to 0.4 m bin consisted of the additional tests. The proximity of tests with very low and very high shear strengths, as noted above, supported the short range. Additional support for correlation at short distances came from experience through the field season. If the operator felt a test was

faulty, a second test was often placed as closely as possible to the first test. Unless the initial fault was due to an improperly prepared test, the second result tended to be more similar to the "faulty" test than two tests at the standard distance of 0.5 m.

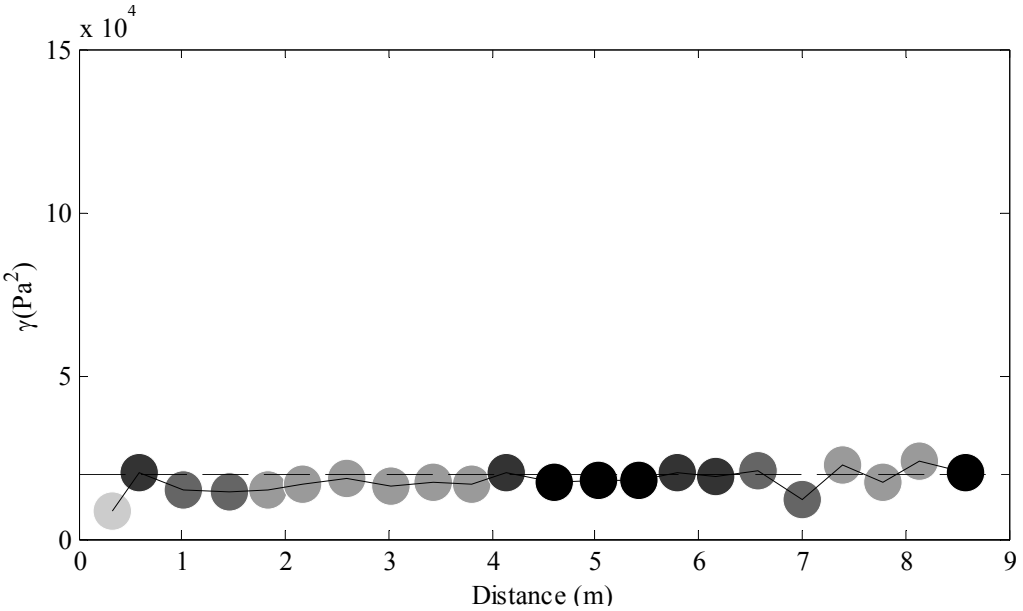

Figure 34. Variogram of Spanky's Plot 1, plotted with a lag distance of 0.4 m. All tests included. Gray circles indicate the number of point pairs within bins: 20% gray less than 50 point-pairs, 40% gray 51-100 point-pairs, 60% gray 101-150 point- pairs, and 80% gray more than 151 point-pairs.

The semivariance at the second bin, 0.4 to 0.8 m, increased higher than the overall variance, and indicated no spatial correlation at those distances (Figure 34). This point seemed anomalously "spiked," but this was common to all four plots; semivariance around 1 m was higher than the semivariance in bins to either side. Removing the two strongest and weakest results (N = 88) from the analysis reduced the overall semivariance, but the spike was still present.

At distances larger than 1 m semivariance decreased, then gradually increased at longer distances. Another spike occurred at 4 m, at distances influenced by tests in different pits. The overall variance was reached at 5 m. The spikes could be reduced by using large bin widths, but at the expense of increasing the nugget ratio (Figure 17, p.

48). The sampling array had several distances with a disproportionately large number of point pairs—0.5 m, 5 to 6 m, and around 9 m. Because these distances involved so many point-pairs, the variance tended to be higher because the extreme values were included in more point pairs than at other distances.

Pit 1 was not representative of the plot shear strength ($p = 0.05$), and some evidence existed that Pit 3 was not representative of the plot shear strength ($p = 0.07$; Figure 35). Pits 1 and 3 were not representative of the stability indices of the plot ($p < 0.05$; Figure 36).

Median shear strength of Pit 1 was higher than the other four pits, and resulted in high calculated stability indices. In Pit 3, the generally lower median shear strength led to lower values of calculated stability indices. While sampling the plot, the operator noted that Pit 2 had more variable results than other pits, as can be seen in the box plots (Figure 35).

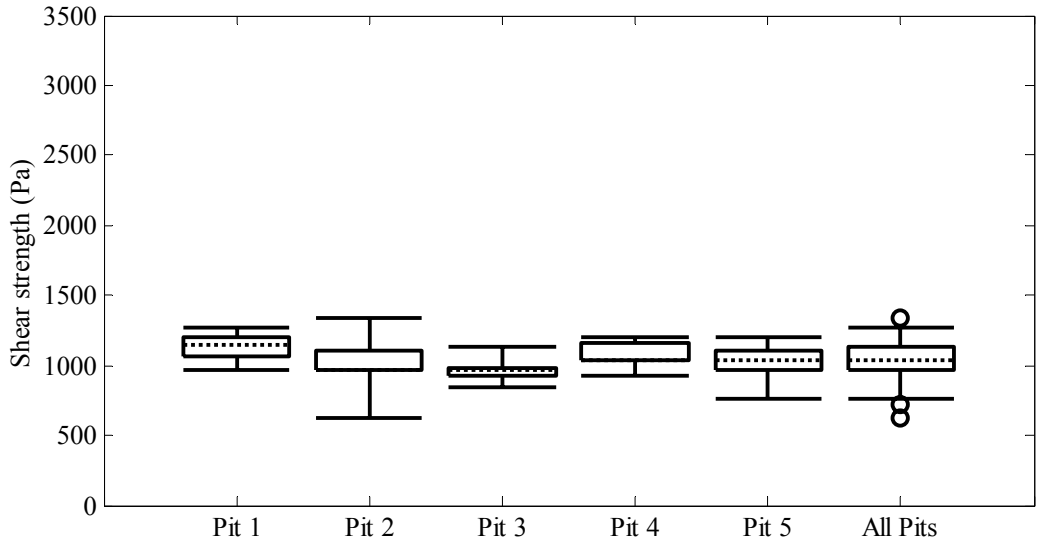

Figure 35. Box plots for pit-to-plot comparison of shear strength for Spanky's Plot 1. Pits 1 and 3 were not representative of plot shear strength. All pits were representative of the plot. Dotted

lines indicate medians, boxes the interquartile range, whiskers extend to 0.05 and 0.95 quantiles, and circles indicate outliers.

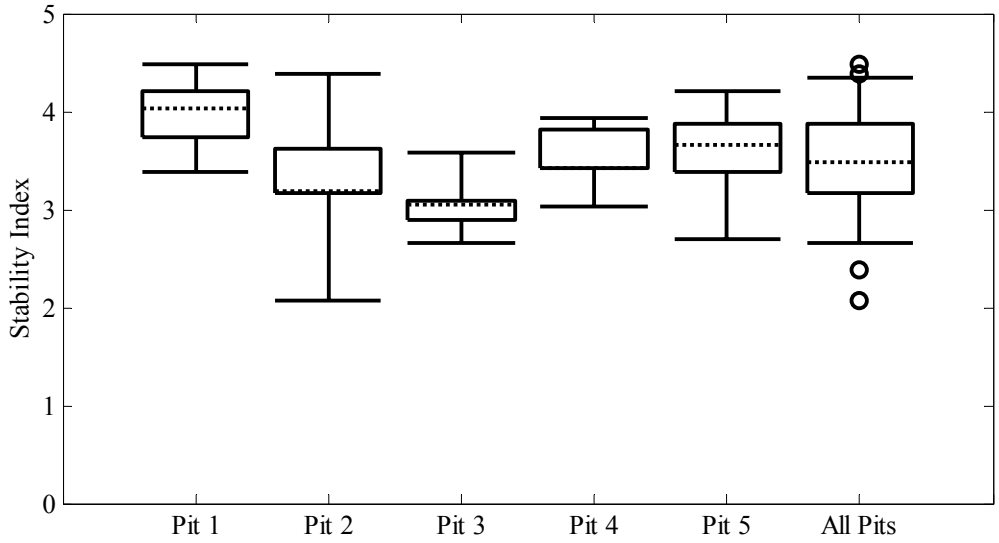

Figure 36. Box plots for pit-to-plot comparison of stability indices for Spanky's Plot 1. Pits 1 and 3 were not representative of the plot. All pits were representative of the plot. Dotted lines indicate medians, boxes the interquartile range, whiskers extend to 0.05 and 0.95 quantiles, and circles indicate outliers.

Plot 2

When we sampled Plot 2 on February 5th, grains in the oldest slab layers had begun to round. Small facets occurred between the surface hoar grains. Light snowfall occurred throughout the week between sampling of Plots 1 and 2, which increased the median slab thickness and density (Table 5). Again, small facets occurred between the surface hoar. Bonding between the smaller grains may have contributed to the increase in median shear strength and median stability index (Table 5). No manual profile was available.

The variogram had a nugget ratio estimate of 0.6 (Figure 37). The nugget ratio estimate increased compared to Plot 1, indicating less spatial correlation (Myers 1997).

Overall, the variogram indicated negative spatial correlation, meaning that test results more than 2 m apart were more similar than test results 1 m apart. Test results 1 to 2 m apart drove the overall variance within the data.

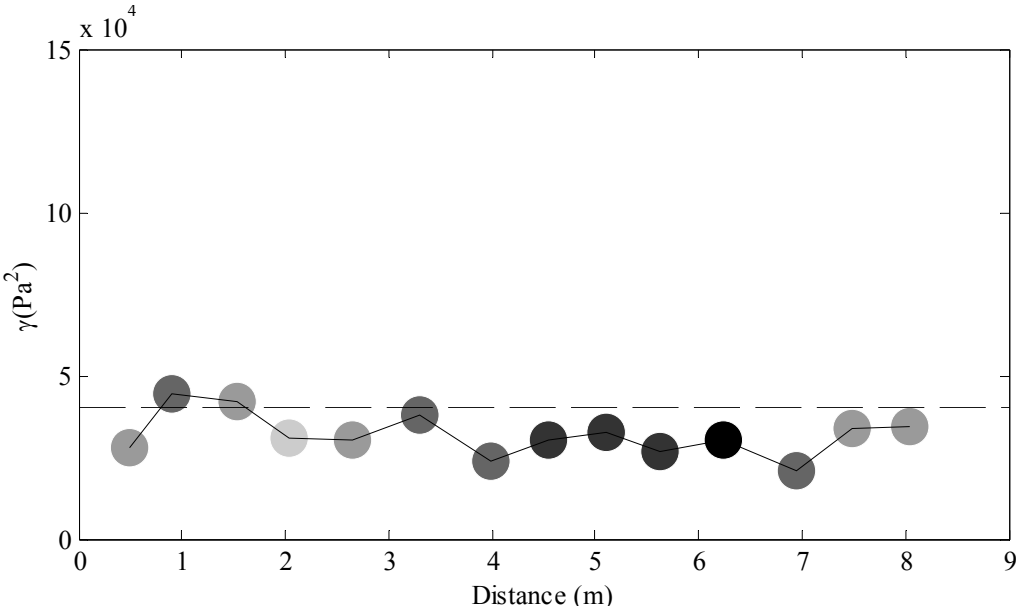

Figure 37. Variogram of Spanky's Plot 2, plotted with a lag distance of 0.6 m. Gray circles indicate the number of point-pairs within bins: 20% gray less than 50 point-pairs, 40% gray 51-100 point-pairs, 60% gray 101-150 point-pairs, and 80% gray more than 151 point-pairs

.

I spent a considerable amount of time attempting to "improve" the variograms by removing outliers, transforming the data, or fitting higher order trend surfaces. None of the methods attempted made significant differences in the variogram pattern. Negative spatial correlations were indicated by all the variograms.

All pits were representative of the plot in both shear strength (Figure 38) and stability (Figure 39). By this measure, Plot 2 was spatially uniform. A sufficient number of tests from any location within the plot would capture the overall variability of the plot. A pure nugget variogram, rather than the variogram indicating a decrease in variability, would have been more consistent with the lack of spatial variability.

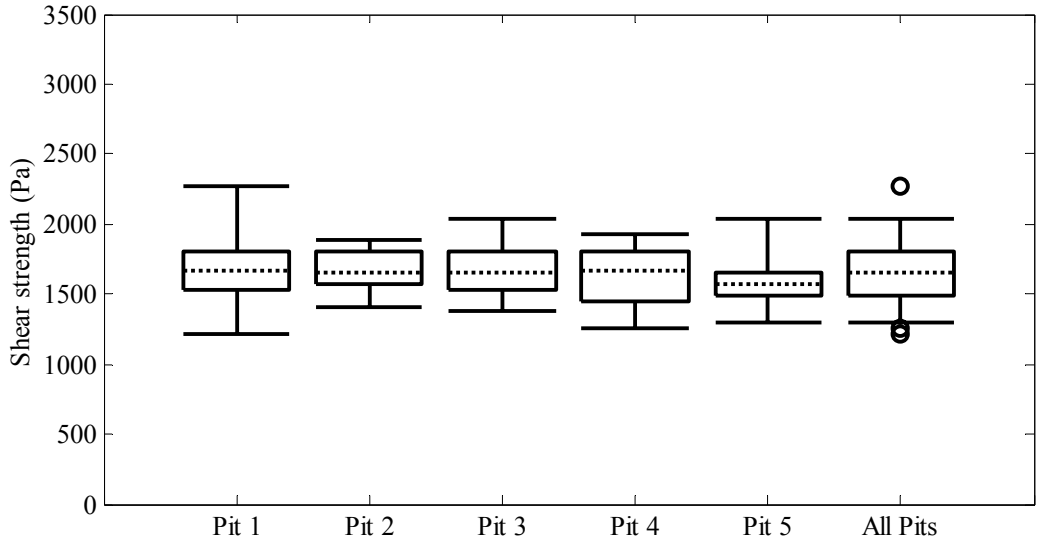

Figure 38. Box plots for the pit-to-plot comparison of shear strength for Spanky's Plot 2. All pits were representative of the plot. All pits were representative of the plot. Dotted lines indicate medians, boxes the interquartile range, whiskers extend to 0.05 and 0.95 quantiles, and circles indicate outliers.

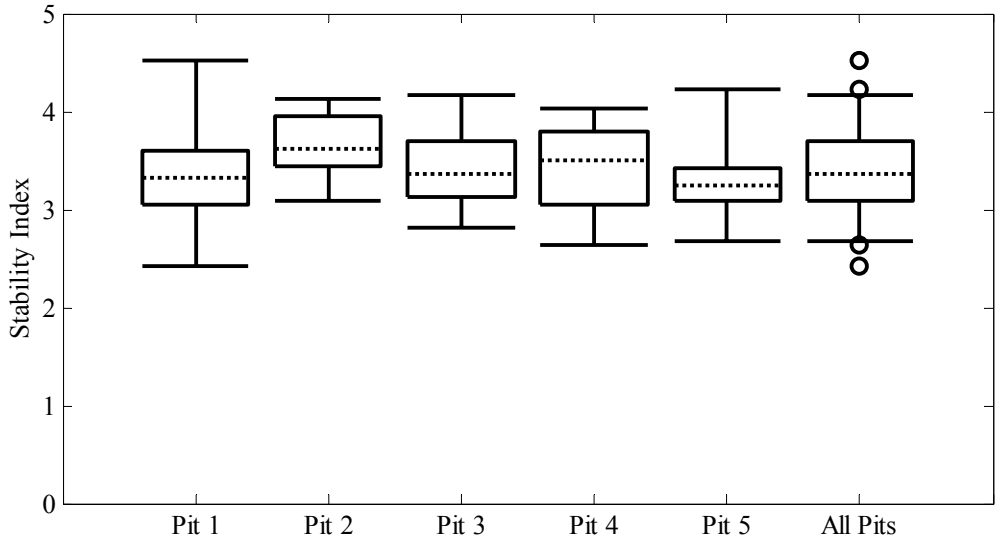

Figure 39. Box plots for the pit-to-plot comparison of stability ratios for Spanky's Plot 2. All pits were representative of the plot. All pits were representative of the plot. Dotted lines indicate medians, boxes the interquartile range, whiskers extend to 0.05 and 0.95 quantiles, and circles indicate outliers.

Plot 3

Snowfall occurred for several days following the sampling of Plot 2, with the heaviest snowfall occurring on February 8 and 9. During that period, observers noted several natural avalanches near the study site, and surrounding ski patrols released several avalanches (Gallatin National Forest Avalanche Center 2004). There was not sufficient information reported to determine if these failed on the layer sampled, or higher in the snowpack. When Plot 3 was sampled February 12, the surface hoar layer was under a 66 cm thick slab (Table 4; Figure 40).

Location	Spanky's Plot 3
Date	20040214
Time	1000
Observer	KB
Aspect	80
Inclination	28

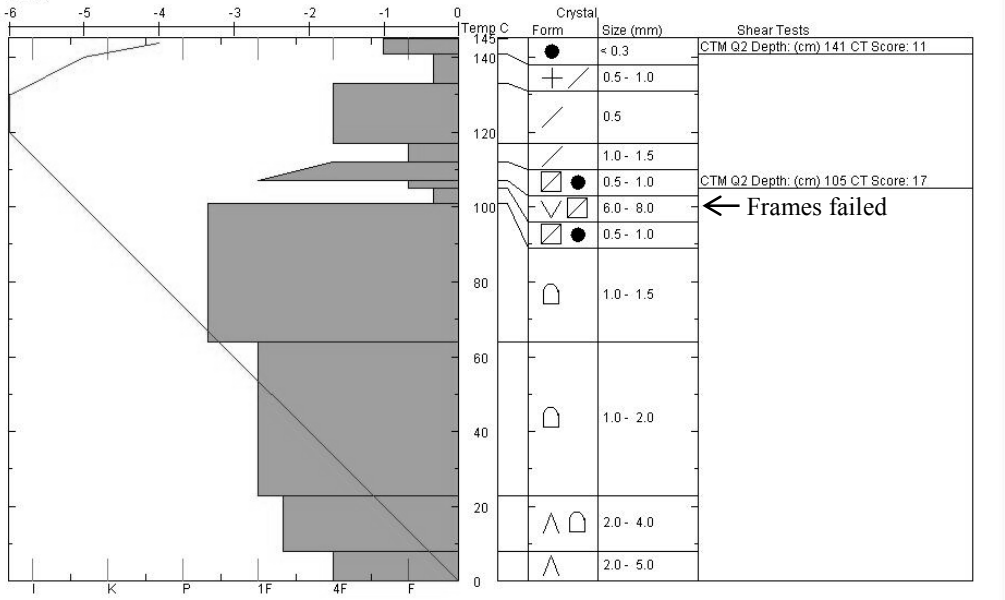

Figure 40. Manual profile for Spanky's Plot 3

Stuffblock tests and compression tests conducted on the layer indicated a strengthening snowpack (Figure 40). Other easier, but poorer quality, failures occurred

on interfaces above the surface hoar layer. The surface hoar layer was no longer the weakest layer, but was still the layer producing the cleanest, high quality shears, and therefore remained a critical layer within the snowpack (Figure 40).

The median shear strength and median stability index continued to increase (Table 5). Again, strong and weak test results were observed within 1m of each other. No evidence suggested a significant trend in shear strength (Table 6).

The variogram had a nugget ratio estimate of 0.44, and a range around 3 m (Figure 41). The 3 m range was resistant to changing the bin widths. Like the previous plots, the spike in the bin near 1 m indicated that much of the overall variance occurred at that distance. The Plot 3 variogram indicated little spatial correlation.

The semivariance increased at the inter-pit distance of 3 to 3.6 m. The increase in semivariance indicated differences among the pits. From the variogram, the pit-to-plot ratios could be expected to indicate several pits to be not representative of the plot.

However, the pit-to-plot comparisons for shear strength indicated that all pits were representative of the plot (Figure 42). In the pit-to-plot comparisons of the stability index, Pit 1 was found to be not representative of the plot ($p < 0.05$; Figure 43). The slab density measured at Pit 1 was the lowest of the plot. Pit 1 had the second highest median stability, and had the highest minimum stability of any pit within the plot. The minimum stability index was 2.1, and occurred in Pit 4, which also had the largest variance of the pits.

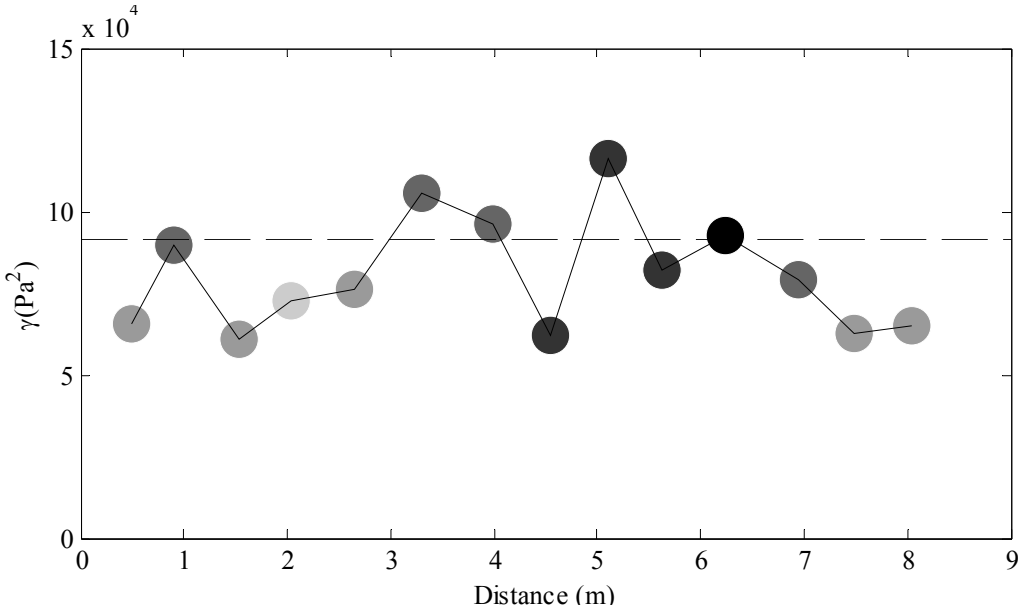

Figure 41. Variogram of Spanky's Plot 3, plotted with a lag distance of 0.6 m. Gray circles indicate the number of point-pairs within bins: 20% gray less than 50 point-pairs, 40% gray 51-100 point-pairs, 60% gray 101-150 point-pairs, and 80% gray more than 151 point-pairs.

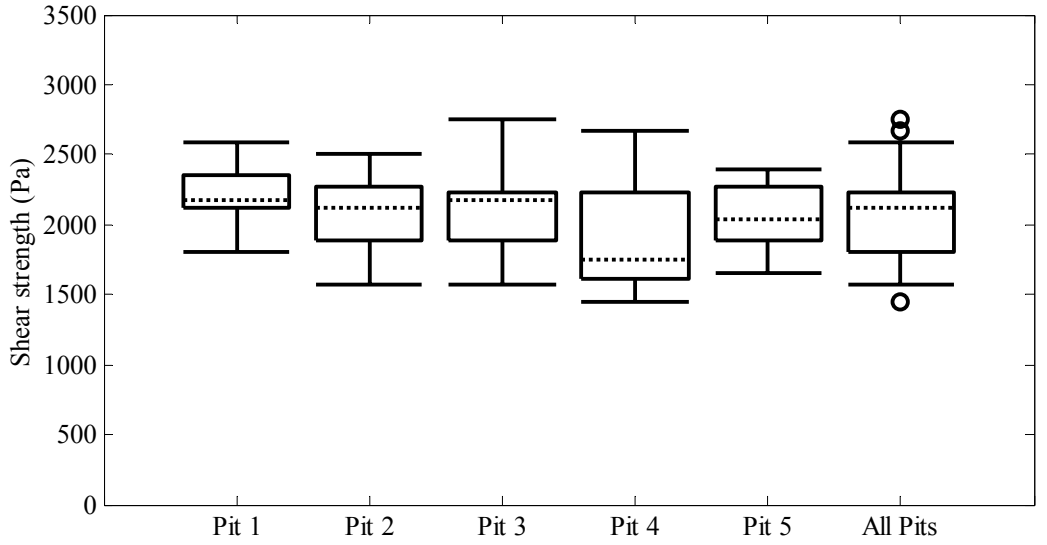

Figure 42. Box plots for pit-to-plot comparison of shear strength for Spanky's Plot 3. All pits were representative of the plot. All pits were representative of the plot. Dotted lines indicate medians, boxes the interquartile range, whiskers extend to 0.05 and 0.95 quantiles, and circles indicate outliers.

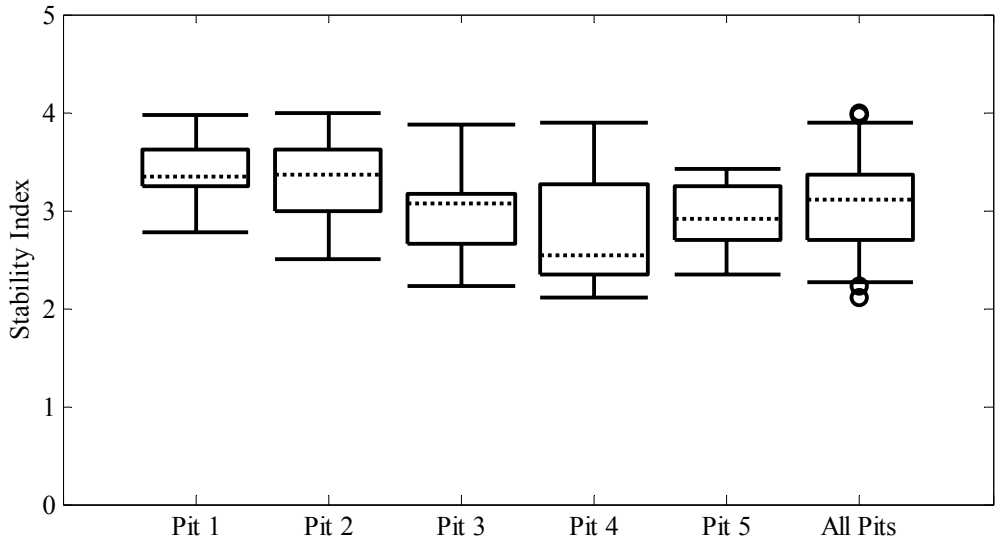

Figure 43. Box plots for pit-to-plot comparison of stability indices for Spanky's Plot 3. Pit 1 was not representative of the plot. All pits were representative of the plot. Dotted lines indicate medians, boxes the interquartile range, whiskers extend to 0.05 and 0.95 quantiles, and circles indicate outliers.

In conjunction with relatively high strength measurements, the low-density slab of Pit 1 resulted in high calculated stabilities within the pit. We measured slab properties at only one location within each pit. This proved to be problematic in the analysis, because the stability indices were effectively binned by pit. The differences of shear strength within a pit were dampened by using the same slab characteristics to calculate the stability indices. Additional slab measurements would reduce the problem but significantly complicate the sampling. Incorporating stratigraphic measurements from the SMP would be ideal.

A significant linear trend explained almost 15% of the variance in the stability indices (Table 6). The trend indicated stability indices for tests along the lower edge of the plot tended to be higher than tests in the middle (where variability among the tests was highest) and the upper portion of the plot. The trend was apparent in the box plot (Figure 43), with Pits 1 and 2 having a higher median stability indices than the other pits.

Slab properties did not exhibit strong trends across the plot, but the nine measurements were not sufficient to determine if a trend in slab properties existed. Additional stratigraphic data from SMP measurements could be utilized to see if trends within the slab existed, or if the linear trend was an artifact of the data collection.

Plot 4

Snowfall between sample days continued, with 15-20 cm of dense snow falling on February 18 (Gallatin National Forest Avalanche Center 2004). When Plot 4 was sampled on February 20, the surface hoar layer could be found in stuffblock and rutschblock tests, with results similar to those of Plot 3 (Figure 44). The surface hoar layer no longer seemed

to be the critical layer to the field crew; we felt that weaker interfaces above posed a greater avalanche problem.

The weak layer continued to strengthen, although the median stability index decreased slightly when compared to Plot 3 (Table 5). A significant linear trend existed within the stability indices but explained less of the variance than did the trend in Plot 3 (Table 6). As in Plot 3, the linear trend indicated that tests along the lower portion of the plot had a higher stability ratio than tests along the top of the plot. Further, as in Plot 3, the nine measurements of slab properties did not indicate strong trends in slab density or thickness. Additional measurement of slab properties from SMP data would be useful in determining the importance of this trend.

In both Plot 3 and 4, the trends were stronger upslope than across the slope. Other research showed that trends tended to be strongest in the upslope direction (Kronholm 2004). The across slope components of the two plots were mirror images, indicating that

shear strength was slightly stronger towards the interior of the site. Because the trend was not apparent in the Alley samples, earlier sampling may have affected these two plots.

Location	Spanky's Plot 4
Date	20040220
Time	1030
Observer	KB
Aspect	80
Inclination	26

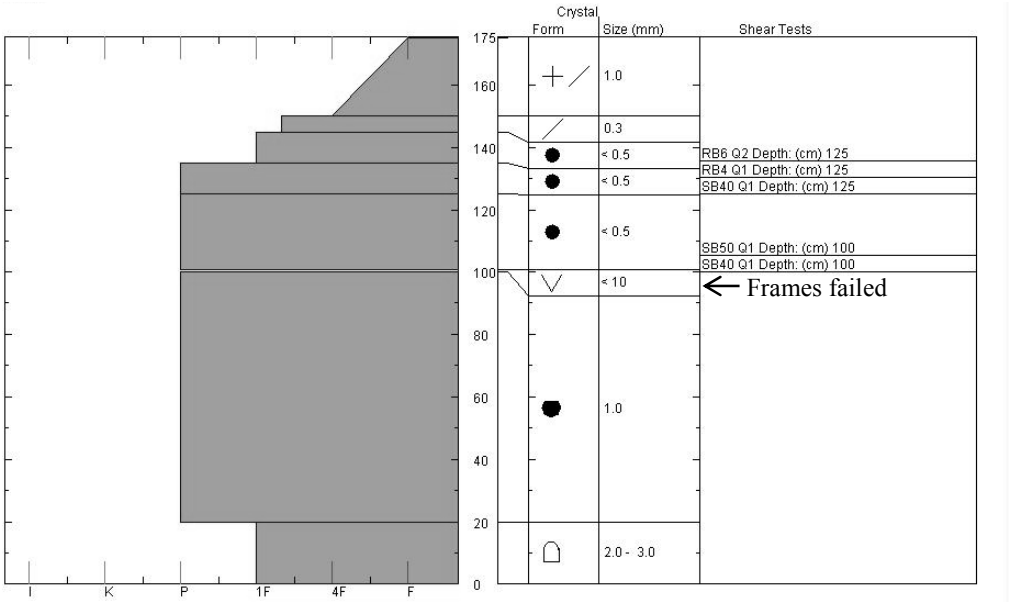

Figure 44. Manual profile for Spanky's Plot 4

The variogram for Plot 4 had a nugget ratio estimate of 0.53 and range of 3.3 m, at the inter-pit distance (Figure 45). The spike near 1 m was not as pronounced as in the previous plots. Again, tests within a pit were more likely to be similar than tests from different pits. Removing the strongest and weakest tests (N = 70) reduced the overall variance but had no effect on the range or nugget ratio estimate.

All pits were representative of the shear strength of Plot 4 (Figure 46). Minimum shear strength was measured in Pit 5, and seemed to be an anomalous value because it was much lower than the surrounding tests. All pits were found to be representative of

the plot stability index, but some evidence (p = 0.052) existed that Pit 4 was not representative (Figure 46).

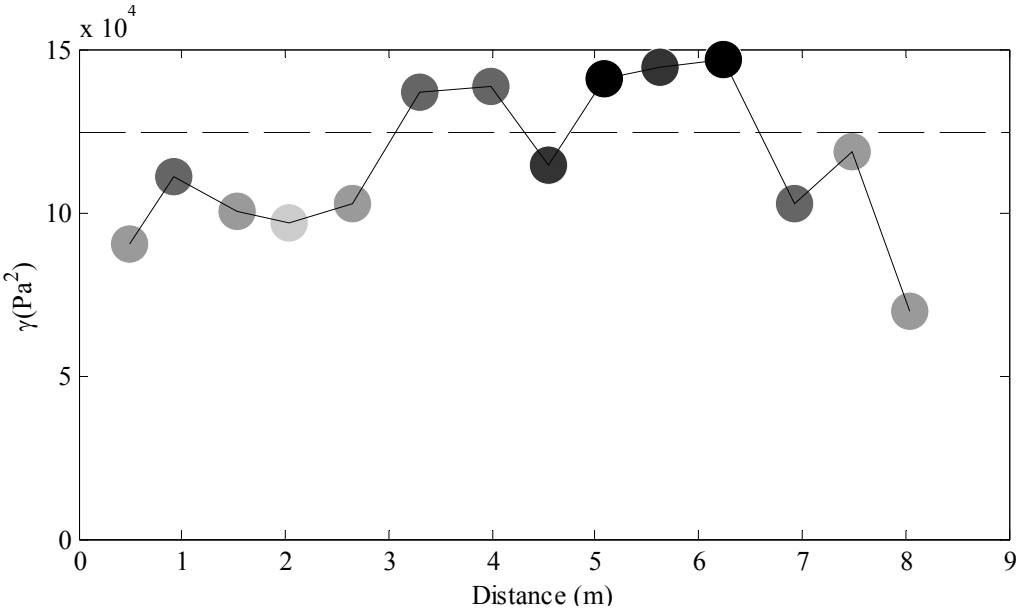

Figure 45. Variogram for Spanky's Plot 4, plotted with a lag distance of 0.6 m. Gray circles indicate the number of point-pairs within bins: 20% gray less than 50 point-pairs, 40% gray 51-100 point-pairs, 60% gray 101-150 point-pairs, and 80% gray more than 151 point-pairs.

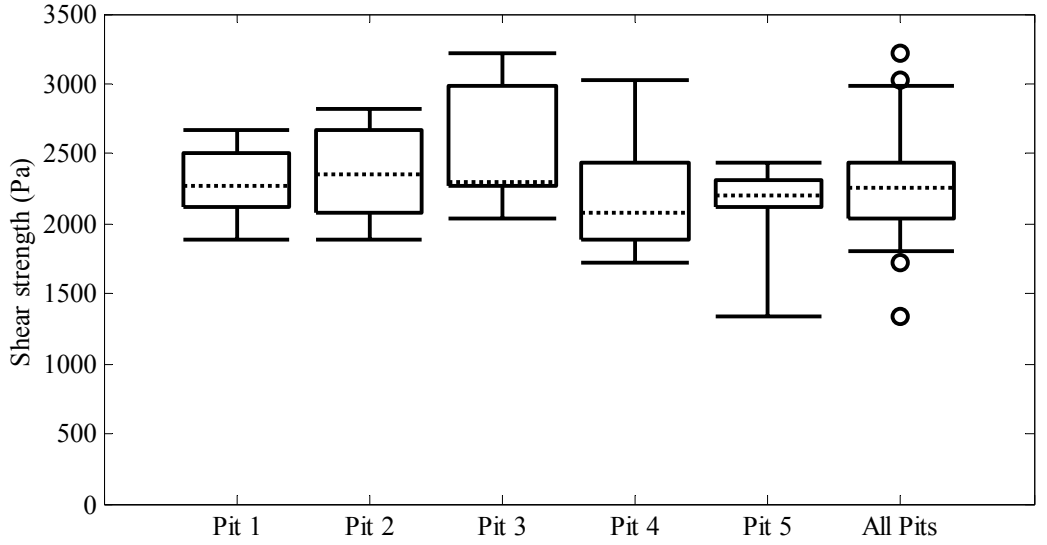

Figure 46. Box plots for pit-to-plot comparison of shear strength for Spanky's Plot 4. All pits were representative of the plot. All pits were representative of the plot. Dotted lines indicate medians, boxes the interquartile range, whiskers extend to 0.05 and 0.95 quantiles, and circles indicate outliers.

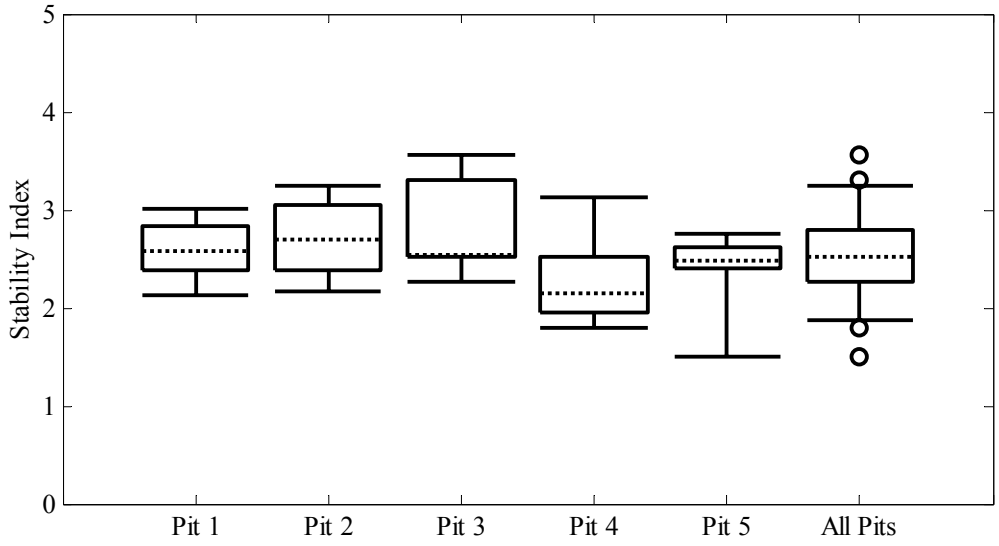

Figure 47. Box plots for pit-to-plot comparison of stability indices for Spanky's Plot 4. Some evidence existed ($p = 0.052$) that Pit 4 was not representative of the plot. All pits were representative of the plot. Dotted lines indicate medians, boxes the interquartile range, whiskers extend to 0.05 and 0.95 quantiles, and circles indicate outliers.

Temporal Change

Shear strength and the stability indices increased significantly from the Alleys to Plot 1 (Table 5). On a per day basis, the change was an order of magnitude greater than observed between other plots. This rapid increase occurred as the weak layer adjusted to the loading of new snow (Jamieson and Johnston 1999). The increase in strength could have been accelerated as small facets interpenetrated the surface hoar layer, increasing the bonding and, hence, strength within the layer. The increase in the non-spatial QCV indicated an increase in the variability of shear strength in the three days between samples.

Spatial correlation was found for distances less than 0.7 m on Plot 1. The range, around 5 m, indicated some correlation of test results between pits. Therefore, some differences in pit-to-plot ratios could be expected, because results would be correlated

with the two nearest pits, but not the two farthest. The pit-to-plot ratios indicated that one pit was not representative of the plot strength, and two pits were not representative of the plot stability index, consistent with the variogram interpretation.

The difference in strength between Plot 1 and 2 was significant, while the difference in stability indices was not (Table 5). Although shear strength increased rapidly between Plot 1 and 2, the additional snowfall increased the load on the weak layer by a proportional amount, and little net change in the stability indices resulted.

The variogram range increased between Plots 1 and 2, the pit-to-plot ratios increased, and the QCV of shear strength decreased, all indicators of convergence. However, neither of the variograms offered easy interpretation or conclusive evidence.

The rate of strengthening between Plot 2 and 3 decreased compared to rates measured earlier but the difference in strength remained significant (Table 5). The difference in the stability indices between Plot 2 and 3 was significant (Table 5). The stability indices decreased between the plots as stress from the slab continued to increase, but the field crew did not feel that the avalanche danger had increased.

The QCV of both strength and the stability indices increased between Plot 2 and 3 and indicated divergence as the layer aged (Figure 30). The decrease in the pit-to-plot ratio of the stability index was an additional indication of divergence. However, the variogram range increased, indicating convergence. Indications of both divergence and convergence were present. Given the poor quality of the variograms, I would discount their indication of convergence.

The difference in strength between Plot 3 and 4 was significant, even as the rate of strengthening continued to decrease (Table 5). The stability indices decreased significantly (Table 5). The QCVs of both increased, suggesting continued divergence.

The variograms indicated little change in the spatial correlation of strength between Plots 3 and 4. The pit-to-plot ratio for stability increased, but the ratios for strength did not change. Both the variograms and pit-to-plot ratios suggest little change, or slight convergence.

Lionhead

Conditions Prior to Sampling

An extensive layer of surface hoar formed during the middle of January 2004 throughout the intermountain west. Reports of "trophy-sized" surface hoar came from Utah; in the mountains around the Lionhead study site observers found grains measuring 50 mm (Chabot 2004; Utah Avalanche Center 2004). Observations made near the study site on January 22 found two layers of surface hoar, separated by a thin layer of precipitation particles, and buried under layer of recent snow 5 cm thick (Figure 48).

Figure 48. Close up photo of the double surface hoar layers. Ruler marked in centimeters.

A storm system on January 24-26 buried and preserved the surface hoar layer (Figure 49). Storm totals of 20 cm were reported for the Lionhead area (Chabot 2004). On January 26, natural avalanche activity was reported on the avalanche paths near the study site (Chabot 2004). Stormy weather continued, with daily snowfall of 2 to 10 cm (Chabot 2004). A widespread avalanche cycle occurred at the end of the month, with an Avalanche Warning issued by the Gallatin National Forest Avalanche Center for January 31 through February 2 (Gallatin National Forest Avalanche Center 2004).

Small snowstorms continued to deposit snow through the week prior to the sampling of the Alleys (Figure 49). Avalanche conditions remained interesting: many slopes had slid on the surface hoar layer, effectively removing it as a hazard on those slopes. Slopes that had not avalanched remained quite sensitive to human triggering, and posed a hazard to backcountry travelers. On February 3, an observer reported that the surface hoar layer was so sensitive they "did not want to get on anything over 30^{o}" (Chabot 2004). Results from stability tests conducted by the observer on slopes near the study site were moderate (SB 30 Q1, CT 16 Q1).

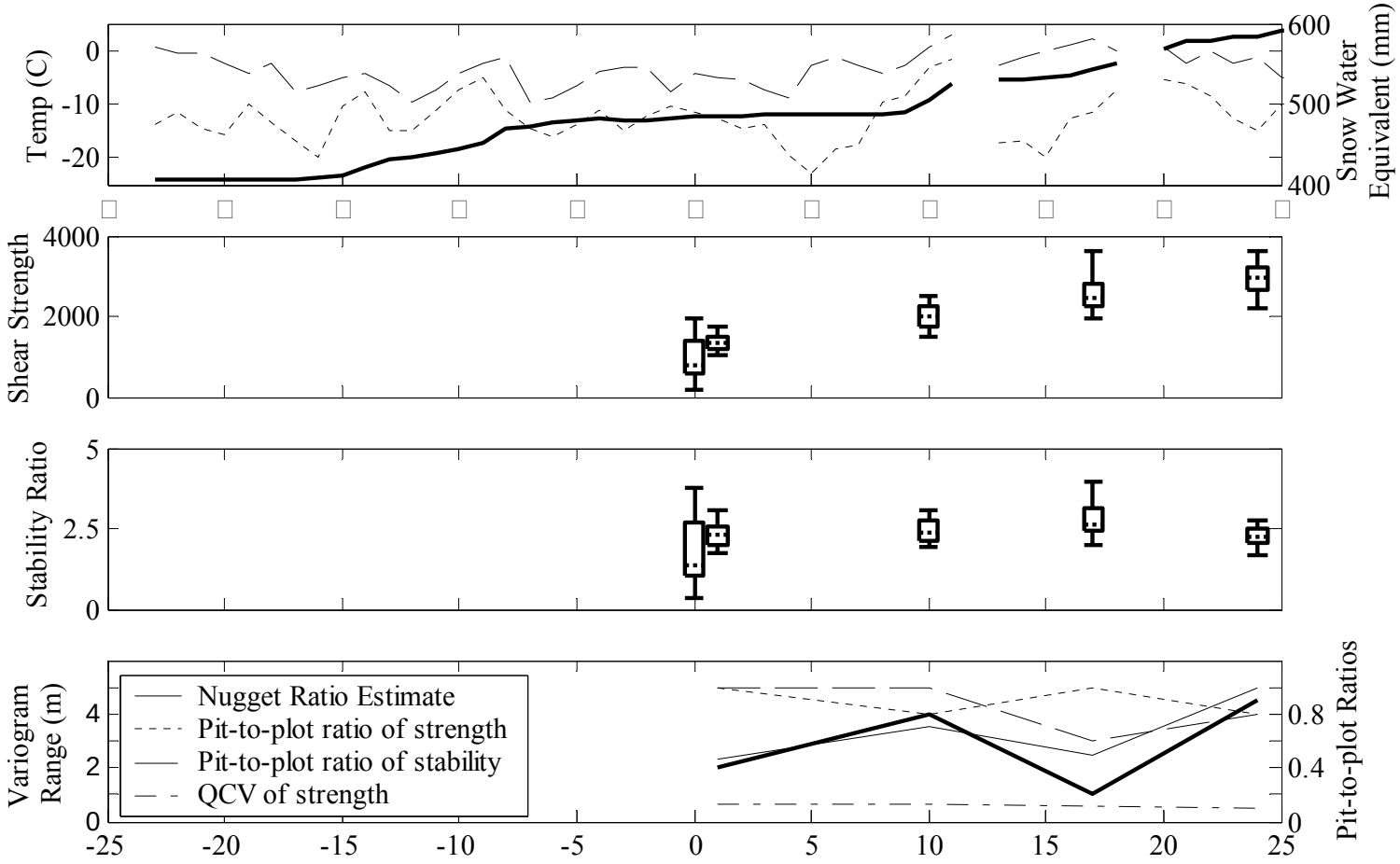

Figure 49. Weather data (top), box plots of shear strength and stability ratios (middle; dotted lines indicate medians, boxes the interquartile range, whiskers extend to 0.05 and 0.95 quantiles), and summaries of the statistical and spatial characteristics (bottom) of the Lionhead site. The weather data was collected at the Madison Plateau Snotel site, 25 km east of the Lionhead site.

The Alleys

We sampled the Alleys on February 7. Slab and weak layer characteristics are summarized in Table 7 and Table 8. Avalanches had run adjacent to the site, probably during the January 26 avalanche cycle, allowing for safe access. The field crew was concerned that the avalanches had collapsed the surface hoar layer across the site, but both layers of surface hoar were upright in pits dug around the site during the initial setup (Figure 50). Debris had come within 3 m of the eastern edge of the site, along the outside margins of Plots 2 and 3 (Figure 51).

Table 7. Characteristics of the slab and weak layer for each plot at the Lionhead site.

	Alley	Plot 1	Plot 2	Plot 3	Plot 4
Median Thickness (cm)	53.25	53	61	61	86
QCV of Thickness	0.011	0.009	0.008	0.016	0.006
Median Density (kg m^{-3})	151	158	182	213	209
QCV of Density	0.051	0.021	0.018	0.030	0.011
Median Shear Strength (Pa)	775	1363	2001	2551	2927
QCV of Strength	0.440	0.125	0.130	0.108	0.093
Median Stability Index	1.37	2.29	2.38	2.65	2.45
QCV of Stability Index	0.440	0.125	0.130	0.124	0.104

Table 8. Rates of change of slab and plot characteristics between Lionhead plots.

	Alley and Plot 1	Plots 1 and 2	Plots 2 and 3	Plots 3 and 4
Number of days between:	1	9	7	9
Change in Median Slab Thickness (cm d^{-1})	-0.25	0.89	0.00	2.78
Change in Median Slab Density (kg m^{-3} d^{-1})	7	0.26	4.5	-0.4
Change in Median Shear Strength (Pa d^{-1})	588	71	79	42
Change in Median Stability (d^{-1})	0.92	0.01	0.04	-0.02
Significance, change in Strength	<0.001	<0.001	<0.001	<0.001
Significance, change in Stability	<0.001	0.037	<0.001	<0.001

Location Lionhead Alleys
Date 20040207
Time 1030
Observer KK
Aspect 80
Inclination 26

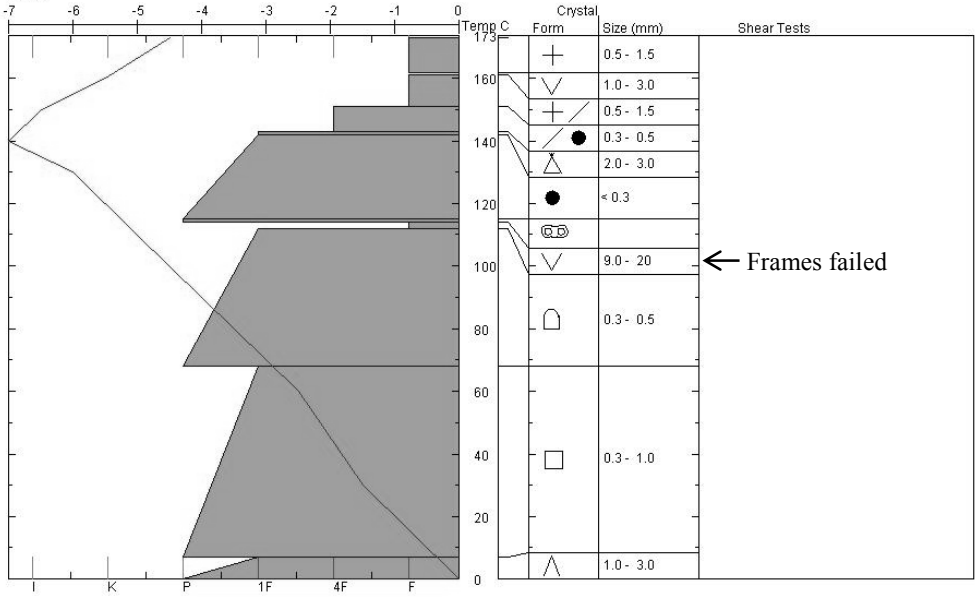

Figure 50. Manual profile for Lionhead Alleys and Plot 1

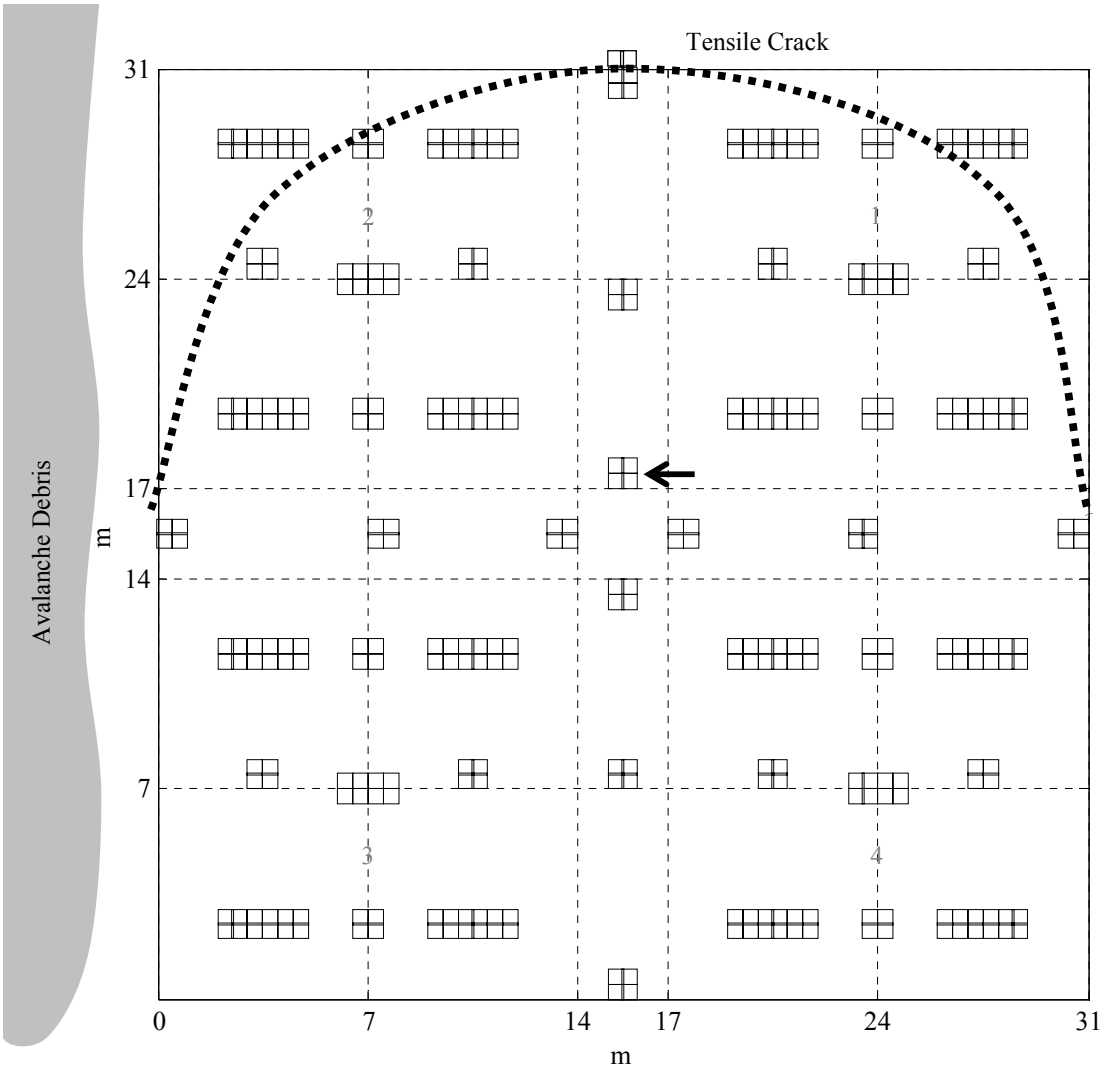

Figure 51. Layout of the Lionhead site. Plots were sampled in the order indicated in gray. The avalanche debris, in solid gray, was from avalanches prior to sampling. The arrow indicates the location of shear frames 14 and 15, down-slope of the arrow, and 16 and 17, up-slope of the arrow. The dashed line indicates the tensile crack.

One quarter of the way into the sampling of the alleys, the upper surface hoar layer collapsed. The lower surface hoar layer remained upright and intact (Figure 52). The collapse occurred between shear frame measurement 15 and 16 (Figure 53). A tensile crack opened up across the site, arcing from the corner of the cross-slope alley, up and across the upper two plots to the top of the up-slope alley (Figure 51).

Figure 52. Close-up photo of the tensile crack and collapsed surface hoar, taken shortly after the collapse. Ruler marked in centimeters.

Prior to the collapse, it was hard to determine which of the surface hoar layers failed in the shear frame tests, because both layers were disrupted as the test failed. After the collapse, the shear frames tended to fail on the upper, collapsed layer. The shear strength measured decreased dramatically after the collapse (Figure 53; Table 9). The median shear strength prior to the collapse was 1697 Pa, with median stability index of 3.08. Post collapse, the median shear strength dropped to 657 Pa, and median stability index to 1.16. Two additional measurements were made above the fracture at the upslope end of the alley. These two tests, 25 and 26, were more than 1000 Pa stronger than the adjacent tests below the fracture (Figure 53).

Table 9. Comparison of tests made in the collapsed and un-collapsed areas of the Lionhead Alley and Plot 1

	Alley	Plot 1
Median Shear Strength, un-collapsed	1697	1432
Median Shear Strength, collapsed	657	1314
Median Stability Index, un-collapsed	3.08	2.32
Median Stability Index, collapsed	1.16	2.26

Using test order as a proxy for time, increase in shear strength through time after the collapse was significant ($p < 0.0143$; $R^2 = 0.174$; Figure 53). Sometimes, observers note that shear strength increases dramatically after the collapse of a weak layer (Landry 2002). That was not the case with this layer. The presence of the second, un-collapsed surface hoar layer may have confounded the trend.

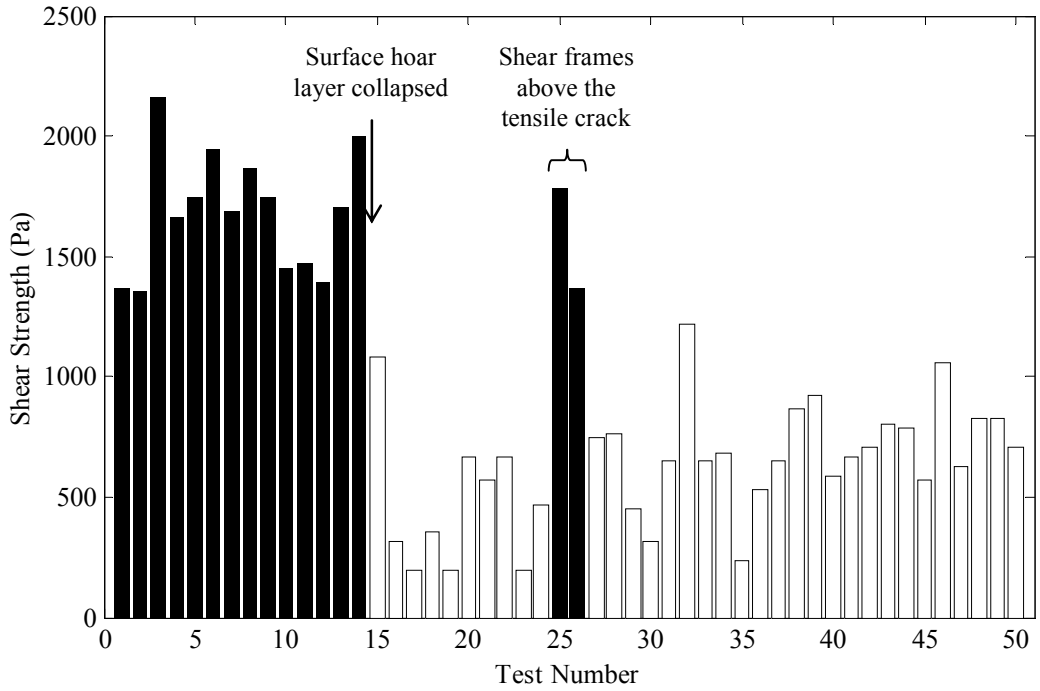

Figure 53. The Alley samples, in measurement order. The collapse occurred between tests 15 and 16, and the white bars indicate tests conducted on the collapsed layer. Tests 25 and 26 were made above the tensile crack, just upslope of tests 23 and 24.

It was not possible to determine from the Alley data if any site-wide trends existed. The number of pre-collapse tests was insufficient, and concentrated within the lower limb of the upslope alley, and the post collapse results changed through the sample period.

Plot 1

We sampled the upper right plot on the following day, February 8 (Figure 51). The slab changed little overnight (Table 8; Figure 50). The presence of the tensile crack dictated our choice of the first plot, because we wanted to compare collapsed and un-collapsed tests.

The location of the tensile crack was still apparent, so tests could be classified as un-collapsed if above the crack, and collapsed if below. Although the collapsed and un-collapsed tests still differed ($p = 0.061$), the difference was much less than the day before (Table 9). The post-collapse strengthening observed in the alley sample continued through the night. It appeared that the un-collapsed areas weakened slightly, although the presence of the double surface hoar layer complicates interpretation because it was hard to tell in which layer the shear frames produced fractures.

A significant ($p = 0.002$) linear trend was present in the Plot 1 shear strength data, but it explained too little of the variance ($R^2 = 0.005$) to affect the variogram analysis (Table 10). The trend indicated that tests at the top of the plot tended to be stronger. The un-collapsed tests occurred in the upper portion of the plot, and potentially explained the trend.

Table 10. Significance, correlation, and coefficients of the linear trends in shear strength and stability indices at the Lionhead site. Trends that were significant and explained more than 10% of the variability are indicated in bold.

		p-value	R^2	a_1	a_2	a_3
Alley	Shear Strength	**0.002**	**0.246**	1464.3	4.5	-35.2
	Stability Index	**0.006**	**0.274**	2.8221	0.0045	-0.0708
Plot 1	Shear Strength	0.002	0.005	1195.6	11.8	-4.9
	Stability Index	**0.005**	**0.116**	2.4423	0.0271	-0.0327
Plot 2	Shear Strength	0.3117	0.239	2645.3	31.8	-36.1
	Stability Index	0.017	0.085	3.1735	0.005	-0.0325
Plot 3	Shear Strength	< **0.000**	**0.128**	2217.2	3.5	43.9
	Stability Index	< **0.000**	**0.289**	2.5702	-0.0391	0.0724

Plot 4	Shear Strength	0.003	0.063	3710.4	-36.8	14.2
	Stability Index	0.0906	0.04	2.8206	-0.0257	0.008

The variogram of Plot 1 had a nugget ratio estimate of 0.66, and range of 1.5 m, within the intra-pit distance (Figure 54). This relatively short range meant all the spatial correlation occurred within the individual pits. Because there was no significant spatial structure at the inter-pit distances, any pit should have represented the plot. This was reflected in the pit-to-plot ratios, with all pits representative of Plot 1 strength (Figure 55) and stability (Figure 56).

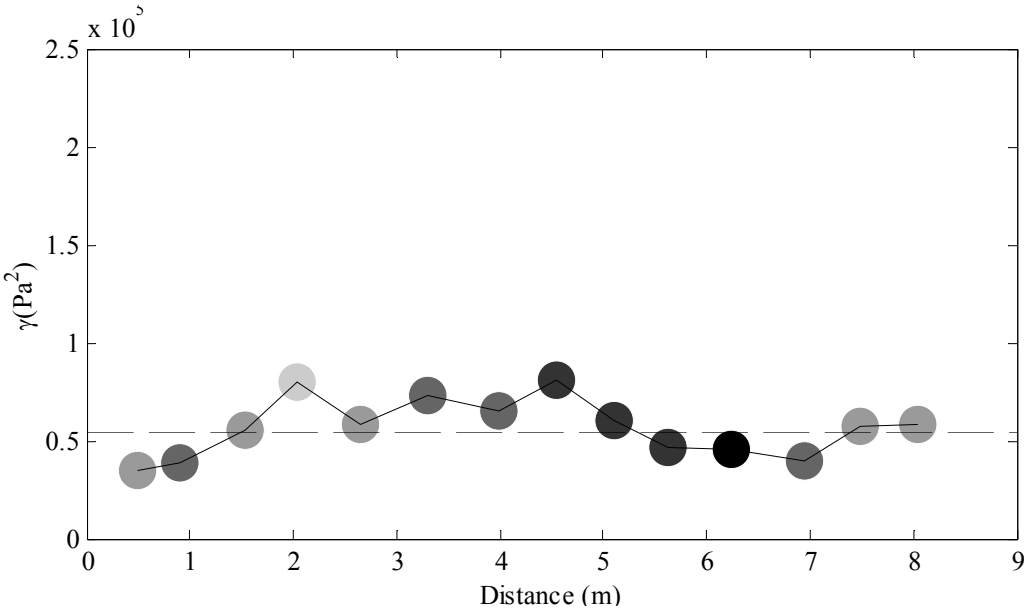

Figure 54. Variogram for Lionhead Plot 1, plotted with a lag distance of 0.6 m. Gray circles indicate the number of point-pairs within bins: 20% gray less than 50 point-pairs, 40% gray 51-100 point-pairs, 60% gray 101-150 point-pairs, and 80% gray more than 151 point-pairs.

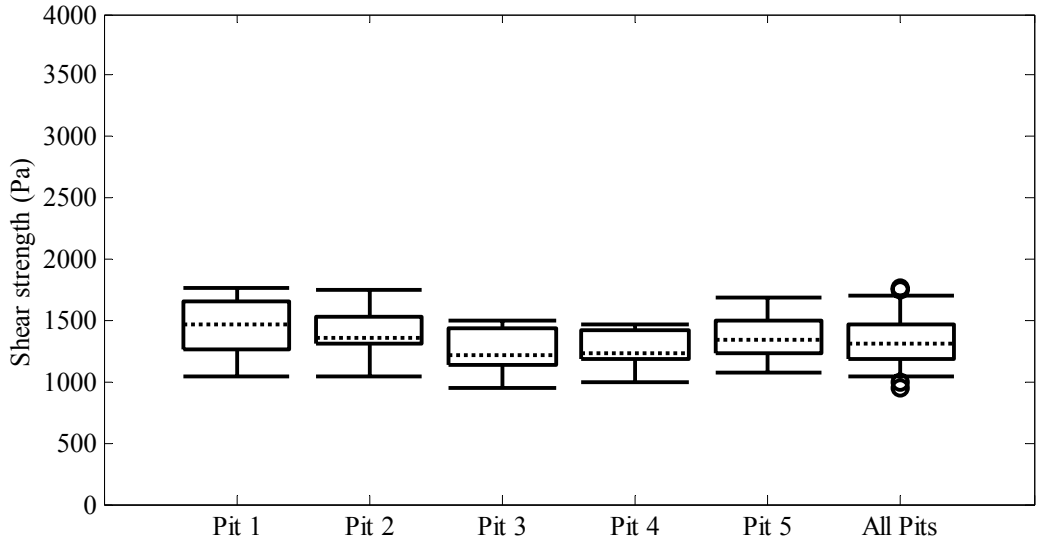

Figure 55. Box plots for the pit-to-plot comparisons of shear strength for Lionhead Plot 1. All pits were representative of the plot. Dotted lines indicate medians, boxes the interquartile range, whiskers extend to 0.05 and 0.95 quantiles, and circles indicate outliers.

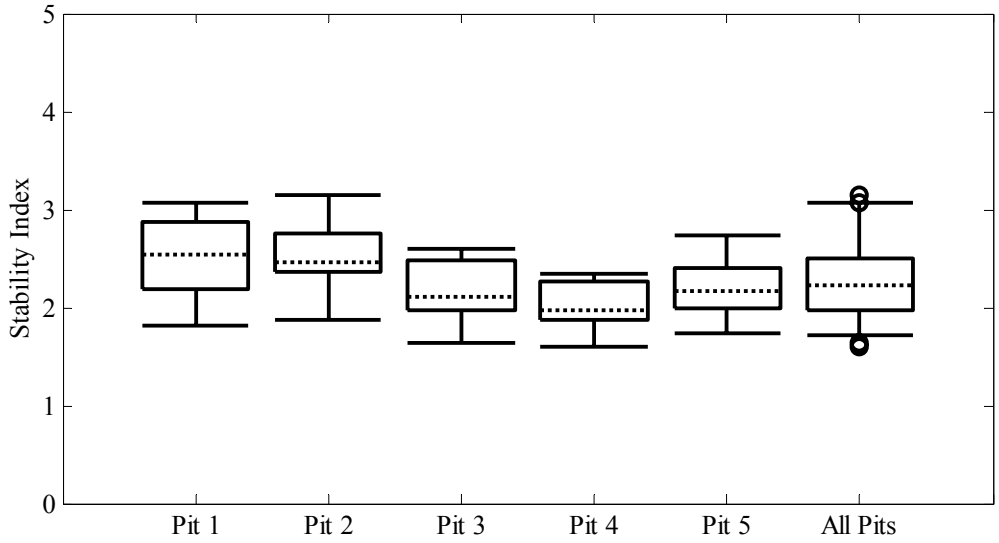

Figure 56. Box plots for the pit-to-plot comparisons of stability indices for Lionhead Plot 1. All pits were representative of the plot. Dotted lines indicate medians, boxes the interquartile range, whiskers extend to 0.05 and 0.95 quantiles, and circles indicate outliers.

Plot 2

After sampling Plot 1, a thin layer of surface hoar formed, then was buried by light snowfall on February 9-12 (Figure 57; Figure 49). Storm totals for the region of the field site were estimated at 15 cm, with an additional 10 cm falling on February 15 and 16 (Gallatin National Forest Avalanche Center 2004). The snowfall obscured all traces of the tensile crack. Although the crack was somewhat symmetrical around the up-slope alley, there were not obvious differences in shear strength or test behavior to differentiate collapsed or un-collapsed tests and accurately separate the tests into two groups.

Location	Lionhead Plot 2
Date	20040217
Time	1130
Observer	KB, KK
Aspect	36
Inclination	31

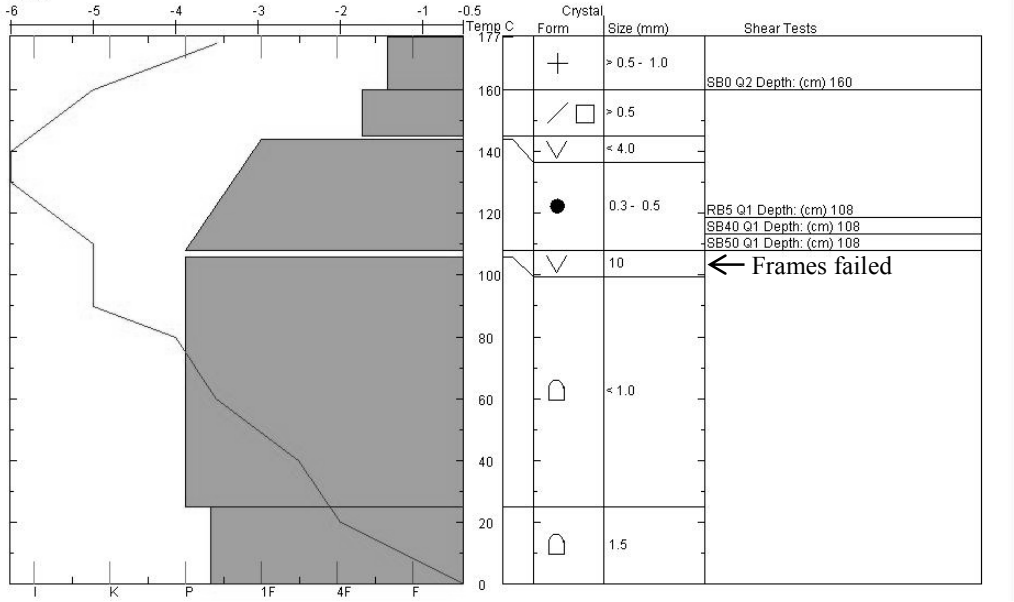

Figure 57. Manual profile for Lionhead Plot 2

A significant linear trend existed within the shear strength across Plot 2 (Table 10), with tests in Pit 2 having a greater probability of lower strength than tests in Pit 4. The trend reflected the location of the tensile crack, with tests below the tensile crack tending to be stronger than tests above. The collapsed surface hoar layer may have contributed to the strengthening in several ways. The grains in the upper layer were flattened down-slope. The contact between grains would have increased, leading to increased bonding and therefore increased strength between the lower layer of the slab, the collapsed surface hoar grains, and the underlying snow. The force of the collapse may have compacted the lower surface hoar layer, forcing the bottom of those surface hoar grains deeper into the underlying snow. The interpenetration would have lead to increased bonding and strengthening at the interface between the lower surface hoar layer and the underlying snow, one mechanical explanation for strengthening of surface hoar layers (Jamieson and Schweizer 2000). Unfortunately, reliable SMP measurements were not available from Plot 2, so detailed structural differences between collapsed and un-collapsed areas can only be hypothesized.

The variogram of the de-trended data had a nugget ratio estimate of 0.55, indicating little spatial autocorrelation (Figure 58). The range was 4 m, suggesting inter-pit differences. The pit-to-plot ratios for Plot 2 also suggested inter-pit differences, with the location of the tensile crack explaining some of the differences. The tensile crack ran below or across the corner of Pit 4. Pit 4, with the lowest median strength, was not representative of the plot strength ($p < 0.001$; Figure 59). Some evidence existed that Pit 3, with the highest median strength, may not have been representative of the plot strength

(p = 0.07) and the pit was not representative of Plot 2 stability index (p = 0.003; Figure 60).

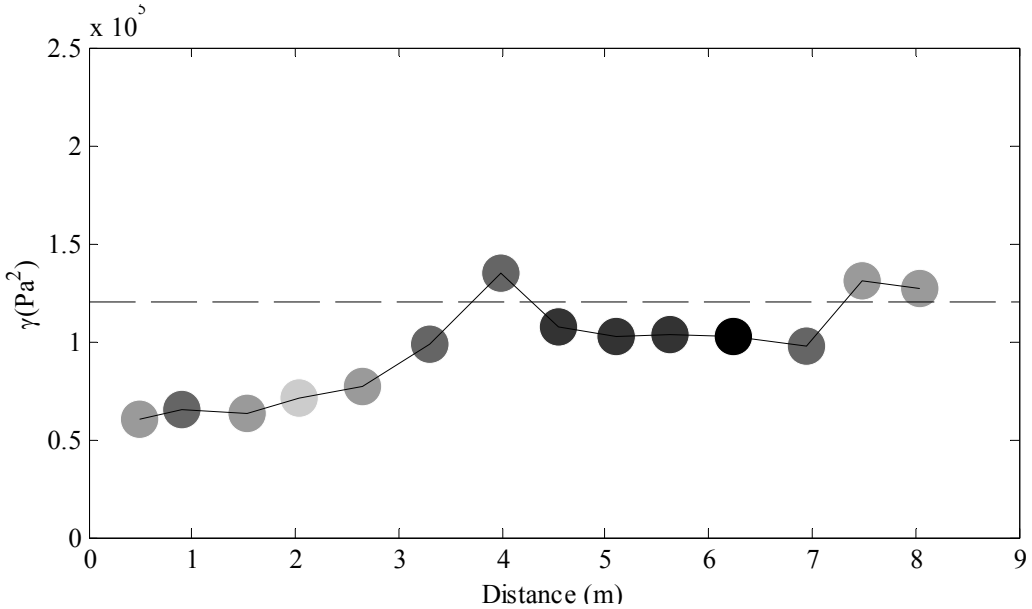

Figure 58. Variogram for Lionhead Plot 2, plotted with a lag distance of 0.6 m. Gray circles indicate the number of point-pairs within bins: 20% gray less than 50 point-pairs, 40% gray 51-100 point-pairs, 60% gray 101-150 point-pairs, and 80% gray more than 151 point-pairs.

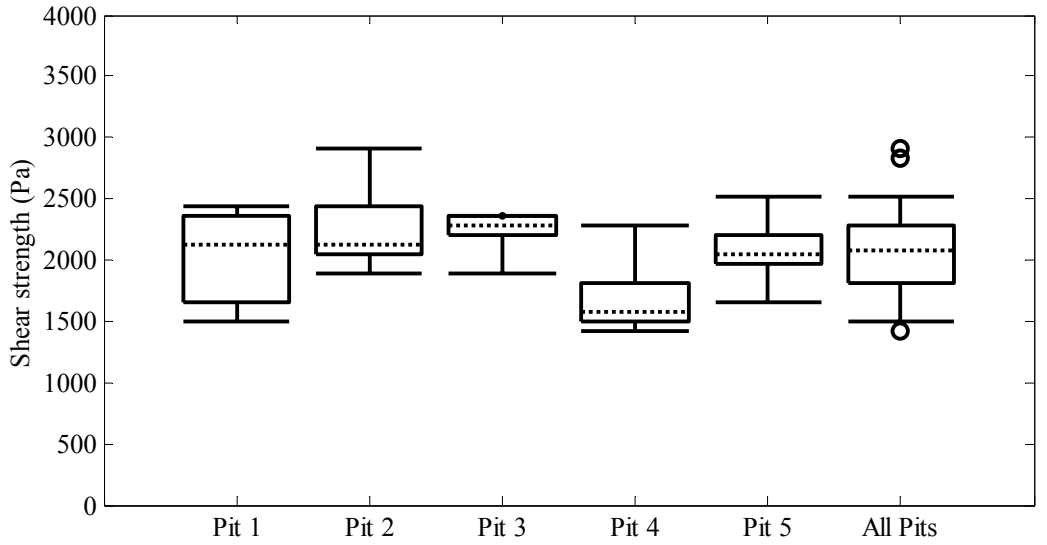

Figure 59. Box plots for the pit-to-plot comparisons of shear strength for Lionhead Plot 2. Pit 4 was not representative (p < 0.001), and some evidence existed that Pit 3 was not representative of the plot strength (p = 0.07). Dotted lines indicate medians, boxes the interquartile range, whiskers extend to 0.05 and 0.95 quantiles, and circles indicate outliers.

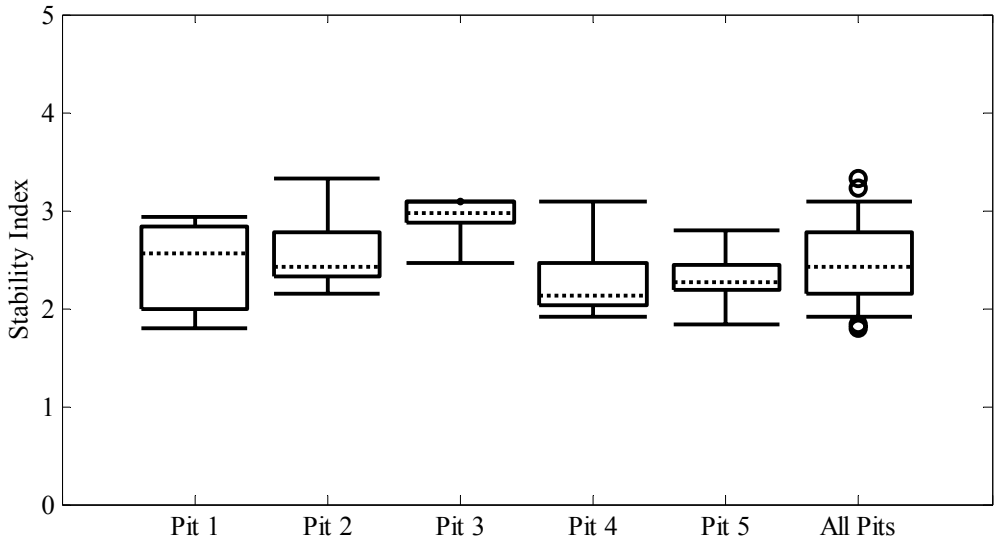

Figure 60. Box plots for the pit-to-plot comparisons of stability indices for Lionhead Plot 2. Pit 3 was not representative of plot stability ($p = 0.003$). Dotted lines indicate medians, boxes the interquartile range, whiskers extend to 0.05 and 0.95 quantiles, and circles indicate outliers.

Plot 3

A warm storm occurred on February 18 and 19, with 30 to 45 cm of dense snow falling at the Lionhead site (Gallatin National Forest Avalanche Center 2004). The minimum temperature recorded at the Madison Plateau Snotel site was -1.6° C for February 18. The station then experienced problems, so no data was recorded for February 19. A period of high pressure followed the storms, with clear skies and temperatures dropping to -20° C on February 22. Plot 3 was sampled on February 24, as snowfall began (Figure 49). Although slightly more variable, the slab thickness did not differ markedly from Plot 2, but density did increase (Table 7). No manual profile was available.

The shear strength in Plot 3 was quite skewed, with several very strong measurements occurring at the top of the plot. There was a significant linear trend across the site ($p < 0.001$, $R^2 = 0.128$; Table 10). Shear strength tended to be lower at the bottom

of the site than at the top. It appeared that the entire plot collapsed while sampling the Alleys, so the trend should not reflect the presence of an un-collapsed weak layer. If Plot 3 was affected by prior sampling, Plot 4 should have a similar or reflected trend, as did Spanky's Plots 3 and 4. However, there were no significant trends in the Lionhead Plot 4 data.

The trend was removed and the variogram analysis utilized the residuals. The nugget ratio estimate was 0.5, indicating little spatial autocorrelation. The variogram was almost pure nugget (Figure 61).

The pit-to-plot ratios for shear strength indicated that all pits were representative of Plot 3 (Figure 62). However, Pits 2 and 4 were not representative of the plot stability index ($p = 0.009$, $p < 0.001$; Figure 63). Because stability indices were calculated from a single set of slab properties for each pit, spatial variations in slab properties may not have been reflected in the stability index.

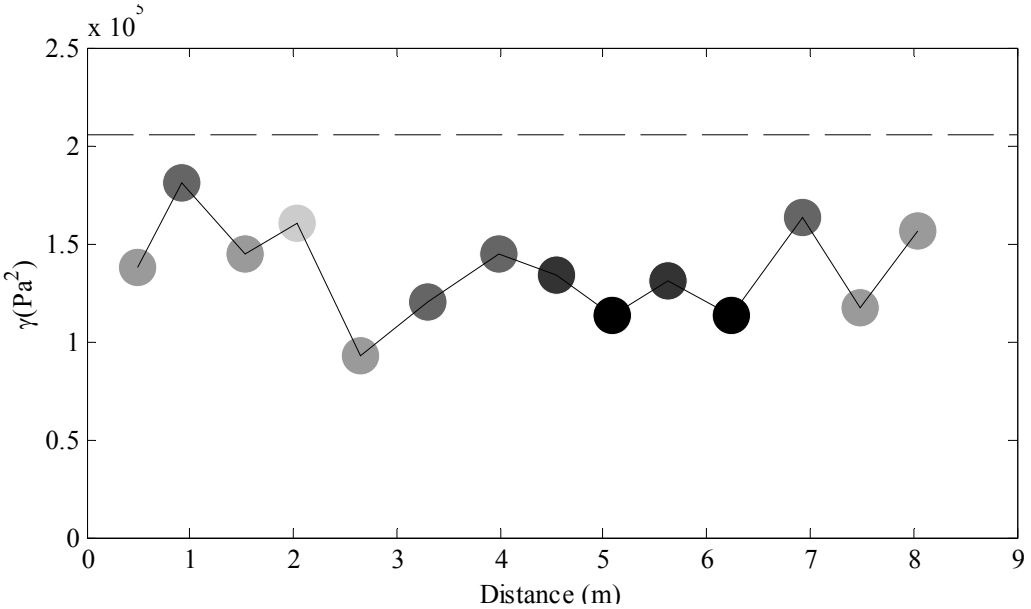

Figure 61. Variogram for Lionhead Plot 3, plotted with a lag distance of 0.6 m. Gray circles indicate the number of point-pairs within bins: 20% gray less than 50 point-pairs, 40% gray 51-

100 point-pairs, 60% gray 101-150 point-pairs, and 80% gray more than 151 point-pairs.

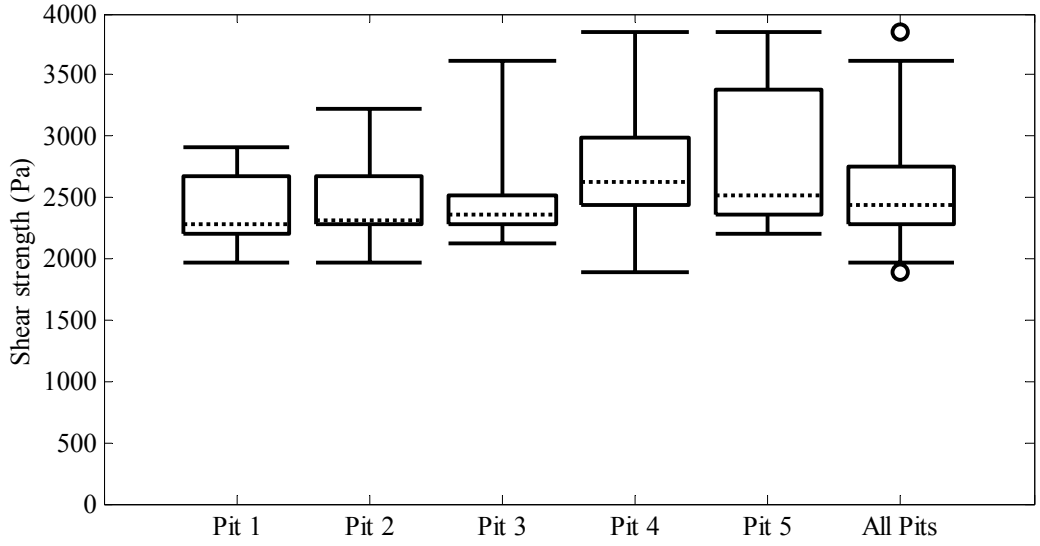

Figure 62. Box plots for the pit-to-plot comparisons of shear strength for Lionhead Plot 3. All pits were representative of the plot. Dotted lines indicate medians, boxes the interquartile range, whiskers extend to 0.05 and 0.95 quantiles, and circles indicate outliers.

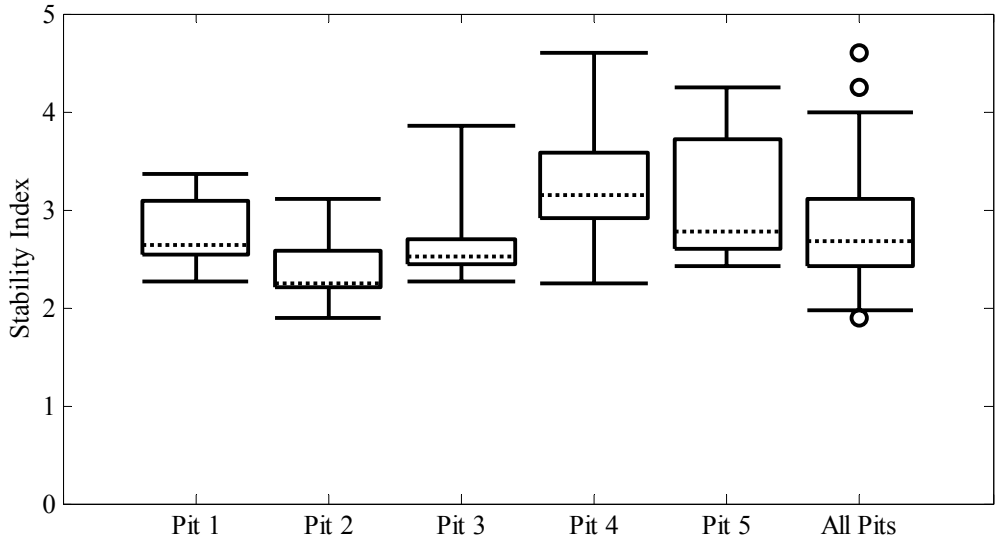

Figure 63. Box plots for the pit-to-plot comparisons of stability indices for Lionhead Plot 3. Pits 2 and 4 were not representative of the plot. ($p = 0.009$, $p < 0.001$). Dotted lines indicate medians, boxes the interquartile range, whiskers extend to 0.05 and 0.95 quantiles, and circles indicate outliers.

Structural data from SMP measurements provide some interesting additional information. Slab thickness was autocorrelated, and the thickness was kriged to coordinates of the shear frame tests (Lutz 2004). There was a significant linear trend within the kriged slab thickness ($p < 0.001$, $R^2 = 0.764$), with the slab at the top of the plot tending to be 1 or 2 cm thicker than the slab at the bottom. Other studies have found that slabs have more spatial structure than weak layers, and trends in slab characteristics and strength are similar in direction (Birkeland et al. 2004; Kronholm et al. 2004; Kronholm 2004).

I attempted to relate slab thickness to density, and recalculate the stability indices for each test using the kriged thicknesses. Unfortunately, there was not enough correlation within the nine slab thickness and water content measurements to build a relationship between the two ($p = 0.38$, $R^2 = 0.107$). Recalculating the stability indices using kriged slab thickness and the measured water content changed the calculated stability indices by no more than 0.25.

Plot 4

Another storm moved through southwestern Montana on February 25-29 (Figure 49). Reports of storm totals of 35 cm came from the Lionhead area (Gallatin National Forest Avalanche Center 2004). Avalanches occurred in the new snow, probably running on near-surface facets formed February 20-24 (Figure 64), but the Gallatin National Forest Avalanche Center (2004) did not report any avalanches fracturing on the January surface hoar layer. Stability tests conducted on February 27, on a slope similar to the study site, produced very hard or no results on the surface hoar layer (Chabot 2004). Only trace amounts of snowfall accumulated between February 29 and March 2 (Figure

49), when Plot 4 was sampled (Gallatin National Forest Avalanche Center 2004). The slab measurements in Plot 4 were the most uniform of the five sample days (Table 7).

A significant linear trend existed within the shear strength data, but explained too little of the variance to be removed from the data (Table 10). The non-spatial QCVs indicated that Plot 4 was the most uniform of the plots (Table 7).

The variogram for Plot 4 was similar to a pure nugget variogram, indicating that what little correlation existed was not strong (Figure 65). With such little spatial autocorrelation indicated by the variogram, all pits could be expected to be representative of the plot in the pit-to-plot ratios. However, Pit 4, with the highest median pit strength, was not representative of either plot strength ($p = 0.019$; Figure 66) or stability index ($p = 0.033$; Figure 67).

Slab thickness kriged from SMP data (Lutz 2004) again indicated a significant slope-scale trend ($p = 0.012$, $R^2 = 0.121$). The slab tended to thicken slightly towards the top of the plot. Unfortunately, as in the case of Plot 3, there was not a strong relationship between the kriged and measured slab properties ($p = 0.162$, $R^2 = 0.260$) so stability indices could not be recalculated.

Location	Lionhead Plot 4
Date	20040302
Time	1000
Observer	KK
Aspect	38
Inclination	33

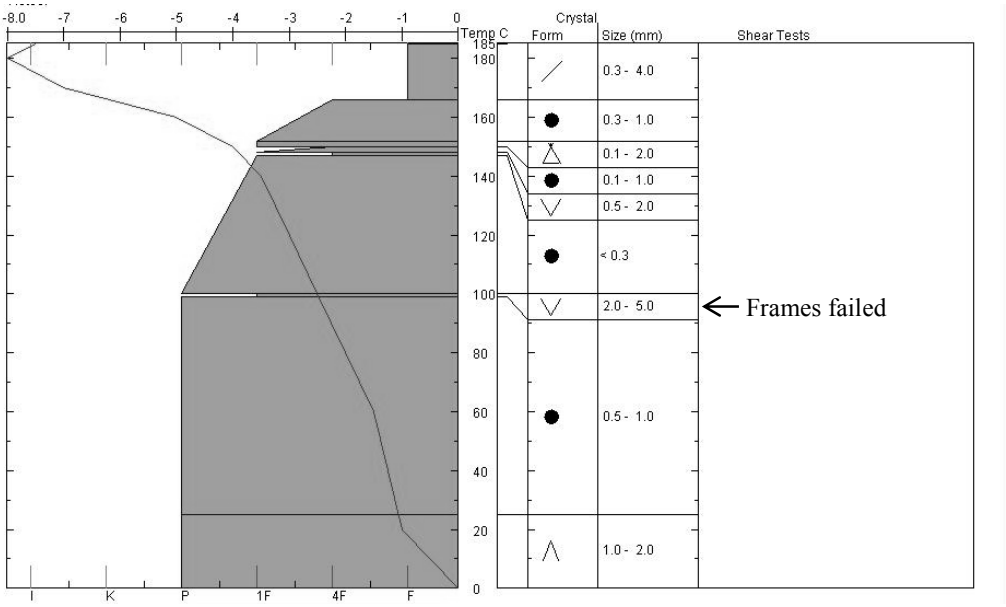

Figure 64. Manual profile for Lionhead Plot 4

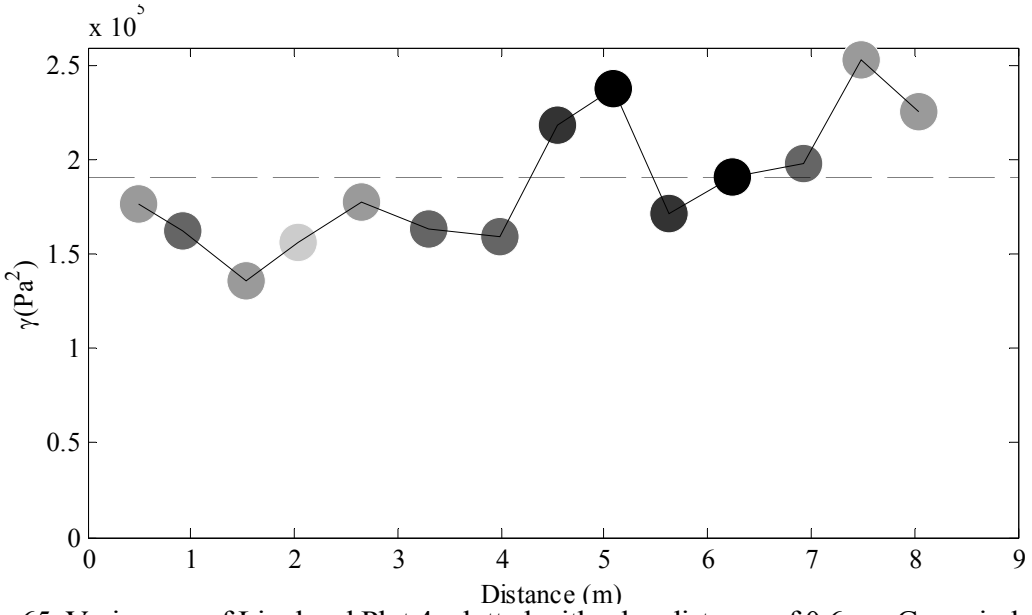

Figure 65. Variogram of Lionhead Plot 4, plotted with a lag distance of 0.6 m. Gray circles indicate the number of point-pairs within bins: 20% gray less than 50 point-pairs, 40% gray 51-100 point-pairs, 60% gray 101-150 point-pairs, and 80% gray more than 151 point-pairs.

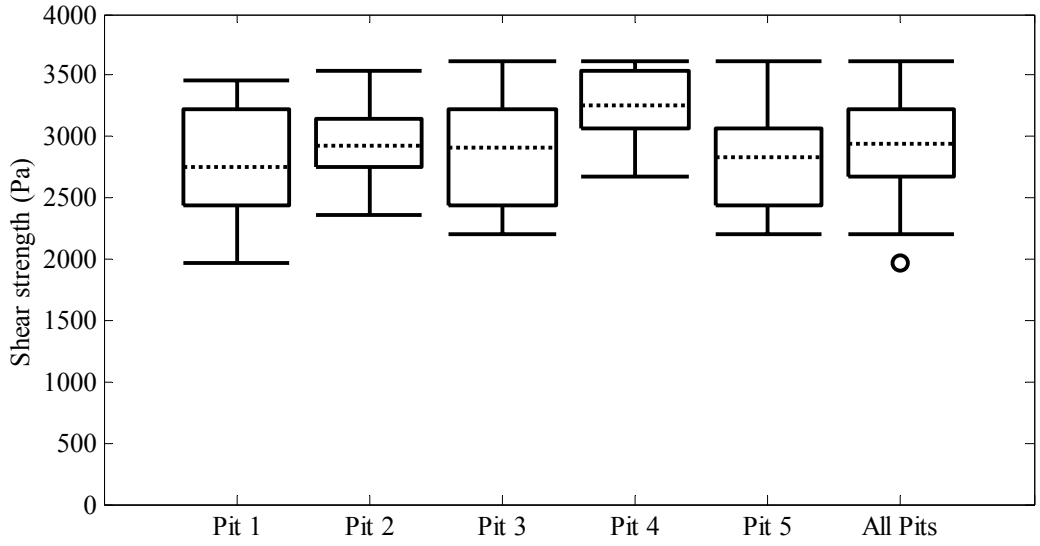

Figure 66. Box plots for the pit-to-plot comparisons of shear strength for Lionhead Plot 4. Pit 4 was not representative ($p = 0.019$) of the plot. Dotted lines indicate medians, boxes the interquartile range, whiskers extend to 0.05 and 0.95 quantiles, and circles indicate outliers.

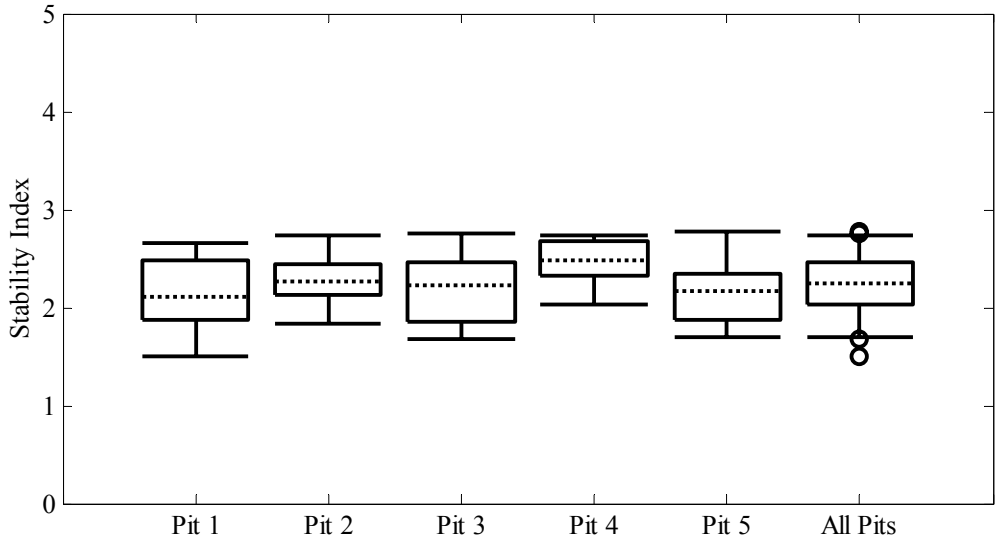

Figure 67. Box plots for the pit-to-plot comparisons of stability indices for Plot 4. Pit 4 was not representative ($p = 0.033$) of the plot. Dotted lines indicate medians, boxes the interquartile range, whiskers extend to 0.05 and 0.95 quantiles, and circles indicate outliers.

Temporal Change

The collapse of the upper surface hoar layer allowed the comparison of both a weak layer and a collapsed weak layer over a ten-day period, although the doubled surface hoar layer added some complication. The shear strength measured after the collapse increased significantly through the day. We were able to capture the rapid strengthening of a weak layer after a collapse. A day later, there was little difference in strength between collapsed and un-collapsed tests.

The change in median shear strength between the Alleys and Plot 1 could not be directly compared. Instead, I compared the differences between the collapsed and un-collapsed tests on each day. The difference in shear strength between un-collapsed tests of the Alley to Plot 1 was significant, as was the difference between collapsed tests (Table 9). The lack of significant difference in shear strength of collapsed and un-collapsed tests in Plot 1 (Table 9) could have been due to the presence of the second, un-collapsed surface hoar layer. It was quite hard to determine in which of the two surface hoar layers the shear frames failed. If the shear frames failed in both surface hoar layers prior to the collapse, and only in the lower layer after the collapse, the difference between tests would be lower in Plot 1.

The differences in both shear strength and stability indices between Plot 1 and 2 were significant (Table 8). The surface hoar layers continued to strengthen through time. The linear trend fit did reflect the presence of the crack, but explained little of the variance across the plot. Although the change in stability was slight, the median increased enough to be significant. The increase in range between Plot 1 and 2 suggested

divergence. So did the decrease in the pit-to-plot ratio and slight increase in the QCV of shear strength.

The increases in shear strength and stability indices between Plots 2 and 3 were significant (Table 8). The increase in shear strength was greater than the proportional increase in shear stress. Although the slab thickness did not change, the density increased. Divergence would be expected, based on my hypothesis, as the layer gained strength without significant change in the slab. Unfortunately, the Plot 3 variogram did not allow much interpretation, although the range decreased between the two. The pit-to-plot ratio for strength increased, and the ratio for the stability index decreased. The QCVs of both strength and stability indices deceased. The changes between the plots indicated both divergence and convergence, with no one indicator providing strong evidence of the temporal trend.

The increase in shear strength between Plots 3 and 4 was significant (Table 8). The decrease in the stability indices between Plots 3 and 4 was also significant (Table 8). The QCVs of both strength and stability decreased, indicating convergence. The range increased between the variograms, but neither indicated spatial correlation, so provided little evidence of change. Again, the pit-to-plot ratios indicated opposite trends, divergence indicated by the pit-to-plot ratios of strength, and convergence indicated by the pit-to-plot ratios of the stability index.

CHAPTER 5

DISCUSSION AND CONCLUSIONS

This study focused on the spatial structures of shear strength and stability on a single day, how the spatial structure changed between sample days, and how the changes in spatial structure were related to changes in the snowpack. I anticipated that changes in the shear stress of the slab would be a primary driver of change in spatial patterns, with small changes in shear stress allowing for increasing spatial variability, and large increases in stress causing decreases in spatial variability. I tried, through site selection and sampling protocol, to find sites that would offer an initially uniform snowpack. The uniform sites and sampling methodology facilitated comparisons of adjacent plots, and allowed for most of the differences between adjacent plots to be attributed to temporal change.

Spatial Structure of Shear Strength and Stability

Spatial structures in the data proved difficult to identify. Slope-scale trends, shown to be significant spatial patterns in strength and stability on less uniform slopes (Kronholm 2004), did not prove to be important in my study. Variograms indicated little autocorrelation or spatial structure. Pit-to-plot ratios indicated little spatial variability within the plots.

Linear Trends

Linear trend surfaces estimated slope-scale trends. To affect variogram analysis, a linear trend had to be both significant ($p < 0.05$) and explain more than 10% of the variation within the data. Only one plot, Lionhead Plot 3, had a trend in shear strength that had to be removed ($p < 0.001$, $R^2 = 0.123$). Four plots, Spanky's 3 and 4, and Lionhead 1 and 3, had trends in stability, and only the Lionhead 3 trend explained more than 15% of the variation in stability. The five slope-scale trends present in my data did trend up-slope, as did the trends present in Kronholm's (2004) data from Switzerland.

The stability trend in Lionhead Plot 1 was related to the collapse of the surface hoar layer and reflected the slightly stronger shear strength of the un-collapsed surface hoar. There was no significant trend in Lionhead 2 shear strength, and tests above and below the tensile crack were indistinguishable.

The trend in strength in Lionhead Plot 3 ran up-slope, with the top of the plot stronger. Several strong measurements occurred in Pits 4 and 5, and certainly biased the trend. The trend in stability followed the trend in strength, even though the slab was thicker at the top of the plot. Measurements from the SMP indicated that the slab was thicker at the top of the plot (Lutz 2004), which should exert more stress on the weak layer and decrease stability. The difference in strength was sufficient to counteract the changes in slab thickness. Other studies have found that slabs tend to have more spatial structure than weak layers, and trends in slab characteristics and strength are similar in direction (Birkeland et al. 2004; Kronholm et al. 2004; Kronholm 2004).

In both Spanky's Plot 3 and 4, the linear trend indicated stability indices were higher along the lower edge of the plots than in the upper portion (Figure 68). These

trends were not apparent in the Alley samples or in Plots 1 and 2. The earlier sampling may have affected the slab in Plots 3 and 4. As creep occurred within the snowpack, the slab may have been pinned in place by the hardened snow in the Alleys, or the disturbed snow within the Alleys may have caused slight differences in drifting along the bottom of the plots. Unfortunately, SMP data was not available, and there were not sufficient manual measurements to determine if trends in slab properties could have explained the trends in stability indices. I can only speculate at the influence of previous sampling, and the causes of the trends.

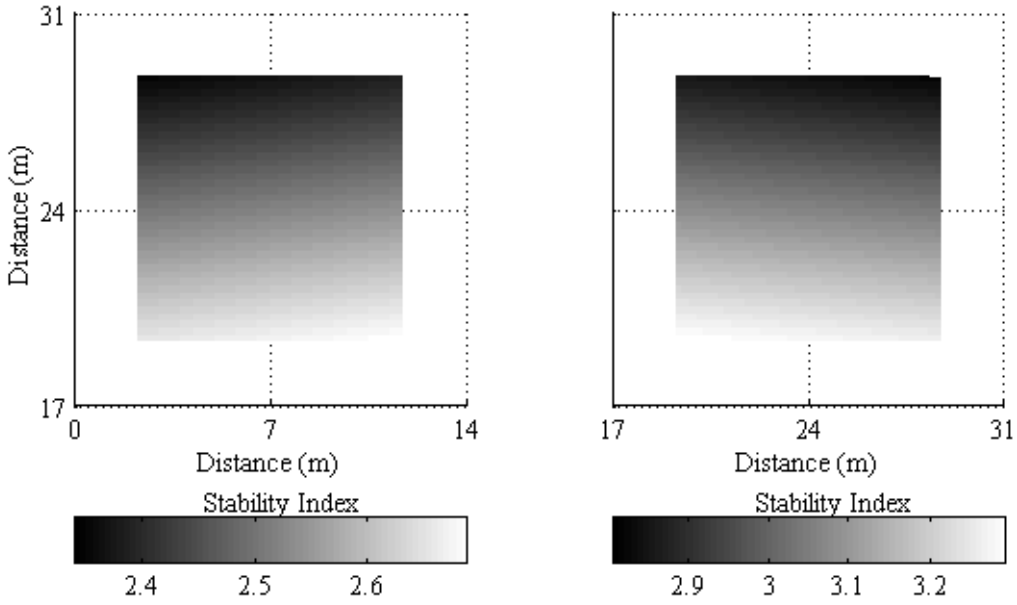

Figure 68. The two trend surfaces in Spanky's 3 and 4 stability indices.

One of the primary differences between my study and others was the wind-sheltered location of the study sites. Conway and Abrahamson (1988) related the autocorrelation within their data to the size of wind ripples preserved in the old snow. Kronholm (2004) used alpine sites, and attributed the slope-scale trends to wind effects.

If wind was the primary cause, removing wind effects from my sites should greatly reduce the resultant slope-scale trends, as seen in my results.

Slope angles varied considerably at some of Kronholm's (2004) sites, by as much as 24°. This would also explain some of the slope scale trends. Stability should be lower on steeper slopes because the gravitational component exerts a greater force on the snowpack. Therefore, changes in slope angle would be seen in trend surfaces, with the trends reflecting changes in the underlying terrain. With the planar slopes I used, there should be no such trends driven by slope angle.

Variogram Analysis

The variograms indicated little autocorrelation even after removing the few trends present in my data. There may be several reasons, including error inherent to the shear frame test, and problems with the sampling array. For shear strength, our plot-wide coefficients of variation ranged from 12% to 24%, which compared favorably with the coefficients of variation ranging from 3% to 66% (with a mean of 15%) reported by Jamieson and Johnston (2001) for 809 sets of shear frame measurements.

Even with favorable comparisons to other studies, my shear frame measurements could still contain considerable error inherent to the shear frame. Shear frames can be challenging to conduct. Improper test preparation can influence the test result, and operator errors may contribute to the fundamental error of the test. I sought to minimize operator error with a consistent methodology and by using the same operator for all plots at a site.

The measurement support directly influences the fundamental error of sampling, with larger measurement support reducing the amount of fundamental error, essentially

binning some variability of smaller tests into one result (Myers 1997). Shear frame measurements, with measurement support of 0.025 m^2, could contain considerable fundamental error which would account for the considerable nugget ratio estimates.

Another potential source of error in the shear frame measurements were the gages used. While only one gage was used within a plot, different gages were used as the weak layers strengthened, complicating plot comparisons somewhat when the gage resolution differed. The 0.2 to 5 kg gage read in 0.05 kg increments, the 2 to 20 kg gage in 0.5 kg increments (Figure 69). The larger increments effectively grouped the shear frame results into bins 0.5 kg wide when using the 2 to 20 kg gage. The grouping reduced the apparent variability of test results. With the 0.2 to 5 kg gage, there were usually 60-70 different values for the 72 shear frame results. With the 2 to 20 kg gage, there were usually 35-45 different values for the 72 shear frame results.

The sampling array could be another reason that the variograms indicated little correlation, if the spatial autocorrelation of shear strength occurs at distances less than 1 m. With measurements spaced 0.5 m apart, the sampling array would miss correlation at distances less than one meter. Both Spanky's Plot 1 and results from my field experience, where tests placed closer than 0.5 m were more similar than tests spaced at or greater than 0.5 m, support such short correlation distances. Other research on similar slopes supports short correlation distances, with the strongest and weakest tests sometimes adjacent (Landry 2002). In a continental snowpack,, researchers found autocorrelation lengths for shear strength between 0.2 and 1.3 meters (Conway and Abrahamson 1988).

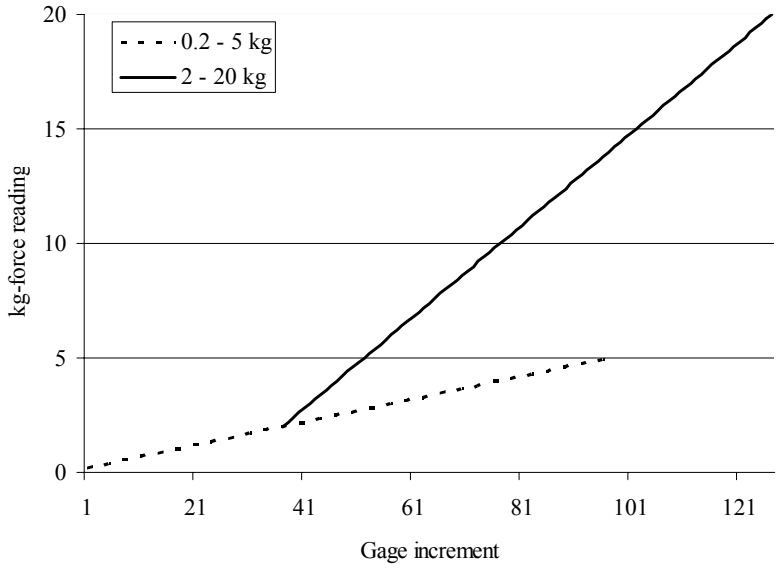

Figure 69. Diagram of the gage increments (or resolution) and resulting kg-force readings.

On slopes that had strong slope-scale trends, Kronholm (2004) found adjacent test results were much more correlated. This suggests that trends imposed by wind or slope angle exerted considerable influence on shear strength, and may be strong enough to override measurement errors. Without trends from wind or changes in slope angle, my sites were essentially uniform. If the variations in measurements were due primarily to measurement error, there would be no spatial structure or autocorrelation.

Pit-to-Plot Ratios

I expected that more pits would not be representative of the plot based on Landry's work (Landry 2002, Landry et al. 2004). In that work, 40% of the pits were not representative of the plots, while I had only four of 60 pits (6%) that were statistically not representative. Because the pit-to-plot ratios changed little, they did not provide much indication of temporal trends. Several differences between the studies might explain the differences.

One difference was the size of the plots, or the measurement extent (Blöschl 1999). My plots were about a fourth of the area of Landry's (2002), with distances between pits about a fourth of the distance between Landry's pits (Figure 70). Spatial trends at scales that Landry's plot layout could detect might be undetectable with my layouts. This would be especially true of slope-scale trends, which would cause much greater differences at the extent of Landry's study.

To examine the effects of linear trends and plot sizes, I fitted the linear trend from Lionhead Plot 4 shear strength (Table 8, p. 87) to the coordinates of Landry's tests. The Lionhead Plot 4 trend was significant, but explained too little of the variability to remove before variogram analysis. To the fitted values I added normally distributed, random values with a standard deviation of 411 Pa, the standard deviation of the pooled Lionhead Plot 4 shear strength. The resulting values in each pit were then used to calculate the pit-to-plot ratio.

In the Lionhead Plot 4 data, all pits were representative of the plot shear strength. In the extrapolated data, 3 pits were not representative (Table 11). Compare the box plot of the extrapolated values (Figure71) to the box plot for Lionhead 4 (Figure 66, p. 103). The trend is apparent in the extrapolated data, even with a large amount of random error added. Slope scale trends that were not significant at the scale of my study could influence the results at the larger scale of Landry's research.

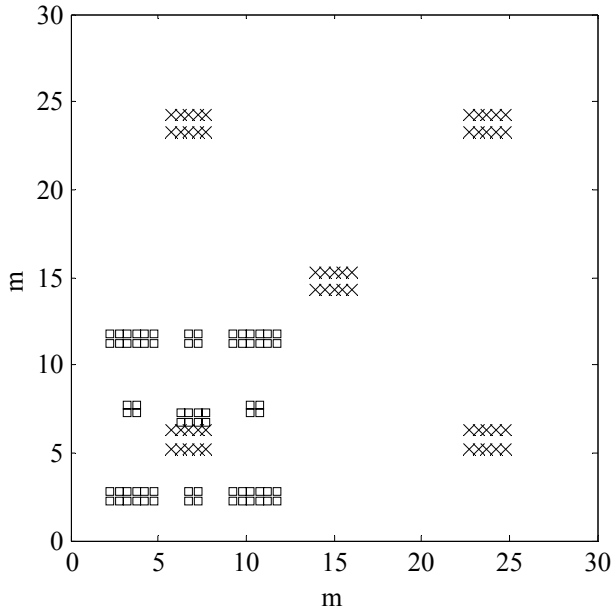

Figure 70. Comparison of test locations for Landry (2002) (x's) and the current study (squares).

Table 11. Significance of the pit-to-plot ratios of the extrapolated values. Pits 1, 4, and 5 (bold) were not representative of the plot shear strength.

	Pit 1	Pit 2	Pit 3	Pit 4	Pit 5
Significance	**0.005**	0.196	0.243	**0.019**	**0.036**

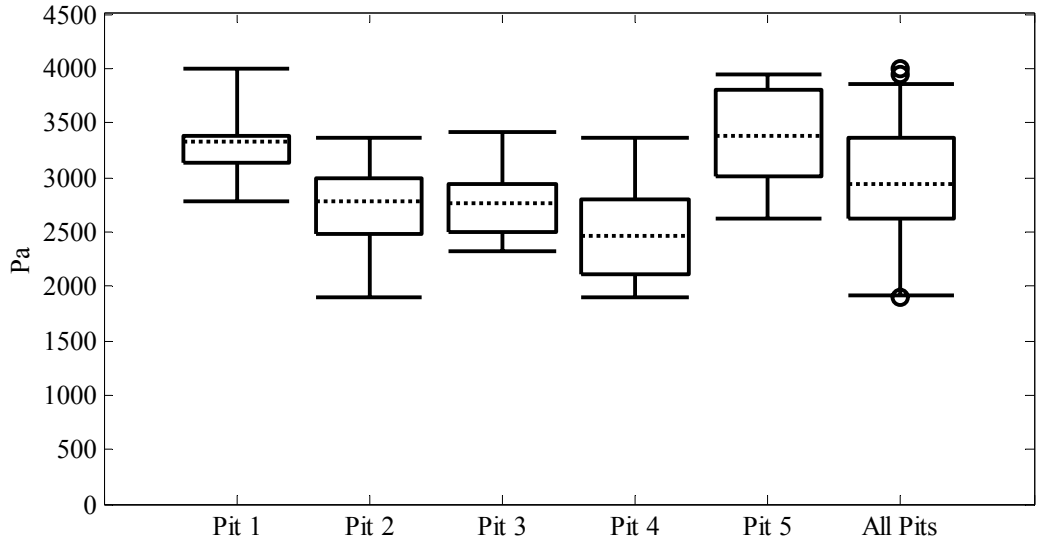

Figure 71. Box plots for pit-to-plot comparisons of extrapolated shear strength. Dotted lines indicate medians, boxes the interquartile range, whiskers extend to 0.05 and 0.95 quantiles, and circles indicate outliers.

The type of test used was another difference between the current study and Landry's (2002) work. Landry used the quantified loaded column test (Landry et al. 2001), which integrates slab characteristics into the test result. The shear frame test removes the slab from the test, and test only the weak layer. Slab properties can exhibit greater spatial correlation than weak layers (Kronholm 2004). Inclusion of the correlated slab could possibly increase the correlation between the tests, as the spatial structure of the slab is added to the lack of structure in the weak layer.

Temporal Change in Spatial Structure

The second and third questions central to my research examined temporal change in the spatial structures and factors causing change. I expected decreasing variogram ranges, increasing nugget ratio estimates, decreasing pit-to-plot ratios, and increasing QCVs to indicate divergence between samples if the slab stress increased slowly. Opposite trends were indicative of convergence: increasing variogram ranges, increasing pit-to-plot ratios, and decreasing QCVs if the slab stress increased rapidly.

The measures of divergence and convergence I chose did not provide clear indicators of temporal trends. The variograms indicated little spatial correlation, and were hard to interpret. The pit-to-plot ratios indicated few differences across the plots. Medians and QCVs of strength and stability were the only measures that changed definitively between plots, but they provided no spatial information.

At both the Spanky's and Lionhead sites, the indications of temporal change were strongest between Plots 1 and 2. As the sampling progressed, the indicators became weaker or contradictory. This suggested that the potential for changes in spatial patterns is greatest within the first weeks of burial, when the shear strength is increasing most

rapidly. The potential for changes in the spatial patterns decreased as the layer aged, and the rate of strengthening slowed. Future research may benefit by concentrating on the early temporal changes in shear strength and stability.

Spanky's Site

Convergence occurred between Plots 1 and 2 at the Spanky's site. The pit-to-plot ratios increased, and the QCV of shear strength decreased, both indicators of convergence. Although shear strength increased rapidly between the plots, additional snowfall increased the load on the weak layer an amount proportional to the strengthening, and little net change in stability resulted. The variogram range increased, but so did the nugget ratio estimate, providing contradictory indicators.

Between Plots 2 and 3, the temporal trend switched to divergence, indicated by the increasing QCV of both strength and stability, and decreasing pit-to-plot ratio of stability. I expected the relatively rapid increase in slab thickness (Table 4, p. 64) to force convergence, but there were no strong indicators. The variogram ranges increased, but given the high nugget estimate ratios, I would discount that indication of convergence.

It appeared that little change occurred between Plots 3 and 4. The rate of strengthening was slight, and the only slab property to change was density, which increased. The variograms indicated little change in the spatial correlation of strength between Plots 3 and 4. The pit-to-plot ratio for stability increased, but the ratios for strength did not change. Both the variograms and pit-to-plot ratios suggested little change.

Lionhead Site

At the Lionhead site, strengthening occurred after the collapse during the Alley sample. Although there were no spatial measures the two distinct collapsed and un-collapsed groups were almost indistinguishable by the following day.

Divergence occurred between Plots 1 and 2. The light snowfall that occurred between samples was not sufficient to force the weak layer to converge. There were four indicators of convergence, with the nugget ratio estimate increasing, decreasing pit-to-plot ratios of strength and stability, and a slight increase in the QCV of shear strength. The variogram range increased, providing a contradictory indicator.

There were no strong indications of divergence or convergence after sampling Plot 2. Divergence would be expected as the layer gained strength without significant change in the slab between Plot 2 and 3. A few of the stronger tests in Plots 3 and 4 had poorer quality shears (Q2). The tests were adjacent, and possibly resulted from the surface hoar layers locally gaining strength. Unfortunately, the Plot 3 and 4 variograms did not allow much interpretation because of the large nugget ratio estimates, and little autocorrelation.

Soccer Field Site

The depth hoar at the Soccer Field aged differently than did the buried surface hoar layers at the other sites. With a thinner snowpack, changes in the slab had a much more dramatic effect on the metamorphism of the depth hoar, and resultant changes in temperature gradients may have had more effect on the depth hoar layer than changes in load. The effects of the gradients were most noticeable as the bottom layers of the slab faceted.

The change in shear strength between Plots 1 and 2 was significant (Table 1, p. 51). The relative spread of the results decreased slightly, although two strong tests skewed the Plot 2 results. Shear quality of the fractures became more planar between the two days.

Shear strength decreased significantly ($p < 0.001$) between Plots 2 and 3. Relative variability changed little, though the distribution of Plot 3 was more symmetrical than Plot 2. A consolidating slab usually strengthens the underlying layers. In the case of the Soccer Field plots, where the snowpack was thin, the consolidating slab may have increased the rate of formation of depth hoar by increasing the potential temperature gradient.

More developed depth hoar grains could have lead to the increasingly planar shear quality between Plots 1, 2, and 3. Typically, shear quality becomes less planer as a weak layer strengthens and ages. As the depth hoar grains metamorphosed, though, the relative size of the bonds between the grains and the crust above would have decreased, and the bonds could fracture easier. The rate of faceting around the crust could be higher than lower in the depth hoar, further weakening the interface. Such changes would be very hard to observe in the field

Changes between the Plot 1, 2, and 3 variograms indicated convergence. The nugget estimates decreased and the ranges increased, indicating increasing spatial correlation through time. However, the variograms all indicated little autocorrelation, and nugget estimates were high, so the changes should be interpreted cautiously. The QCV decreased between Pits 1 and 2, and did not change between Pits 2 and 3, supporting convergence. However, the pit-to-plot ratios did not change.

The snowpack structure of Plot 4 was very different from the earlier plots. The presence of the variable ice lens complicated the spatial analysis. Results were different enough from the previous plots that, possibly, too much change had occurred between the samples for comparison.

Site Comparisons

With the two buried surface hoar layers, the rate of strengthening decreased through time. Shear strength increased through time and became more variable as the weak layer aged and strengthened. The change in the rate of strengthening and increasing spread of strength has been shown for other buried surface hoar layers (Jamieson and Schweizer 2000).

This increase in the QCV of strength across what the analyses show are relatively spatially uniform sites demonstrates how evaluating stability becomes more difficult and less reliable as the weak layer ages. This becomes problematic in forecasting, especially when dealing with deep slabs and old weak layers (Greene and Johnson 2002; Tremper 2001). Weak layers several months old can become active on pockets where the layer has remained very weak.

The weak pockets may develop even over relatively uniform slopes, not just around topographic features, as indicated by the increasing plot-wide variability measured as the surface hoar layers aged. A forecaster testing a portion of the slope may miss the weak pockets, leading to an over-estimation of the slope stability. Therefore, older layers would require more tests to characterize properly the range of stability.

Temporal changes in stability were related to changes in the slab thickness, density, and weak layer strengthening. Seen at both the Spanky's and Lionhead site, the

stability ratio decreased between the final few samples, even as the field crew felt that the layer was a decreasing avalanche hazard. This illustrates a disadvantage of the shear frame test, that factors important to evaluating avalanche danger other than the layer of interest are discarded. On the other hand, shear frames allowed me to track the same weak layer, rather than having tests fail on multiple or different weak layers.

On the Soccer Field, the weak layer was depth hoar. The shallow snowpack and flat site meant that snowpack thickness and resulting metamorphic rates might have had a larger effect on the snowpack than did changes in slab loading. Several measures indicated convergence between Plots 1, 2, and 3. The variograms indicated an increasing range and decreasing nugget estimates, suggesting an increase in the spatial correlation of shear strength as the snowpack aged. Considerable changes in snowpack structure, including formation of the ice lens, complicated comparisons between Plots 3 and 4. The increasing variogram range and snowpack differences suggest considerable divergence.

Implications for Forecasting

This research aimed to improve avalanche forecasting. The analysis allowed me to examine the ability of a forecaster to extrapolate stability tests a short distance across uniform sites. On these layers, over relatively uniform slopes, stability results could be statistically extrapolated at least 17 m (the diagonal distance across the plot) on all but two plots—provided sufficient tests were conducted to characterize properly the distribution of test results. For an avalanche forecaster, the ability to extrapolate reliably even over such short distances is encouraging, given some previous work (Landry 2002).

To represent adequately the potential variability, tests need to be spaced at distances greater than the correlation length. A sufficient number of tests must be made

to represent statistically the variability. As the correlation length changes, the distance between tests would change. Therefore, it is important to consider the potential temporal trends when considering the appropriate test spacing.

The number of tests required becomes a problem of sample design, and is dependent upon the variability present in the results. There are many ways to estimate the necessary sample size. One method (Neter et al. 1996) estimates the sample size (n) based on the desired absolute error (δ),

$$n \approx z_{\alpha}^{2}\left(\frac{\sigma^{2}}{\delta^{2}}\right)$$

using an estimate of the population standard deviation (σ), where $\alpha = 0.1$ and $z = 2$, and the measurements are not autocorrelated. Using Spanky's Alley (mean shear strength of 758 Pa, $\sigma = 105$ Pa) and Plot 4 (mean shear strength of 2249 Pa, $\sigma = 353$ Pa) as examples, and constraining the absolute error to within 10% of the mean ($\delta = 40$ Pa and 105 Pa respectively), 28 tests were required during the Alley sample, and 45 during the sampling of Plot 4. Using a fixed constraint, 100 Pa for example, 5 tests were required during the Alley sample, and 50 during the sampling of Plot 4. Performing a sample size calculation in the field would be practical only in the case of uniform slopes. This does illustrate that layers that are more variable require more tests to capture the distribution of shear strength.

Would results from a single pit with a sufficient number of tests have helped to evaluate the avalanche hazard in terrain near the study area? Yes, but not directly. Because the surrounding, avalanche prone slopes are steeper and more wind affected, results from the study area would need to be interpreted, just as most forecasting requires.

This returns to earlier researcher's suggestions of groups of tests 5 to 10 m apart (Jamieson and Johnston 2001) or targeted sampling (McClung 2002a, 2002b). Avalanche forecasting and assessment has never been a matter of using one test result. The process of forecasting is inductive, and integrates many pieces of information of which stability tests are but a part (LaChapelle 1980; McClung 2002b; McClung and Schaerer 1993; Tremper 2001).

One important issue is the potential correlation of adjacent tests. Commonly, groups of stability tests are conducted adjacent to each other, at intervals somewhat closer than tests in this study. If the correlation length of shear strength is shorter that 1 m, as suggested by results from Spanky's Plot 1, results of adjacent tests would be related, and under-represent the potential variability of stability or shear strength across the slope.

Most stability tests used in the field are not measured on a continuous scale, and have a coarser resolution than tests used in research. Combined with potential correlation of adjacent tests, that could be one reason that field tests are often similar, and detect less variability than is found in research studies. A test with coarser resolution would also detect less fundamental error, as would tests with larger spatial areas, resulting in less test variability. However, tests with large spatial areas and coarse resolution can demonstrate substantial variations in results (Campbell and Jamieson 2004).

Suggestions for Future Research

This study provides encouraging preliminary answers to the initial research questions. The results of this thesis, while based on one of the most extensive spatial datasets of stability measurements collected, is still based on limited data. Collecting additional similar data would be extremely valuable. Additional layers and different

types of change would increase the value of the three field sites already sampled. However, future research should include several improvements.

First, the sampling array should be improved. Efficient geostatistical surveys are often conducted in stages, with the first sample used to determine the process scale. Additional samples are then made at locations that will improve the geostatistics (Webster and Oliver 1990, 2001). Resampling is not a luxury that the snowpack allows. The only method to refine the sampling is to take measurements, analyze the results, and try to make improvements to the future sample array.

There are two directions to take the current sampling array. One is to sample tests at finer intervals. Doing so should improve the resolution at shorter distances, and provide a better measure of correlation at distances closer than 1 m. The other direction is to sample larger plots to see if the slope-scale trends become more prevalent. Doing so may provide results more similar to Landry (2002), but with the ability to detect trends better. However, achieving both of these results simultaneously will be difficult since collecting enough measurements has proven difficult to do in a single day.

Second, future researchers may want to examine carefully the utility of pit-to-plot ratios. With plots similar in size to those used here, the method does not seem to be useful. Abandoning the pit-to-plot technique would allow tests to be located to better optimize the variograms.

Another avenue of future research would be to sample across slopes with strong trends in variability. Sampling a weak layer in a wind-affected site could prove interesting. Would the weak layer exhibit little correlation? Is the lack of spatial

structure I found typical? Would there be strong isotropic correlation following the wind-imposed trend?

I had hoped to sample both before and after an avalanche cycle. However, a slab sturdy enough to sample never formed prior to the avalanche cycle on the two layers of buried surface hoar. Bracketing an avalanche cycle with measurements may help substantiate or repudiate the hypothesized divergence. Additionally, each of the layers sampled was unique. The spatial characteristics and temporal changes of many more layers may need to be sampled before a picture of the trends and patterns emerges.

I see this research as only an important, additional step in improving our understanding of the spatial variability of snow. Variability is critically important for snow avalanches, as well as related fields such as snow hydrology. This work demonstrates that, even with such a large spatial dataset, the spatial variability is hard to quantify over uniform slopes. Future work on spatial variability within the snowpack will continue to be challenging.

REFERENCES

Arons, E. M., S. C. Colbeck, and J. Gray. 1998. Depth-hoar growth rates near a rocky outcrop. *Journal of Glaciology* 44 (148):477-484.

Birkeland, K. W. 1997. Spatial and temporal variations in snow stability and snowpack conditions throughout the Bridger Mountains, Montana. Ph. D. Dissertation, Department of Geography, University of Arizona, Tempe.

Birkeland, K. W. 1998. Terminology and predominant processes associated with the formation of weak layers of near-surface faceted crystals in the mountain snowpack. *Arctic and Alpine Research* 30 (2):193-199.

Birkeland, K. W. 2001. Spatial patterns of snow stability throughout a small mountain range. *Journal of Glaciology* 47 (157):176-186.

Birkeland, K. W., K. J. Hansen, and R. L. Brown. 1995. The spatial variability of snow resistance on potential avalanche slopes. *Journal of Glaciology* 41 (137):183-190.

Birkeland, K. W., K. Kronholm, M. Schneebeli, and C. Pielmeier. 2004. Temporal changes in the shear strength and hardness of a buried surface hoar layer. *Annals of Glaciology* 38: 223-228.

Birkeland, K. W., and C. C. Landry. 2002. Changes in spatial patterns of snow stability through time. In *Proceedings of the 2002 International Snow Science Workshop*, Penticton, British Columbia, Canada [CD-ROM].

Blöschl, G. 1999. Scaling issues in snow hydrology. *Hydrological Processes* 13 (14-15):2149-2175.

Burrough, P. A. 1983. Multiscale sources of spatial variation in soil .1: The application of fractal concepts to nested levels of soil variation. *Journal of Soil Science* 34 (3):577-597.

Campbell, C. and B. Jamieson. 2004. Spatial variability of rutschblock results in avalanche start zones. In *Proceedings of the 2004 International Snow Science Workshop*, Jackson Hole, Wyoming, USA [CD-ROM].

Chabot, D. 2004. Personal communication. Director, Gallatin National Forest Avalanche Center, U. S. Forest Service, Bozeman, Montana, USA.

Colbeck, S. C. 1991. The layered character of snow covers. *Reviews of Geophysics* 29 (1):81-96.

Colbeck, S. C., E. Akitaya, R. Armstrong, H. Gubler, J. Lafeuille, K. Leid, D. M. McClung, and E. Morris. 1990. *The International Classification for Seasonal Snow on the Ground*. Boulder: World Data Center A for Glaciology.

Conway, H., and J. Abrahamson. 1984. Snow stability index. *Journal of Glaciology* 30 (106):321-327.

Conway, H., and J. Abrahamson. 1988. Snow-slope stability - a probabilistic approach. *Journal of Glaciology* 34 (117):170-177.

Cressie, N. A. C. 1993. *Statistics for Spatial Data*. Chichester: John Wiley and Sons.

Deutsch, C. V., and A. G. Journel. 1998. *GSLIB: Geostatistical Software Library and User's Guide*. New York: Oxford University Press.

Easterbrook, D. J. 1993. *Surface Processes and Landforms*. Englewood Cliffs: Prentice-Hall.

Föhn, P. M. B. 1987a. The 'rutschblock" as a parcticle tool for slope stability evaluation. In *Avalanche Formation, Movement, and Effects*, eds. B. Salm and H. Gubler, 195-211: IASH-AISH.

Föhn, P. M. B. 1987b. The stability index and various triggering mechanisms. In *Avalanche Formation, Movement, and Effects*, eds. B. Salm and H. Gubler, 195-211: IASH-AISH.

Gallatin National Forest Avalanche Center. 2004. *Gallatin National Forest Avalanche Center Backcountry avalanche advisories.* Web page, www.mtavalanche.com/archives/index.shtml [cited 2004].

Greene, E., K. W. Birkeland, K. Elder, G. Johnson, C. C. Landry, I. McCammon, M. Moore, D. Sharaf, C. Sterbenz, B. Tremper, and K. Williams. 2004. *Snow, Weather, and Avalanches: Observational Guidelines for Avalanche Programs in the United States*. 1st ed. Pagosa Springs: American Avalanche Association.

Hageli, P., and D. M. McClung. 1999. Classification in avalanche forecasting. Paper presented at the International Conference on Avalanches, at Saint Vincent, Italy.

Harper, J. T., and J. H. Bradford. 2003. Snow stratigraphy over a uniform depositional surface: spatial variability and measurement tools. *Cold Regions Science and Technology* 37 (3):289-298.

Jamieson, B. 1995. Avalanche prediction for persistent snow slabs. Ph.D. Dissertation, Department of Civil Engineering, University of Calgary, Calgary.

Jamieson, B. 1999a. Skier triggering of slab avalanches: concepts and research. *The Avalanche Review* 18 (2):8-10.

Jamieson, B. 1999b. Snowpack factors associated with strength changes of buried surface hoar layers. *Cold Regions Science and Technology* 30 (1-3):19-34.

Jamieson, B., and C. D. Johnston. 1993. Rutschblock precision, technique variations and limitations. *Journal of Glaciology* 39 (133):666-674.

Jamieson, B. and C. D. Johnston. 2001. Evaluation of the shear frame test for weak snowpack layers. *Annals of Glaciology* 32:59-69.

Jamieson, J. B., and J. Schweizer. 2000. Texture and strength changes of buried surface-hoar layers with implications for dry snow-slab avalanche release. *Journal of Glaciology* 46 (152):151-160.

Johnson, J. B., and M. Schneebeli. 1999. Characterizing the microstructural and micromechanical properties of snow. *Cold Regions Science and Technology* 30 (1-3):91-100.

Johnson, R. F., and K. W. Birkeland. 2002. Integrating shear quality into stability test results. In *Proceedings of the 2002 International Snow Science Workshop*, Penticton, British Columbia, Canada [CD-ROM].

Kronholm, K. 2004. Spatial variability of snow mechanical properties with regard to avalanche formation. Ph.D. Dissertation, Mathematisch-naturwissenschaftlichen, Universitat Zurich, Zurich.

Kronholm, K., M. Schneebeli, and J. Schweizer. 2004. Spatial variability of penetration resistance in snow layers on a small slope. *Annals of Glaciology* 38: 202-208.

Kronholm, K., and J. Schweizer. 2003. Snow stability variation on small slopes. *Cold Regions Science and Technology* 37 (3):453-465.

LaChapelle, E. R. 1980. The fundamental processes in conventional avalanche forecasting. *Journal of Glaciology* 26 (94):75-84.

Landry, C. C. 2002. Spatial variations in snow stability on uniform slopes: Implications for extrapolation to surrounding terrain. MS Thesis, Department of Earth Sciences, Montana State University, Bozeman.

Landry, C. C., J. J. Borkowski, and R. L. Brown. 2001. Quantified loaded column stability test: mechanics, procedure, sample-size selection, and trials. *Cold Regions Science and Technology* 33 (2-3):103-121.

Landry, C. C., K. W. Birkeland, K. J. Hansen, J. J. Borkowski, R. L. Brown, and R. Aspinall. 2004. Variations in snow strength and stability on uniform slopes. *Cold Regions Science and Technology* 39 (2-3):205-218.

Lark, R. M. 2000. A comparison of some robust estimators of the variogram for use in soil survey. *European Journal of Soil Science* 51 (1):137-157.

Leonard, Tom. 2004. Personal communication. Snow safety director, The Yellowstone Club, Montana, USA.

Louchet, F. 2000. A simple model for dry snow slab avalanche triggering. *Comptes Rendus De L Academie Des Sciences Serie Ii Fascicule a- Sciences De La Terre Et Des Planetes* 330 (12):821-827.

Lutz, E. 2004. Personal communication. Doctoral student, Department of Earth Sciences, Montana State University, Bozeman, Montana, USA.

McClung, D. M. 2002a. The elements of applied avalanche forecasting - Part I: The human issues. *Natural Hazards* 26 (2):111-129.

McClung, D. M. 2002b. The elements of applied avalanche forecasting - Part II: The physical issues and the rules of applied avalanche forecasting. *Natural Hazards* 26 (2):131-146.

McClung, D. M., and P. Schaerer. 1993. *The Avalanche Handbook*. Seattle: The Mountaineers.

Mock, C. J., and K. W. Birkeland. 2000. Snow avalanche climatology of the western United States mountain ranges. *Bulletin of the American Meteorological Society* 81 (10):2367-2392.

Myers, J. C. 1997. *Geostatistical Error Management: quantifying uncertainty for environmental sampling and mapping*. New York: Van Nostrand Reinhold.

National Geographic Holdings. 2003. *TOPO! Montana*, version 3.4.2.

National Resources Conservation Service. 2004. Madison Plateau Snotel data. Web page, www.wcc.nrcs.usda.gov/snotel/snotel.pl?sitenum=609&state=mt [cited 2003].

Neter, J., M. H. Kutner, C. J. Nachtsheim, and W. Wasserman. 1996. *Applied Linear Statistical Models*. 4th ed. Boston: WCB/McGraw Hill.

O'Sullivan, D., and D. Unwin. 2003. *Geographic Information Analysis*. Hoboken: John Wiley and Sons.

Phillips, J. D. 1993. Chaotic evolution of some coastal-plain soils. *Physical Geography* 14 (6):566-580.

Phillips, J. D. 1995. Nonlinear dynamics and the evolution of relief. *Geomorphology* 14 (1):57-64.

Phillips, J. D. 1999. *Earth Surface Systems; Complexity, Order and Scale*. Oxford: Blackwell Publishers, Ltd.

Phillips, J. D. 2000. Signatures of divergence and self-organization in soils and weathering profiles. *Journal of Geology* 108:91-102.

Pielmeier, C., and M. Schneebeli. 2003. Stratigraphy and changes in hardness of snow measured by hand, ramsonde and snow micro penetrometer: a comparison with planar sections. *Cold Regions Science and Technology* 37 (3):393-405.

Schneebeli, M., C. Pielmeier, and J. B. Johnson. 1999. Measuring snow microstructure and hardness using a high resolution penetrometer. *Cold Regions Science and Technology* 30 (1-3):101-114.

Schweizer, J. 1999. Review of dry snow slab avalanche release. *Cold Regions Science and Technology* 30 (1-3):43-57.

Spiegel, M. R., and L. J. Stephens. 1999. *Schaum's Outline of Theory and Problems of Statistics*. Third edition. New York: McGraw-Hill.

Stewart, K., and B. Jamieson. 2002. Spatial variability of slab stability in avalanche start zones. In *Proceedings of the 2002 International Snow Science Workshop*, Penticton, British Columbia, Canada [CD-ROM].

Tremper, B. 2001. *Staying Alive in Avalanche Terrain*. Seattle: The Mountaineers.

Tufte, E. R. 1983. *The Visual Display of Quantitative Information.* Chelshire: Graphics Press.

Utah Avalanche Center. 2004. *Archived Backcountry Avalanche advisories* Web page, www.avalanche.org/~uac/archive/2003-2004/ [cited 2004].

Webster, R. 2000. Is soil variation random? *Geoderma* 97:149-163.

Webster, R., and M. A. Oliver. 1990. *Statistical Methods in Soil and Land Resource Survey*. New York: Oxford University Press.

Webster, R., and M. A. Oliver. 2001. *Geostatistics for Environmental Scientists*. Chichester: John Wiley and Sons.

Western Regional Climate Center. 2004. Bozeman Montana State Univ climate summary. Web page, www.wrcc.dri.edu/cgi-bin/cliMAIN.pl?mtboze [cited 2004]

APPENDIX A

FIELD DATA

Site SOCCER FIELD
Date 20031231 Q notes
Name Plot One 2 is planar failure
Operator SL 3 is irregular failure with no plane
FRAME: 0.025 GAGE 5 kg 2.5 is "rough," irregular plane

PIT	TEST	kg fail	H fail	Shear Quality	Failure (N)	Shear Strength (Pa)	Notes
SLAB cm		mmH2O	55	Density	---		
1	1	1.9	7	3	18.62	744.8	
1	2	1.65	4	3	16.17	646.8	
1	3	2.2	4.5	2.5	21.56	862.4	
1	4	2.2	4.5	3	21.56	862.4	
1	5	1.8	4	3	17.64	705.6	
1	6	2.25	3.5	3	22.05	882	
1	7	2.3	7	2.5	22.54	901.6	
1	8	2.55	3	3	24.99	999.6	
1	9	1.55	7.5	2.5	15.19	607.6	
1	10	2.1	4	3	20.58	823.2	
1	11	2	6	3	19.6	784	
1	12	2.1	4	2.5	20.58	823.2	
SLAB cm		mmH2O	55	Density	---		
2	1	2.45	7	3	24.01	960.4	
2	2	1.6	3	2	15.68	627.2	base of crust
2	3	JUNK					
2	4	1.7	7.5	3	16.66	666.4	
2	5	2.15	8	3	21.07	842.8	
2	6	2.5	4.5	3	24.5	980	
2	7	1.95	3.5	2	19.11	764.4	
2	8	2.7	7	2.5	26.46	1058.4	
2	9	1.9	6	3	18.62	744.8	
2	10	1.8	5	3	17.64	705.6	
2	11	2	8.5	2.5	19.6	784	
2	12	2	8	3	19.6	784	
SLAB cm		mmH2O	55	Density	---		
3	1	2.5	4	3	24.5	980	
3	2	2.15	5	2.5	21.07	842.8	
3	3	2.05	5.5	2.5	20.09	803.6	
3	4	1.75	5	2.5	17.15	686	
3	5	1.8	5	3	17.64	705.6	
3	6	1.95	3	3	19.11	764.4	
3	7	1.7	4	3	16.66	666.4	
3	8	2.1	5.5	3	20.58	823.2	
SLAB cm		mmH2O	55	Density	---		
4	1	1.55	6	2.5	15.19	607.6	

4	2	2.1	6	3	20.58	823.2	
4	3	1.3	5	3	12.74	509.6	
4	4	1.3	5	3	12.74	509.6	
4	5	2.9	6	2.5	28.42	1136.8	
4	6	2.4		63	23.52	940.8	
4	7	1.1	5	3	10.78	431.2	
4	8	1.75	4	3	17.15	686	
4	9	1	5	2.5	9.8	392	
4	10	1.6	3	3	15.68	627.2	
4	11	1.9	6	3	18.62	744.8	
4	12	2.1	7	2.5	20.58	823.2	
SLAB cm		mmH2O	55	Density	---		
5	1	1.75	4	2	17.15	686	
5	2	2.25	4.5	3	22.05	882	
5	3	JUNK					
5	4	1.25	6	3	12.25	490	
5	5	2.55	4	3	24.99	999.6	
5	6	1.6	7	2.5	15.68	627.2	
5	7	2	4	2.5	19.6	784	
5	8	1.4	3	3	13.72	548.8	
5	9	2.3	6	3	22.54	901.6	
5	10	1	6.5	2	9.8	392	Failure less than 1 kg (min on gage); tried three times with same result
5	11	2.15	7	3	21.07	842.8	
5	12	2	5	3	19.6	784	

Site	SOCCER FIELD						
Date	20040106						
Name	Plot 2						
Operator:	SL						
FRAME:	0.025	GAGE		5 kg	2 is planar failure		
PIT	TEST	kg fail	H fail	Q	Failure (N)	Shear Strength (Pa)	Notes
SLAB cm	24.8	mmH2O	43	Density	173.3871	TAU250	
1	1	3.45	4.5	2.5	33.81	879.06	
1	2	2.75	7.5	2	26.95	700.7	
1	3	2.95	8	2	28.91	751.66	
1	4	3.3	6.5	2	32.34	840.84	
1	5	2.65	5	2	25.97	675.22	
1	6	3.65	5	2	35.77	930.02	
1	7	3.45	7.5	2	33.81	879.06	
1	8	2.4	8	2.5	23.52	611.52	
1	9	3	9	2	29.4	764.4	
1	10	2.9	8	2	28.42	738.92	
1	11	3.25	7	2	31.85	828.1	
1	12	3.7	7	2	36.26	942.76	
SLAB cm	24.2	mmH2O	46	Density	190.0826		
2	1	3.3	7	2	32.34	840.84	
2	2	3.9	8	3	38.22	993.72	
2	3	3.2	9	3	31.36	815.36	
2	4	4.05	8	2	39.69	1031.94	
2	5	3.1	7	2	30.38	789.88	
2	6	2.7	6	2	26.46	687.96	
2	7	3.55	8	3	34.79	904.54	
2	8	4.1	9	2	40.18	1044.68	
2	9	3.5	8	2	34.3	891.8	
2	10	4.5	7	1	44.1	1146.6	
2	11	4.95	7	1	48.51	1261.26	
2	12	2.95	8	2.5	28.91	751.66	
SLAB cm	23.2	mmH2O	41	Density	176.7241		
3	1	2.95	7	2	28.91	751.66	
3	2	3.1	7	3	30.38	789.88	
3	3	5.8	3	3	56.84	1477.84	Very thick ice at base
3	4	3	7.5	2	29.4	764.4	
3	5	3.2	8	2	31.36	815.36	
3	6	3.15	7.5	1	30.87	802.62	
3	7	4	7	2	39.2	1019.2	
3	8	2.75	7	2.5	26.95	700.7	
SLAB cm	24.2	mmH2O	44	Density	181.8182		
4	1	2.9	5.5	2	28.42	738.92	
4	2	3.6	9	3	35.28	917.28	
4	3	2.85	10	3	27.93	726.18	

4	4	3.3	7	1	32.34	840.84
4	5	3	7	1	29.4	764.4
4	6	3	7	1	29.4	764.4
4	7	5.55	2	3	54.39	1414.14
4	8	3.7	7	2.5	36.26	942.76
4	9	3.8	6.5	3	37.24	968.24
4	10	3.3	9	2	32.34	840.84
4	11	2.8	7	3	27.44	713.44
4	12	4.6	8	2	45.08	1172.08
SLAB cm	25	mmH2O	47	Density	188	
5	1	4.35	8	3	42.63	1108.38
5	2	3.15	8	1	30.87	802.62
5	3	3.1	4	1	30.38	789.88
5	4	3.25	8	2	31.85	828.1
5	5	4.05	7	1	39.69	1031.94
5	6	3.4	8	1	33.32	866.32
5	7	3.45	8	1	33.81	879.06
5	8	3.25	6	2	31.85	828.1
5	9	2.95	9	2	28.91	751.66
5	10	4.1	5	3	40.18	1044.68
5	11	3.45	7	2	33.81	879.06
5	12	3.9	6	1	38.22	993.72

Site	SOCCER FIELD					
Date	20040114					
Name	Plot 3					
Operator:	SL			Q notes		
FRAME:	0.025	GAGE	5 kg	2 is planar failure		
PIT	TEST	kg fail	H fail	Q	Failure (N)	Shear Strength (Pa)
SLAB cm	22.8	mmH2O	48	Density	210.52632	
1	1	3.2	7	1	31.36	1254.4
1	2	3.1	6	1	30.38	1215.2
1	3	2.75	7	1	26.95	1078
1	4	2.7	6	1	26.46	1058.4
1	5	2.95	6	2	28.91	1156.4
1	6	2.85	7	1	27.93	1117.2
1	7	4.2	9	1	41.16	1646.4
1	8	2.75	7	1	26.95	1078
1	9	2.85	7	1	27.93	1117.2
1	10	3	8	1	29.4	1176
1	11	2.2	6	1	21.56	862.4
1	12	2.05	7	1	20.09	803.6
SLAB cm	22	mmH2O	41	Density	186.36364	
2	1	2.4	9	1	23.52	940.8
2	2	2.6	8	2	25.48	1019.2
2	3	2.85	9	1	27.93	1117.2
2	4	2.65	6	1	25.97	1038.8
2	5	1.75	7	1	17.15	686
2	6	2.9	6	2	28.42	1136.8
2	7	3.35	9	1	32.83	1313.2
2	8	3.3	8	1	32.34	1293.6
2	9	3.5	9	1	34.3	1372
2	10	2.5	6	1	24.5	980
2	11	2.6	6	1	25.48	1019.2
2	12	2.55	6	1	24.99	999.6
SLAB cm	22.8	mmH2O	48	Density	210.52632	
3	1	3	5	1	29.4	1176
3	2	2.7	7	1	26.46	1058.4
3	3	2.5	6	1	24.5	980
3	4	3.15	9	2	30.87	1234.8
3	5	4.35	8	2	42.63	1705.2
3	6	4.05	8	1	39.69	1587.6
3	7	4.4	7	1	43.12	1724.8
3	8	2.15	7	1	21.07	842.8

SLAB cm	23	mmH2O	50	Density	217.3913	
4	1	2.25	8	1	22.05	882
4	2	2.7	7	1	26.46	1058.4
4	3	3.05	7	1	29.89	1195.6
4	4	3.5	6	1	34.3	1372
4	5	4	6	1	39.2	1568
4	6	2.3	6	1	22.54	901.6
4	7	2	7	1	19.6	784
4	8	3.35	7	1	32.83	1313.2
4	9	3.65	8	1	35.77	1430.8
4	10	2.8	5	2	27.44	1097.6
4	11	2.5	5	1	24.5	980
4	12	2.7	7	1	26.46	1058.4

SLAB cm	22	mmH2O	47	Density	213.63636	
5	1	2.5	7	1	24.5	980
5	2	2.25	7	1	22.05	882
5	3	3.3	8	1	32.34	1293.6
5	4	2.95	7	1	28.91	1156.4
5	5	2.5	7	1	24.5	980
5	6	2.2	5	2	21.56	862.4
5	7	2.65	7	1	25.97	1038.8
5	8	2.7	6	1	26.46	1058.4
5	9	2.95	6	1	28.91	1156.4
5	10	2.6	7	1	25.48	1019.2
5	11	1.45	8	1	14.21	568.4
5	12	2.35	8	2	23.03	921.2

Site	SOCCER FIELD			
Date	20040203			
Name	Plot 4			
Operator:	SL			
FRAME:	0.025	GAGE	5 kg	

PIT	TEST	kg fail 1	kg fail 2	H fail	Failure (N)	Shear Strength (Pa)	Notes
SLAB cm	21	mmH20	52	Rho	247.62		
1	1		3.6	5	35.28	1411.20	
1	2		3.6	2	35.28	1411.20	
1	3		4.05	2	39.69	1587.60	
1	4		3.5	5	34.30	1372.00	
1	5	5.8		6	56.84	2273.60	
1	6		3.95	8	38.71	1548.40	
1	7		3	5	29.40	1176.00	
1	8	4.3		7	42.14	1685.60	
1	9	5.8		6	56.84	2273.60	thick ice @ ground
1	10		4.55	4	44.59	1783.60	
1	11		4.75	4	46.55	1862.00	
1	12		3.2	4	31.36	1254.40	
SLAB cm	22.5	mmH20	50.4	Rho	224.00	234.78	
2	1		3.4	2	33.32	1332.80	
2	2	5.6		6	54.88	2195.20	
2	3	6		7.5	58.80	2352.00	
2	4	7.2		7	70.56	2822.40	
2	5		2.85	7	27.93	1117.20	
2	6	4.5		8	44.10	1764.00	
2	7		3.4	4	33.32	1332.80	
2	8		4.2	4	41.16	1646.40	
2	9		3.4	5	33.32	1332.80	
2	10		4.6	5	45.08	1803.20	
2	11		3.4	6	33.32	1332.80	
2	12		3.4	8	33.32	1332.80	
SLAB cm	22	mmH20	58	Rho	263.64	263.64	
3	1		3.28	6	32.14	1285.76	
3	2		3	4	29.40	1176.00	
3	3	5.2		8	50.96	2038.40	
3	4	5.5		7	53.90	2156.00	
3	5	5		7	49.00	1960.00	
3	6		4.55	4	44.59	1783.60	
3	7		3.85	6	37.73	1509.20	
3	8	9.2		6	90.16	3606.40	thick ice lens @ top of SH

SLAB cm	22	mmH20	54	Rho	245.45	245.45
4	1	6		9	58.80	2352.00
4	2		3.55	6	34.79	1391.60
4	3		4.6	7	45.08	1803.20
4	4		2.8	4	27.44	1097.60
4	5		3.45	5	33.81	1352.40
4	6		3.8	6	37.24	1489.60
4	7		4.7	6	46.06	1842.40
4	8		3.9	6	38.22	1528.80
4	9		3.9	5	38.22	1528.80
4	10		3.5	5	34.30	1372.00
4	11		3.05	4	29.89	1195.60
4	12		3.15	6	30.87	1234.80
Slab cm	21	mmH20	52	Rho	247.62	247.62
5	1		3.9	6	38.22	1528.80
5	2		2.75	4	26.95	1078.00
5	3		3.6	4	35.28	1411.20
5	4		3.2	5	31.36	1254.40
5	5		3.75	4	36.75	1470.00
5	6	3		8	29.40	1176.00
5	7		4.5	7	44.10	1764.00
5	8		3.9	6	38.22	1528.80
5	9		4.6	6	45.08	1803.20
5	10		4	6	39.20	1568.00
5	11	Large ice lens in test cell--no results, because faceted layer was not present				
5	12		3.85	6	37.73	1509.20

Site SPANKY'S
Date 20040126
Name Alleys
Operator: KK
FRAME: 0.025 GAGE 5 kg

X	Y	Pit	test	kg	mmH20	HN	Slope	Rho	Failure (N)	(Pa)	Stability Index
15.25	0.25	1	1	2.1	44	45.5	25	96.7033	20.59	461.30	2.53
15.75	0.25	1	2	2					19.61	439.34	2.41
15.25	0.75	1	3	1.8					17.16	384.42	2.11
15.75	0.75	1	4	2					19.61	439.34	2.41
15.25	7.25	2	1	2.1	45	47	26	95.74468	20.59	461.30	2.39
15.75	7.25	2	2	2					19.61	439.34	2.27
15.25	7.75	2	3	1.9					18.63	417.37	2.16
15.75	7.75	2	4	1.6					15.69	351.47	1.82
15.25	13.25	3	1	2.1	42	45.5	25	92.30769	20.10	450.32	2.59
15.75	13.25	3	2	1.9					18.63	417.37	2.40
15.25	13.75	3	3	2					19.61	439.34	2.53
15.75	13.75	3	4	2					19.12	428.35	2.46
15.25	17.25	4	1	1.8	46	50	25	92	17.16	384.42	2.02
15.75	17.25	4	2	2.2					21.08	472.29	2.48
15.25	17.75	4	3	2.2					21.08	472.29	2.48
15.75	17.75	4	4	1.8					17.16	384.42	2.02
15.25	24.25	5	1	1.6	45	41	25	109.7561	15.69	351.47	1.89
15.75	24.25	5	2	2.2					21.08	472.29	2.53
15.25	24.75	5	3	2.6					25.50	571.14	3.06
15.75	24.75	5	4	1.5					14.22	318.52	1.71
15.25	30.25	6	1	1.9	42	44	28	95.45455	18.63	417.37	2.16
15.75	30.25	6	2	1.6					15.69	351.47	1.82
15.25	30.75	6	3	1.7					16.67	373.44	1.93
15.75	30.75	6	4	2					19.61	439.34	2.27
0.25	15.25	7	1	2.1	47	45	25	104.4444	20.59	461.30	2.37
0.25	15.75	7	2	1.9					18.14	406.39	2.09
0.75	15.25	7	3	1.9					18.14	406.39	2.09
0.75	15.75	7	4	2.1					20.59	461.30	2.37
7.25	15.25	8	1	1.6	43	43	23	100	15.69	351.47	2.13
7.25	15.75	8	2	1.5					14.71	329.50	2.00
7.75	15.25	8	3	2					19.61	439.34	2.67
7.75	15.75	8	4	1.5					14.71	329.50	2.00
13.25	15.25	9	1	2.2	43	45	25	95.55556	21.08	472.29	2.65
13.25	15.75	9	2	2.2					21.08	472.29	2.65
13.75	15.25	9	3	1.9					18.63	417.37	2.34
13.75	15.75	9	4	1.8					17.65	395.40	2.22
17.25	15.25	10	1	1.4	46	44	26	104.5455	13.73	307.53	1.56
17.25	15.75	10	2	2					19.12	428.35	2.17
17.75	15.25	10	3	2.5					24.03	538.19	2.72
17.75	15.75	10	4	1.9					18.63	417.37	2.11
24.25	15.25	11	1	2.2	45	43.5	24	103.4483	21.08	472.29	2.63

24.25	15.75	11	2	1.9					18.63	417.37	2.33
24.75	15.25	11	3	2.1					20.59	461.30	2.57
24.75	15.75	11	4	1.8					17.16	384.42	2.14
30.25	15.25	12	1	2	45	44	26	102.2727	19.12	428.35	2.22
30.25	15.75	12	2	2.7					26.48	593.10	3.07
30.75	15.25	12	3	1.9					18.14	406.39	2.10
30.75	15.75	12	4	2					19.61	439.34	2.27

Site	SPANKY'S						
Date	20040129						
Name	Plot 1						
Operator:	KK						
FRAME:	0.025	GAGE	5 kg				
X	Y	Pit	Test	Fail (kg)	Fail (N)	Shear Strength (Pa)	Stability Index
SLAB cm	34	mmH20	43	Rho	126.47059	SLOPE	26
2.25	2.25	1	1	2.9	28.44	1137.57	4.00
2.75	2.25	1	2	2.5	24.52	980.66	3.45
3.25	2.25	1	3	3.25	31.87	1274.86	4.49
3.75	2.25	1	4	2.7	26.48	1059.11	3.73
4.25	2.25	1	5	2.55	25.01	1000.27	3.52
4.75	2.25	1	6	2.45	24.03	961.05	3.38
4.75	2.75	1	7	3	29.42	1176.79	4.14
4.25	2.75	1	8	2.95	28.93	1157.18	4.07
3.25	2.75	1	9	2.9	28.44	1137.57	4.00
2.75	2.75	1	10	3.15	30.89	1235.63	4.35
2.25	2.75	1	11	3.05	29.91	1196.41	4.21
3.75	2.75	1	12	3.05	29.91	1196.41	4.21
SLAB cm	34	mmH20	46	Rho	135.29	SLOPE	26
9.25	2.25	2	1	2.7	26.48	1059.11	3.48
9.75	2.25	2	2	2.1	20.59	823.75	2.71
10.25	2.25	2	3	1.85	18.14	725.69	2.39
10.75	2.25	2	4	1.6	15.69	627.62	2.06
11.25	2.25	2	5	2.45	24.03	961.05	3.16
11.75	2.25	2	6	2.8	27.46	1098.34	3.61
9.25	2.75	2	7	2.45	24.03	961.05	3.16
9.75	2.75	2	8	2.5	24.52	980.66	3.23
10.25	2.75	2	9	3.4	33.34	1333.70	4.39
10.75	2.75	2	10	3.25	31.87	1274.86	4.19
11.25	2.75	2	11	2.45	24.03	961.05	3.16
11.75	2.75	2	12	2.7	26.48	1059.11	3.48
SLAB cm	35	mmH20	45	Rho	128.57	SLOPE	28
6.25	6.75	3	1	2.35	23.05	921.82	2.89
6.25	7.25	3	2	2.2	21.57	862.98	2.71
7.75	6.75	3	3	2.5	24.52	980.66	3.08
6.75	7.25	3	4	2.9	28.44	1137.57	3.57
6.75	6.75	3	5	2.15	21.08	843.37	2.65
7.75	7.25	3	6	2.5	24.52	980.66	3.08
7.25	7.25	3	7	2.5	24.52	980.66	3.08
7.25	6.75	3	8	2.45	24.03	961.05	3.02
SLAB cm	34	mmH20	46	Rho	135.29	SLOPE	26
2.25	11.25	4	1	2.65	25.99	1039.50	3.42

2.75	11.25	4	2	2.45	24.03	961.05	3.16
3.25	11.25	4	3	3.05	29.91	1196.41	3.94
3.75	11.25	4	4	2.65	25.99	1039.50	3.42
4.25	11.25	4	5	2.35	23.05	921.82	3.03
4.75	11.25	4	6	2.65	25.99	1039.50	3.42
2.25	11.75	4	7	2.35	23.05	921.82	3.03
2.75	11.75	4	8	2.95	28.93	1157.18	3.81
3.25	11.75	4	9	2.65	25.99	1039.50	3.42
3.75	11.75	4	10	2.8	27.46	1098.34	3.61
4.25	11.75	4	11	3.05	29.91	1196.41	3.94
4.75	11.75	4	12	2.95	28.93	1157.18	3.81
SLAB cm	34	mmH20	43	Rho	126.47	SLOPE	26
9.25	11.25	5	1	2.4	23.54	941.43	3.31
9.75	11.25	5	2	2.45	24.03	961.05	3.38
10.25	11.25	5	3	2.4	23.54	941.43	3.31
10.75	11.25	5	4	2.7	26.48	1059.11	3.73
11.25	11.25	5	5	1.95	19.12	764.91	2.69
11.75	11.25	5	6	2.75	26.97	1078.73	3.80
9.25	11.75	5	7	2.55	25.01	1000.27	3.52
9.75	11.75	5	8	2.8	27.46	1098.34	3.86
10.25	11.75	5	9	3.05	29.91	1196.41	4.21
10.75	11.75	5	10	2.6	25.50	1019.89	3.59
11.25	11.75	5	11	2.7	26.48	1059.11	3.73
11.75	11.75	5	12	2.8	27.46	1098.34	3.86
SLAB cm	34	mmH20	45	Rho	132.35	SLOPE	27
6.75	2.25	1.5	1	2.4	23.54	941.43	3.06
7.25	2.25	1.5	2	2.7	26.48	1059.11	3.44
SLAB cm	34	mmH20	42	Rho	123.53	SLOPE	29
10.25	7.25	2.5	1	2.75	26.97	1078.73	3.51
10.75	7.25	2.5	2	3.45	33.83	1353.31	4.41
10.25	7.75	2.5	3	3.1	30.40	1216.02	3.96
10.75	7.75	2.5	4	2.6	25.50	1019.89	3.32
SLAB cm	34	mmH20	43	Rho	126.47	SLOPE	26
3.25	7.25	3.5	1	2.9	28.44	1137.57	4.00
3.75	7.25	3.5	2	2.5	24.52	980.66	3.45
3.25	7.75	3.5	3	2.2	21.57	862.98	3.04
3.75	7.75	3.5	4	2.65	25.99	1039.50	3.66
SLAB cm	32	mmH20	44	Rho	137.50	SLOPE	27
6.75	11.25	4.5	1	2.45	24.03	961.05	3.19
7.25	11.25	4.5	2	2.7	26.48	1059.11	3.52
		Additional measurements					
5.25	2			2.4	23.54	941.43	3.31
5.25	2.5			3.05	29.91	1196.41	4.21
5	2			2.5	24.52	980.66	3.45

5	2.5			2.95	28.93	1157.18	4.07
5.5	2			2.75	26.97	1078.73	3.80
5.5	2.5			2.6	25.50	1019.89	3.59
6	2			2.5	24.52	980.66	3.45
6	2.5			3.4	33.34	1333.70	4.69
6.5	2			3.2	31.38	1255.24	4.42
6	2.5			2.6	25.50	1019.89	3.59
SLAB cm	34	mmH20	45	Rho	132.35	SLOPE	27
6.2	2.5			2.9	28.44	1137.57	3.69
6.7	2.5			3.4	33.34	1333.70	4.33
7.2	2.5			2.85	27.95	1117.95	3.63
7.7	2.5			3.4	33.34	1333.70	4.33
8.2	2			2.55	25.01	1000.27	3.29
8.2	2.5			3	29.42	1176.79	3.87
8.7	2			2.45	24.03	961.05	3.16
8.7	2.5			2.8	27.46	1098.34	3.61
9.2	2			2.65	25.99	1039.50	3.42
9.2	2.5			2.7	26.48	1059.11	3.48
9.7	2			1.95	19.12	764.91	2.52
9.7	2.5			3.2	31.38	1255.24	4.13

Site	SPANKY'S						
Date	20040205						
Name	Plot 2						
Operator:	KK						
FRAME:	0.025	GAGE	5 kg				
X	Y	Pit	Test	Fail (kg)	Fail (N)	Shear Strength (Pa)	Stability Index
SLAB cm	47	mmH20	76	Rho	161.70	SLOPE	26
19.25	2.25	1	1	3.6	35.30	1412.15	2.81
19.75	2.25	1	2	4.3	42.17	1686.74	3.36
20.25	2.25	1	3	4.3	42.17	1686.74	3.36
20.75	2.25	1	4	4.2	41.19	1647.51	3.28
21.25	2.25	1	5	4.3	42.17	1686.74	3.36
21.75	2.25	1	6	3.9	38.25	1529.83	3.05
21.75	2.75	1	7	3.8	37.27	1490.60	2.97
21.25	2.75	1	8	3.1	30.40	1216.02	2.42
20.25	2.75	1	9	4.2	41.19	1647.51	3.28
19.75	2.75	1	10	4.8	47.07	1882.87	3.75
19.25	2.75	1	11	4.6	45.11	1804.41	3.59
20.75	2.75	1	12	5.8	56.88	2275.13	4.53
SLAB cm	49	mmH20	69	Rho	140.82	SLOPE	26
26.25	2.25	2	1	4.2	41.19	1647.51	3.61
26.75	2.25	2	2	4.4	43.15	1725.96	3.78
27.25	2.25	2	3	4.6	45.11	1804.41	3.96
27.75	2.25	2	4	4.8	47.07	1882.87	4.13
28.25	2.25	2	5	4.6	45.11	1804.41	3.96
28.75	2.25	2	6	4	39.23	1569.06	3.44
26.25	2.75	2	7	4.8	47.07	1882.87	4.13
26.75	2.75	2	8	4.2	41.19	1647.51	3.61
27.25	2.75	2	9	4	39.23	1569.06	3.44
27.75	2.75	2	10	3.8	37.27	1490.60	3.27
28.25	2.75	2	11	3.6	35.30	1412.15	3.10
28.75	2.75	2	12	3.7	36.28	1451.38	3.18
SLAB cm	47	mmH20	74	Rho	157.45	SLOPE	26
23.25	6.75	3	1	3.9	38.25	1529.83	3.13
23.25	7.25	3	2	5.2	50.99	2039.77	4.17
24.75	6.75	3	3	4.6	45.11	1804.41	3.69
23.75	7.25	3	4	3.8	37.27	1490.60	3.05
23.75	6.75	3	5	4.2	41.19	1647.51	3.37
24.75	7.25	3	6	4.3	42.17	1686.74	3.45
24.25	7.25	3	7	3.5	34.32	1372.92	2.81
24.25	6.75	3	8	4.2	41.19	1647.51	3.37
SLAB cm	45	mmH20	72	Rho	160.00	SLOPE	26
19.25	11.25	4	1	4.6	45.11	1804.41	3.79
19.75	11.25	4	2	4	39.23	1569.06	3.30
20.25	11.25	4	3	3.7	36.28	1451.38	3.05
20.75	11.25	4	4	4.8	47.07	1882.87	3.96

21.25	11.25	4	5	4.4	43.15	1725.96	3.63
21.75	11.25	4	6	4.2	41.19	1647.51	3.46
19.25	11.75	4	7	4.4	43.15	1725.96	3.63
19.75	11.75	4	8	4.3	42.17	1686.74	3.54
20.25	11.75	4	9	3.5	34.32	1372.92	2.89
20.75	11.75	4	10	3.2	31.38	1255.24	2.64
21.25	11.75	4	11	3.7	36.28	1451.38	3.05
21.75	11.75	4	12	4.9	48.05	1922.09	4.04
SLAB cm	47	mmH20	73	Rho	155.32	SLOPE	26
26.25	11.25	5	1	4.2	41.19	1647.51	3.41
26.75	11.25	5	2	3.8	37.27	1490.60	3.09
27.25	11.25	5	3	5.2	50.99	2039.77	4.23
27.75	11.25	5	4	4.2	41.19	1647.51	3.41
28.25	11.25	5	5	3.9	38.25	1529.83	3.17
28.75	11.25	5	6	3.6	35.30	1412.15	2.93
26.25	11.75	5	7	4.2	41.19	1647.51	3.41
26.75	11.75	5	8	5	49.03	1961.32	4.07
27.25	11.75	5	9	3.9	38.25	1529.83	3.17
27.75	11.75	5	10	3.3	32.36	1294.47	2.68
28.25	11.75	5	11	3.8	37.27	1490.60	3.09
28.75	11.75	5	12	4.1	40.21	1608.28	3.33
SLAB cm	46	mmH20	72	Rho	156.52	SLOPE	25
23.75	2.25	1.5	1	4.3	42.17	1686.74	3.68
24.25	2.25	1.5	2	4.1	40.21	1608.28	3.51
23.75	2.75	1.5	3	4.1	40.21	1608.28	3.51
24.25	2.75	1.5	4	4.2	41.19	1647.51	3.59
SLAB cm	47	mmH20	73	Rho	155.32	SLOPE	25
27.25	7.25	2.5	1	3.9	38.25	1529.83	3.29
27.75	7.25	2.5	2	4	39.23	1569.06	3.37
27.25	7.75	2.5	3	4.3	42.17	1686.74	3.63
27.75	7.75	2.5	4	4.3	42.17	1686.74	3.63
SLAB cm	48	mmH20	72	Rho	150.00	SLOPE	26
20.25	7.25	3.5	1	4.3	42.17	1686.74	3.54
20.75	7.25	3.5	2	4.4	43.15	1725.96	3.63
20.25	7.75	3.5	3	4.3	42.17	1686.74	3.54
20.75	7.75	3.5	4	4.3	42.17	1686.74	3.54
SLAB cm	48	mmH20	77	Rho	160.42	SLOPE	26
23.75	11.25	4.5	1	5	49.03	1961.32	3.85
24.25	11.25	4.5	2	5.8	56.88	2275.13	4.47
23.75	11.75	4.5	3	4.2	41.19	1647.51	3.24
24.25	11.75	4.5	4	4.1	40.21	1608.28	3.16

Site	SPANKY'S						
Date	20040212						
Name	Plot 3						
Operator:	KK						
FRAME:	0.025	GAGE	20 kg				
X	Y	Pit	Test	kg Fail	Failure (N)	(Pa)	Stability Index
SLAB cm	67	mmH20	92	Rho	137.31	SLOPE	28
19.25	19.25	1	1	6.4	62.76	2510.49	3.86
19.75	19.25	1	2	5.2	50.99	2039.77	3.13
20.25	19.25	1	3	5.6	54.92	2196.68	3.37
20.75	19.25	1	4	6	58.84	2353.58	3.61
21.25	19.25	1	5	4.9	48.05	1922.09	2.95
21.75	19.25	1	6	4.6	45.11	1804.41	2.77
21.75	19.75	1	7	5.5	53.94	2157.45	3.31
21.25	19.75	1	8	5.5	53.94	2157.45	3.31
20.25	19.75	1	9	5.8	56.88	2275.13	3.49
19.75	19.75	1	10	6.6	64.72	2588.94	3.98
19.25	19.75	1	11	5.8	56.88	2275.13	3.49
20.75	19.75	1	12	5.4	52.96	2118.23	3.25
SLAB cm	63	mmH20	89	Rho	141.27	SLOPE	28
26.25	19.25	2	1	5.6	54.92	2196.68	3.49
26.75	19.25	2	2	5.8	56.88	2275.13	3.61
27.25	19.25	2	3	6.4	62.76	2510.49	3.99
27.75	19.25	2	4	4.8	47.07	1882.87	2.99
28.25	19.25	2	5	5.4	52.96	2118.23	3.36
28.75	19.25	2	6	5.4	52.96	2118.23	3.36
26.25	19.75	2	7	4.6	45.11	1804.41	2.86
26.75	19.75	2	8	5.8	56.88	2275.13	3.61
27.25	19.75	2	9	5.2	50.99	2039.77	3.24
27.75	19.75	2	10	4.6	45.11	1804.41	2.86
28.25	19.75	2	11	4	39.23	1569.06	2.49
28.75	19.75	2	12	5.4	52.96	2118.23	3.36
SLAB cm	67	mmH20	100	Rho	149.25	SLOPE	28
23.25	23.75	3	1	5.6	54.92	2196.68	3.10
23.25	24.25	3	2	5.6	54.92	2196.68	3.10
24.75	23.75	3	3	5.5	53.94	2157.45	3.05
23.75	24.25	3	4	7	68.65	2745.85	3.88
23.75	23.75	3	5	4.1	40.21	1608.28	2.27
24.75	24.25	3	6	4.8	47.07	1882.87	2.66
24.25	24.25	3	7	5.7	55.90	2235.90	3.16
24.25	23.75	3	8	4	39.23	1569.06	2.22
SLAB cm	64	mmH20	97	Rho	151.56	SLOPE	28
19.25	28.25	4	1	4.1	40.21	1608.28	2.34
19.75	28.25	4	2	3.7	36.28	1451.38	2.11
20.25	28.25	4	3	4.2	41.19	1647.51	2.40
20.75	28.25	4	4	5	49.03	1961.32	2.86

21.25	28.25	4	5	4	39.23	1569.06	2.29
21.75	28.25	4	6	5.6	54.92	2196.68	3.20
19.25	28.75	4	7	4.2	41.19	1647.51	2.40
19.75	28.75	4	8	4.7	46.09	1843.64	2.69
20.25	28.75	4	9	5.7	55.90	2235.90	3.26
20.75	28.75	4	10	5.7	55.90	2235.90	3.26
21.25	28.75	4	11	4	39.23	1569.06	2.29
21.75	28.75	4	12	6.8	66.68	2667.40	3.89
SLAB cm	68	mmH20	99	Rho	145.59	SLOPE	28
26.25	28.25	5	1	5.8	56.88	2275.13	3.25
26.75	28.25	5	2	4.8	47.07	1882.87	2.69
27.25	28.25	5	3	5.8	56.88	2275.13	3.25
27.75	28.25	5	4	6.1	59.82	2392.81	3.41
28.25	28.25	5	5	4.6	45.11	1804.41	2.58
28.75	28.25	5	6	5.5	53.94	2157.45	3.08
26.25	28.75	5	7	4.6	45.11	1804.41	2.58
26.75	28.75	5	8	4.9	48.05	1922.09	2.74
27.25	28.75	5	9	4.2	41.19	1647.51	2.35
27.75	28.75	5	10	5.2	50.99	2039.77	2.91
28.25	28.75	5	11	5.2	50.99	2039.77	2.91
28.75	28.75	5	12	5.2	50.99	2039.77	2.91
SLAB cm	66	mmH20	98	Rho	148.48	SLOPE	28
23.75	19.25	1.5	1	4	39.23	1569.06	2.26
24.25	19.25	1.5	2	4.4	43.15	1725.96	2.49
23.75	19.75	1.5	3	6	58.84	2353.58	3.39
24.25	19.75	1.5	4	5.6	54.92	2196.68	3.17
SLAB cm	64	mmH20	96	Rho	150.00	SLOPE	28
27.25	24.25	2.5	1	4.7	46.09	1843.64	2.71
27.75	24.25	2.5	2	4.8	47.07	1882.87	2.77
27.25	24.75	2.5	3	5	49.03	1961.32	2.89
27.75	24.75	2.5	4	6.9	67.67	2706.62	3.98
SLAB cm	63	mmH20	90	Rho	142.86	SLOPE	27
20.25	24.25	3.5	1	5.6	54.92	2196.68	3.57
20.75	24.25	3.5	2	5.4	52.96	2118.23	3.44
20.25	24.75	3.5	3	4.7	46.09	1843.64	2.99
20.75	24.75	3.5	4	5.6	54.92	2196.68	3.57
SLAB cm	66	mmH20	101	Rho	153.03	SLOPE	28
23.75	28.25	4.5	1	5.9	57.86	2314.36	3.24
24.25	28.25	4.5	2	5.8	56.88	2275.13	3.18
23.75	28.75	4.5	3	3.8	37.27	1490.60	2.09
24.25	28.75	4.5	4	5	49.03	1961.32	2.74

Site	SPANKY'S						
Date	20040220						
Name	Plot 4						
Operator:	KK						
FRAME:	0.025	GAGE	20 kg				
X	Y	Pit	test		Failure (N)	(Pa)	Stability Index
SLAB cm	73	mmH20	134	Rho	183.5616	SLOPE	26
2.25	19.25	1	1	6.5	63.74	2549.72	2.88
2.75	19.25	1	2	6.4	62.76	2510.49	2.83
3.25	19.25	1	3	5.6	54.92	2196.68	2.48
3.75	19.25	1	4	5.8	56.88	2275.13	2.57
4.25	19.25	1	5	4.8	47.07	1882.87	2.13
4.75	19.25	1	6	6.8	66.68	2667.40	3.01
4.75	19.75	1	7	5.2	50.99	2039.77	2.30
4.25	19.75	1	8	5.8	56.88	2275.13	2.57
3.25	19.75	1	9	4.9	48.05	1922.09	2.17
2.75	19.75	1	10	5.8	56.88	2275.13	2.57
2.25	19.75	1	11	5.8	56.88	2275.13	2.57
3.75	19.75	1	12	5.4	52.96	2118.23	2.39
SLAB cm	72	mmH20	132	Rho	183.3333	SLOPE	26
9.25	19.25	2	1	5.3	51.97	2079.00	2.38
9.75	19.25	2	2	6.2	60.80	2432.04	2.79
10.25	19.25	2	3	5	49.03	1961.32	2.25
10.75	19.25	2	4	4.8	47.07	1882.87	2.16
11.25	19.25	2	5	5	49.03	1961.32	2.25
11.75	19.25	2	6	5.6	54.92	2196.68	2.52
9.25	19.75	2	7	5.8	56.88	2275.13	2.61
9.75	19.75	2	8	6.8	66.68	2667.40	3.06
10.25	19.75	2	9	7	68.65	2745.85	3.15
10.75	19.75	2	10	6.4	62.76	2510.49	2.88
11.25	19.75	2	11	6.3	61.78	2471.26	2.83
11.75	19.75	2	12	7.2	70.61	2824.30	3.24
SLAB cm	73	mmH20	132	Rho	180.8219	SLOPE	27
6.25	23.75	3	1	5.2	50.99	2039.77	2.26
6.25	24.25	3	2	7.6	74.53	2981.21	3.30
7.75	23.75	3	3	5.8	56.88	2275.13	2.52
6.75	24.25	3	4	7.4	72.57	2902.75	3.21
6.75	23.75	3	5	5.9	57.86	2314.36	2.56
7.75	24.25	3	6	5.8	56.88	2275.13	2.52
7.25	24.25	3	7	5.7	55.90	2235.90	2.47
7.25	23.75	3	8	8.2	80.41	3216.56	3.56
SLAB cm	70	mmH20	132	Rho	188.5714	SLOPE	29
2.25	28.25	4	1	5.6	54.92	2196.68	2.28
2.75	28.25	4	2	6.2	60.80	2432.04	2.52
3.25	28.25	4	3	7.1	69.63	2785.07	2.89
3.75	28.25	4	4	7.7	75.51	3020.43	3.13

4.25	28.25	4	5	6.2	60.80	2432.04	2.52
4.75	28.25	4	6	4.6	45.11	1804.41	1.87
2.25	28.75	4	7	5.7	55.90	2235.90	2.32
2.75	28.75	4	8	4.4	43.15	1725.96	1.79
3.25	28.75	4	9	5	49.03	1961.32	2.03
3.75	28.75	4	10	4.8	47.07	1882.87	1.95
4.25	28.75	4	11	4.6	45.11	1804.41	1.87
4.75	28.75	4	12	4.8	47.07	1882.87	1.95
SLAB cm	68	mmH20	121	Rho	177.9412	SLOPE	29
9.25	28.25	5	1	5.4	52.96	2118.23	2.39
9.75	28.25	5	2	5.7	55.90	2235.90	2.53
10.25	28.25	5	3	5.6	54.92	2196.68	2.48
10.75	28.25	5	4	6	58.84	2353.58	2.66
11.25	28.25	5	5	5.4	52.96	2118.23	2.39
11.75	28.25	5	6	5.6	54.92	2196.68	2.48
9.25	28.75	5	7	4.8	47.07	1882.87	2.13
9.75	28.75	5	8	3.4	33.34	1333.70	1.51
10.25	28.75	5	9	5.9	57.86	2314.36	2.62
10.75	28.75	5	10	5.8	56.88	2275.13	2.57
11.25	28.75	5	11	6.2	60.80	2432.04	2.75
11.75	28.75	5	12	5	49.03	1961.32	2.22
SLAB cm	72	mmH20	133	Rho	184.7222	SLOPE	25
6.75	19.25	1.5	1	4.7	46.09	1843.64	2.18
7.25	19.25	1.5	2	7	68.65	2745.85	3.24
6.75	19.75	1.5	3	4.5	44.13	1765.19	2.08
7.25	19.75	1.5	4	6.5	63.74	2549.72	3.01
SLAB cm	72	mmH20	130	Rho	180.5556	SLOPE	28
10.25	24.25	2.5	1	5.8	56.88	2275.13	2.47
10.75	24.25	2.5	2	5.4	52.96	2118.23	2.30
10.25	24.75	2.5	3	4.4	43.15	1725.96	1.88
10.75	24.75	2.5	4	5.6	54.92	2196.68	2.39
SLAB cm	71	mmH20	131	Rho	184.507	SLOPE	26
3.25	24.25	3.5	1	6.4	62.76	2510.49	2.90
3.75	24.25	3.5	2	6.2	60.80	2432.04	2.81
3.25	24.75	3.5	3	6	58.84	2353.58	2.72
3.75	24.75	3.5	4	6.8	66.68	2667.40	3.08
SLAB cm	68	mmH20	121	Rho	177.9412	SLOPE	29
6.75	28.25	4.5	1	5	49.03	1961.32	2.22
7.25	28.25	4.5	2	4	39.23	1569.06	1.77
6.75	28.75	4.5	3	5.4	52.96	2118.23	2.39
7.25	28.75	4.5	4	5.8	56.88	2275.13	2.57

Site LIONHEAD
Date 20040207
Name Alleys
Operator: SL
FRAME: 0.025 GAGE 5 kg

X	Y	Pit	Test	kg	HN	mm H2O	Angle	Density	Failure (N)	Shear Strength (Pa)	Stability Index	Notes
15.25	0.25	1	1	3.5	53	77	29	145.28	34.32	1372.92	2.44	
15.75	0.25	1	2	3.45					33.83	1353.31	2.40	
15.25	0.75	1	3	5.5					53.94	2157.45	3.83	
15.75	0.75	1	4	4.25					41.68	1667.12	2.96	
15.25	7.25	2	1	4.45	52	73	28	140.38	43.64	1745.57	3.38	
15.75	7.25	2	2	4.95					48.54	1941.71	3.76	
15.25	7.75	2	3	4.3					42.17	1686.74	3.26	
15.75	7.75	2	4	4.75					46.58	1863.25	3.61	
15.25	13.25	3	1	4.45	53	73	28	137.74	43.64	1745.57	3.38	
15.75	13.25	3	2	3.7					36.28	1451.38	2.81	
15.25	13.75	3	3	3.75					36.77	1470.99	2.85	
15.75	13.75	3	4	3.55					34.81	1392.54	2.70	
15.25	17.25	4	1	4.35	53	73	29	137.74	42.66	1706.35	3.20	
15.75	17.25	4	2	5.1					50.01	2000.55	3.75	pre-collapse
15.25	17.75	4	3	2.75					26.97	1078.73	2.02	
15.75	17.75	4	4	0.8					7.85	313.81	0.59	
15.25	24.25	5	1	0.5	53.5	72	30	134.58	4.90	196.13	0.36	
15.75	24.25	5	2	0.9					8.83	353.04	0.65	
15.25	24.75	5	3	0.5					4.90	196.13	0.36	1330
15.75	24.75	5	4	1.7					16.67	666.85	1.23	1405
15.25	30.25	6	1	1.45	57	88	28	154.39	14.22	568.78	0.91	
15.75	30.25	6	2	1.7					16.67	666.85	1.07	just below fx
15.25	30.75	6	3	0.5					4.90	196.13	0.31	1420
15.75	30.75	6	4	1.2					11.77	470.72	0.76	
0.25	15.25	7	1	1.9	57	88	24	154.39	18.63	745.30	1.38	1550
0.25	15.75	7	2	1.95					19.12	764.91	1.42	1605
0.75	15.25	7	3	1.15					11.28	451.10	0.84	
0.75	15.75	7	4	0.8					7.85	313.81	0.58	
7.25	15.25	8	1	1.65	55	86	26	156.36	16.18	647.24	1.14	1520
7.25	15.75	8	2	3.1					30.40	1216.02	2.14	
7.75	15.25	8	3	1.65					16.18	647.24	1.14	
7.75	15.75	8	4	1.75					17.16	686.46	1.21	1450
13.25	15.25	9	1	0.6	53	80	27	150.94	5.88	235.36	0.43	
13.25	15.75	9	2	1.35					13.24	529.56	0.97	
13.75	15.25	9	3	1.65					16.18	647.24	1.18	1505
13.75	15.75	9	4	2.2					21.57	862.98	1.58	1620
17.25	15.25	10	1	2.35	54	82	27	151.85	23.05	921.82	1.64	
17.25	15.75	10	2	1.5					14.71	588.40	1.05	

17.75	15.25	10	3	1.7					16.67	666.85	1.19	1630
17.75	15.75	10	4	1.8					17.65	706.08	1.26	1645
24.25	15.25	11	1	2.05	54	84	28	155.56	20.10	804.14	1.35	
24.25	15.75	11	2	2					19.61	784.53	1.32	
24.75	15.25	11	3	1.45					14.22	568.78	0.96	1700
24.75	15.75	11	4	2.7					26.48	1059.11	1.78	1710
30.25	15.25	12	1	1.6	53	83	28	156.60	15.69	627.62	1.07	
30.25	15.75	12	2	2.1					20.59	823.75	1.40	
30.75	15.25	12	3	2.1					20.59	823.75	1.40	1770
30.75	15.75	12	4	1.8					17.65	706.08	1.20	
15.25	31.25			4.55	57	88	28		44.62	1784.80	2.87	
15.75	31.25			3.5					34.32	1372.92	2.20	

Site	LIONHEAD							
Date	20040208							
Name	Plot 2							
Operator:	SL							
FRAME:	0.025		GAGE	5 kg				
X	Y	Pit	Test	Fail (kg)	Fail (N)	Shear Strength (Pa)	Stability Index	
SLAB cm	53	mmH20	84	Rho	158.5	SLOPE	27	
2.25	2.25	1	1	3.65	35.79	1431.76	2.49	
2.75	2.25	1	2	2.7	26.48	1059.11	1.84	
3.25	2.25	1	3	3.9	38.25	1529.83	2.66	
3.75	2.25	1	4	2.9	28.44	1137.57	1.98	
4.25	2.25	1	5	3.2	31.38	1255.24	2.18	
4.75	2.25	1	6	3.8	37.27	1490.60	2.59	
4.75	2.75	1	7	4.1	40.21	1608.28	2.80	
4.25	2.75	1	8	4.2	41.19	1647.51	2.87	
3.25	2.75	1	9	3.25	31.87	1274.86	2.22	
2.75	2.75	1	10	2.65	25.99	1039.50	1.81	affected by tracks above?
2.25	2.75	1	11	4.25	41.68	1667.12	2.90	
3.75	2.75	1	12	4.5	44.13	1765.19	3.07	1000
SLAB cm	53	mmH20	84	Rho	158.4906	SLOPE	26	
9.25	2.25	2	1	4.45	43.64	1745.57	3.14	
9.75	2.25	2	2	2.65	25.99	1039.50	1.87	
10.25	2.25	2	3	3.55	34.81	1392.54	2.51	
10.75	2.25	2	4	3.45	33.83	1353.31	2.44	
11.25	2.25	2	5	3.6	35.30	1412.15	2.54	
11.75	2.25	2	6	4.35	42.66	1706.35	3.07	
9.25	2.75	2	7	3.9	38.25	1529.83	2.76	
9.75	2.75	2	8	2.75	26.97	1078.73	1.94	
10.25	2.75	2	9	3.35	32.85	1314.08	2.37	
10.75	2.75	2	10	3.35	32.85	1314.08	2.37	
11.25	2.75	2	11	3.4	33.34	1333.70	2.40	
11.75	2.75	2	12	3.5	34.32	1372.92	2.47	
SLAB cm	53	mmH20	84	Rho	158.4906	SLOPE	27	
6.25	6.75	3	1	3.8	37.27	1490.60	2.59	
6.25	7.25	3	2	3.5	34.32	1372.92	2.39	
7.75	6.75	3	3	3	29.42	1176.79	2.05	
6.75	7.25	3	4	2.9	28.44	1137.57	1.98	
6.75	6.75	3	5	3.2	31.38	1255.24	2.18	
7.75	7.25	3	6	2.8	27.46	1098.34	1.91	
7.25	7.25	3	7	2.4	23.54	941.43	1.64	
7.25	6.75	3	8	3.65	35.79	1431.76	2.49	
SLAB cm	55	mmH20	83	Rho	150.9091	SLOPE	30	
2.25	11.25	4	1	3.3	32.36	1294.47	2.07	
2.75	11.25	4	2	3.3	32.36	1294.47	2.07	

3.25	11.25	4	3	3.75	36.77	1470.99	2.35	
3.75	11.25	4	4	3.2	31.38	1255.24	2.01	
4.25	11.25	4	5	2.55	25.01	1000.27	1.60	just below fx
4.75	11.25	4	6	3.1	30.40	1216.02	1.94	above fx
2.25	11.75	4	7	3	29.42	1176.79	1.88	
2.75	11.75	4	8	2.75	26.97	1078.73	1.72	
3.25	11.75	4	9	3.75	36.77	1470.99	2.35	
3.75	11.75	4	10	3.1	30.40	1216.02	1.94	below fx
4.25	11.75	4	11	3.6	35.30	1412.15	2.26	above fx
4.75	11.75	4	12	2.75	26.97	1078.73	1.72	
SLAB cm	54	mmH20	82	Rho	151.8519	SLOPE	30	
9.25	11.25	5	1	3.8	37.27	1490.60	2.41	
9.75	11.25	5	2	3.5	34.32	1372.92	2.22	
10.25	11.25	5	3	3.35	32.85	1314.08	2.13	
10.75	11.25	5	4	4.3	42.17	1686.74	2.73	
11.25	11.25	5	5	2.75	26.97	1078.73	1.75	
11.75	11.25	5	6	3	29.42	1176.79	1.90	
9.25	11.75	5	7	3.75	36.77	1470.99	2.38	
9.75	11.75	5	8	3.5	34.32	1372.92	2.22	
10.25	11.75	5	9	4.25	41.68	1667.12	2.70	
10.75	11.75	5	10	3.15	30.89	1235.63	2.00	
11.25	11.75	5	11	3.1	30.40	1216.02	1.97	
11.75	11.75	5	12	3.15	30.89	1235.63	2.00	
SLAB cm	53	mmH20	82	Rho	154.717	SLOPE	27	
6.75	2.25	1.5	1	2.45	24.03	961.05	1.71	
7.25	2.25	1.5	2	2.95	28.93	1157.18	2.06	
6.75	2.75	1.5	3	5.1	50.01	2000.55	3.56	weak layer pinned
7.25	2.75	1.5	4	3.1	30.40	1216.02	2.17	
SLAB cm	53	mmH20	84	Rho	158.4906	SLOPE	29	
10.25	7.25	2.5	1	3.55	34.81	1392.54	2.27	
10.75	7.25	2.5	2	2.65	25.99	1039.50	1.69	
10.25	7.75	2.5	3	3	29.42	1176.79	1.92	
10.75	7.75	2.5	4	3.75	36.77	1470.99	2.40	
SLAB cm	53	mmH20	87	Rho	164.1509	SLOPE	27	
3.25	7.25	3.5	1	4.65	45.60	1824.03	3.06	
3.75	7.25	3.5	2	4.2	41.19	1647.51	2.77	
3.25	7.75	3.5	3	3.8	37.27	1490.60	2.50	
3.75	7.75	3.5	4	4.65	45.60	1824.03	3.06	
SLAB cm	54	mmH20	82	Rho	151.8519	SLOPE	30	
6.75	11.25	4.5	1	3.85	37.76	1510.22	2.44	
7.25	11.25	4.5	2	3.65	35.79	1431.76	2.32	
6.75	11.75	4.5	3	4	39.23	1569.06	2.54	
7.25	11.75	4.5	4	4.2	41.19	1647.51	2.67	

Site LIONHEAD
Date 20040217
Name Plot 3
Operator: SL
FRAME: 0.025 GAGE 20 kg

X	Y	Pit	Test	Fail (kg)	Fail (N)	Shear Strength (Pa)	Stability Index	
SLAB cm	61	mmH20	107	Rho	175.41	SLOPE	31	
2.25	19.25	1	1	6.2	60.80	2432.04	2.93	
2.75	19.25	1	2	5.4	52.96	2118.23	2.55	
3.25	19.25	1	3	6	58.84	2353.58	2.83	
3.75	19.25	1	4	5.4	52.96	2118.23	2.55	
4.25	19.25	1	5	5.4	52.96	2118.23	2.55	
4.75	19.25	1	6	6.2	60.80	2432.04	2.93	
4.75	19.75	1	7	4.2	41.19	1647.51	1.98	
4.25	19.75	1	8	3.8	37.27	1490.60	1.79	
3.25	19.75	1	9	5	49.03	1961.32	2.36	
2.75	19.75	1	10	5.8	56.88	2275.13	2.74	
2.25	19.75	1	11	4.2	41.19	1647.51	1.98	
3.75	19.75	1	12	4.2	41.19	1647.51	1.98	
SLAB cm	60	mmH20	116	Rho	193.33	SLOPE	30	
9.25	19.25	2	1	5.8	56.88	2275.13	2.60	
9.75	19.25	2	2	5.4	52.96	2118.23	2.42	
10.25	19.25	2	3	6.2	60.80	2432.04	2.78	
10.75	19.25	2	4	5.2	50.99	2039.77	2.33	
11.25	19.25	2	5	5.2	50.99	2039.77	2.33	
11.75	19.25	2	6	5.2	50.99	2039.77	2.33	
9.25	19.75	2	7	5.4	52.96	2118.23	2.42	
9.75	19.75	2	8	5	49.03	1961.32	2.24	
10.25	19.75	2	9	4.8	47.07	1882.87	2.15	
10.75	19.75	2	10	7.2	70.61	2824.30	3.23	q2 @ top of sh
11.25	19.75	2	11	7.4	72.57	2902.75	3.32	q2
11.75	19.75	2	12	5.8	56.88	2275.13	2.60	q1
SLAB cm	59	mmH20	108	Rho	183.05	SLOPE	28	
6.25	23.75	3	1	5.8	56.88	2275.13	2.98	
6.25	24.25	3	2	5.8	56.88	2275.13	2.98	q2
7.75	23.75	3	3	6	58.84	2353.58	3.08	q3
6.75	24.25	3	4	5.8	56.88	2275.13	2.98	q2
6.75	23.75	3	5	5.6	54.92	2196.68	2.87	
7.75	24.25	3	6	5.4	52.96	2118.23	2.77	
7.25	24.25	3	7	6	58.84	2353.58	3.08	
7.25	23.75	3	8	4.8	47.07	1882.87	2.46	

SLAB	55	mmH20	92	Rho	167.27	SLOPE	32	
cm								
2.25	28.25	4	1	4.8	47.07	1882.87	2.56	
2.75	28.25	4	2	3.6	35.30	1412.15	1.92	
3.25	28.25	4	3	4	39.23	1569.06	2.13	
3.75	28.25	4	4	3.8	37.27	1490.60	2.03	
4.25	28.25	4	5	5.8	56.88	2275.13	3.10	
4.75	28.25	4	6	4.6	45.11	1804.41	2.45	
2.25	28.75	4	7	3.8	37.27	1490.60	2.03	
2.75	28.75	4	8	4.2	41.19	1647.51	2.24	
3.25	28.75	4	9	3.6	35.30	1412.15	1.92	
3.75	28.75	4	10	3.8	37.27	1490.60	2.03	
4.25	28.75	4	11	4	39.23	1569.06	2.13	
4.75	28.75	4	12	4.6	45.11	1804.41	2.45	
SLAB	62	mmH20	116	Rho	187.10	SLOPE	31	
cm								
9.25	28.25	5	1	4.2	41.19	1647.51	1.83	
9.75	28.25	5	2	5	49.03	1961.32	2.18	
10.25	28.25	5	3	4.6	45.11	1804.41	2.00	
10.75	28.25	5	4	5.4	52.96	2118.23	2.35	
11.25	28.25	5	5	4.8	47.07	1882.87	2.09	
11.75	28.25	5	6	5	49.03	1961.32	2.18	
9.25	28.75	5	7	5.4	52.96	2118.23	2.35	
9.75	28.75	5	8	5.8	56.88	2275.13	2.53	
10.25	28.75	5	9	5.6	54.92	2196.68	2.44	
10.75	28.75	5	10	5	49.03	1961.32	2.18	
11.25	28.75	5	11	6.4	62.76	2510.49	2.79	
11.75	28.75	5	12	5.6	54.92	2196.68	2.44	
SLAB	61	mmH20	112	Rho	183.61	SLOPE	30	
cm								
6.75	19.25	1.5	1	4.8	47.07	1882.87	2.23	
7.25	19.25	1.5	2	5.8	56.88	2275.13	2.69	
6.75	19.75	1.5	3	6	58.84	2353.58	2.79	
7.25	19.75	1.5	4	6.4	62.76	2510.49	2.97	
SLAB	63	mmH20	114	Rho	180.95	SLOPE	28	
cm								
10.25	24.25	2.5	1	4.4	43.15	1725.96	2.14	not collapsed
10.75	24.25	2.5	2	5.2	50.99	2039.77	2.53	
10.25	24.75	2.5	3	4.8	47.07	1882.87	2.33	
10.75	24.75	2.5	4	3	29.42	1176.79	1.46	
SLAB	60	mmH20	109	Rho	181.67	SLOPE	30	
cm								
3.25	24.25	3.5	1	5	49.03	1961.32	2.39	
3.75	24.25	3.5	2	5	49.03	1961.32	2.39	
3.25	24.75	3.5	3	4.4	43.15	1725.96	2.10	
3.75	24.75	3.5	4	6.4	62.76	2510.49	3.06	

SLAB	61	mmH20	108	Rho	177.05	SLOPE	30
cm							
6.75	28.25	4.5	1	4	39.23	1569.06	1.93
7.25	28.25	4.5	2	4	39.23	1569.06	1.93
6.75	28.75	4.5	3	4.4	43.15	1725.96	2.12
7.25	28.75	4.5	4	4.6	45.11	1804.41	2.22

Site LIONHEAD
Date 20040217
Name Plot 4
Operator: SL
FRAME: 0.025 GAGE 20 kg

X	Y	Pit	Test	Fail (kg)	Fail (N)	Shear Strength (Pa)	Stability Index	
SLAB cm	61	mmH20	107	Rho	175.41	SLOPE	31	
2.25	19.25	1	1	6.2	60.80	2432.04	2.93	
2.75	19.25	1	2	5.4	52.96	2118.23	2.55	
3.25	19.25	1	3	6	58.84	2353.58	2.83	
3.75	19.25	1	4	5.4	52.96	2118.23	2.55	
4.25	19.25	1	5	5.4	52.96	2118.23	2.55	
4.75	19.25	1	6	6.2	60.80	2432.04	2.93	
4.75	19.75	1	7	4.2	41.19	1647.51	1.98	
4.25	19.75	1	8	3.8	37.27	1490.60	1.79	
3.25	19.75	1	9	5	49.03	1961.32	2.36	
2.75	19.75	1	10	5.8	56.88	2275.13	2.74	
2.25	19.75	1	11	4.2	41.19	1647.51	1.98	
3.75	19.75	1	12	4.2	41.19	1647.51	1.98	
SLAB cm	60	mmH20	116	Rho	193.33	SLOPE	30	
9.25	19.25	2	1	5.8	56.88	2275.13	2.60	
9.75	19.25	2	2	5.4	52.96	2118.23	2.42	
10.25	19.25	2	3	6.2	60.80	2432.04	2.78	
10.75	19.25	2	4	5.2	50.99	2039.77	2.33	
11.25	19.25	2	5	5.2	50.99	2039.77	2.33	
11.75	19.25	2	6	5.2	50.99	2039.77	2.33	
9.25	19.75	2	7	5.4	52.96	2118.23	2.42	
9.75	19.75	2	8	5	49.03	1961.32	2.24	
10.25	19.75	2	9	4.8	47.07	1882.87	2.15	
10.75	19.75	2	10	7.2	70.61	2824.30	3.23	q2 @ top of sh
11.25	19.75	2	11	7.4	72.57	2902.75	3.32	q2
11.75	19.75	2	12	5.8	56.88	2275.13	2.60	q1
SLAB cm	59	mmH20	108	Rho	183.05	SLOPE	28	
6.25	23.75	3	1	5.8	56.88	2275.13	2.98	
6.25	24.25	3	2	5.8	56.88	2275.13	2.98	q2
7.75	23.75	3	3	6	58.84	2353.58	3.08	q3
6.75	24.25	3	4	5.8	56.88	2275.13	2.98	q2
6.75	23.75	3	5	5.6	54.92	2196.68	2.87	
7.75	24.25	3	6	5.4	52.96	2118.23	2.77	
7.25	24.25	3	7	6	58.84	2353.58	3.08	
7.25	23.75	3	8	4.8	47.07	1882.87	2.46	
SLAB cm	55	mmH20	92	Rho	167.27	SLOPE	32	
2.25	28.25	4	1	4.8	47.07	1882.87	2.56	
2.75	28.25	4	2	3.6	35.30	1412.15	1.92	

3.25	28.25	4	3	4	39.23	1569.06	2.13	
3.75	28.25	4	4	3.8	37.27	1490.60	2.03	
4.25	28.25	4	5	5.8	56.88	2275.13	3.10	
4.75	28.25	4	6	4.6	45.11	1804.41	2.45	
2.25	28.75	4	7	3.8	37.27	1490.60	2.03	
2.75	28.75	4	8	4.2	41.19	1647.51	2.24	
3.25	28.75	4	9	3.6	35.30	1412.15	1.92	
3.75	28.75	4	10	3.8	37.27	1490.60	2.03	
4.25	28.75	4	11	4	39.23	1569.06	2.13	
4.75	28.75	4	12	4.6	45.11	1804.41	2.45	
SLAB cm	62	mmH20	116	Rho	187.10	SLOPE	31	
9.25	28.25	5	1	4.2	41.19	1647.51	1.83	
9.75	28.25	5	2	5	49.03	1961.32	2.18	
10.25	28.25	5	3	4.6	45.11	1804.41	2.00	
10.75	28.25	5	4	5.4	52.96	2118.23	2.35	
11.25	28.25	5	5	4.8	47.07	1882.87	2.09	
11.75	28.25	5	6	5	49.03	1961.32	2.18	
9.25	28.75	5	7	5.4	52.96	2118.23	2.35	
9.75	28.75	5	8	5.8	56.88	2275.13	2.53	
10.25	28.75	5	9	5.6	54.92	2196.68	2.44	
10.75	28.75	5	10	5	49.03	1961.32	2.18	
11.25	28.75	5	11	6.4	62.76	2510.49	2.79	
11.75	28.75	5	12	5.6	54.92	2196.68	2.44	
SLAB cm	61	mmH20	112	Rho	183.61	SLOPE	30	
6.75	19.25	1.5	1	4.8	47.07	1882.87	2.23	
7.25	19.25	1.5	2	5.8	56.88	2275.13	2.69	
6.75	19.75	1.5	3	6	58.84	2353.58	2.79	
7.25	19.75	1.5	4	6.4	62.76	2510.49	2.97	
SLAB cm	63	mmH20	114	Rho	180.95	SLOPE	28	
10.25	24.25	2.5	1	4.4	43.15	1725.96	2.14	not collapsed
10.75	24.25	2.5	2	5.2	50.99	2039.77	2.53	
10.25	24.75	2.5	3	4.8	47.07	1882.87	2.33	
10.75	24.75	2.5	4	3	29.42	1176.79	1.46	
SLAB cm	60	mmH20	109	Rho	181.67	SLOPE	30	
3.25	24.25	3.5	1	5	49.03	1961.32	2.39	
3.75	24.25	3.5	2	5	49.03	1961.32	2.39	
3.25	24.75	3.5	3	4.4	43.15	1725.96	2.10	
3.75	24.75	3.5	4	6.4	62.76	2510.49	3.06	
SLAB cm	61	mmH20	108	Rho	177.05	SLOPE	30	
6.75	28.25	4.5	1	4	39.23	1569.06	1.93	
7.25	28.25	4.5	2	4	39.23	1569.06	1.93	
6.75	28.75	4.5	3	4.4	43.15	1725.96	2.12	
7.25	28.75	4.5	4	4.6	45.11	1804.41	2.22	